Title
Low Embodied CO2 Binders using Belitic Calcium Sulfoaluminate Cement

Author
ATEBA ESSOLEBE, Elisabeth

Publication Date
2023

Peer reviewed|Thesis/dissertation

UNIVERSITY OF CALIFORNIA

Los Angeles

Low Embodied CO_2 Binders using Belitic Calcium Sulfoaluminate Cement

A thesis submitted in partial satisfaction

of the requirements for the degree of Master of Science

in Materials Science and Engineering

by

Elisabeth Ateba Essolebe

2023

ABSTRACT OF THE THESIS

Low Embodied CO_2 Binders using Belitic Calcium Sulfoaluminate Cement

by

Elisabeth Ateba Essolebe

Master of Science in Materials Science and Engineering

University of California, Los Angeles, 2023

Professor Jaime Marian, Chair

Using alternative cements or binders is an effective strategy to reduce the overall embodied CO_2 of concrete. Portland limestone cement (PLC) and limestone calcined clay cement (LC^3) are commercially available Portland-based cements with less embodied CO_2 than traditional Portland cement. These binders contain lower amounts of Portland cement and include supplementary cementitious materials (SCMs) that can provide additional cementitious properties. Another class

of cements known as calcium sulfoaluminate or CSA cements, and more specifically, belite CSA or BCSA cements, are becoming increasingly important because of their high performance and low embodied CO_2. One drawback of PLC and LC^3 cements is that they lack early-age strengths, i.e., between 1 and 24 hours; however, BCSA cement, due to its unique chemistry and rapid setting behavior, can provide sufficient high early-age strengths necessary for specific applications. The ability of concrete mixes that provide this advantage and offer lower CO_2 emissions can also have economic benefits. In this study, low embodied CO_2 binders are developed using BCSA and PLC as well as calcined clay to maintain or improve their essential performance characteristics. Cement blends consisting of BCSA, PLC, and calcined clay are prepared, and various properties such as flow, setting time, shrinkage, and compressive strength are measured. The hydration of different phases in these binders and their blends are also evaluated using isothermal calorimetry, TGA/DTG, XRD, and SEM. The results show that replacing only 30% of PLC or LC^3 (i.e., a mix proportioned with PLC and calcined clay) with BCSA can significantly improve early-age performance without affecting later-age strength and achieve a low GWP and carbon intensity.

Keywords: embodied CO_2, belitic calcium sulfoaluminate cement, Portland limestone cement, calcined clay, compressive strengths, carbon intensity

The thesis of Elisabeth Ateba Essolebe is approved.

Bruce S. Dunn

Eric P. Bescher

Jenn-Ming Yang

Jaime Marian, Committee Chair

University of California, Los Angeles

2023

Table of Contents

List of tables

List of figures

Cement chemistry notation

C = CaO, A = Al_2O_3, $\overline{S}$ = SO_3, $\overline{C}$ = CO_3, S=SiO_2, H = H_2O

C_3S Alite or Tricalcium silicate ($3CaO \cdot SiO_2$)

C_2S Belite or Dicalcium silicate ($2CaO \cdot SiO_2$)

C_3A Tricalcium aluminate ($3CaO \cdot Al_2O_3$)

C_4AF Tetracalcium aluminoferrite ($4CaO \cdot Al_2O_3 \cdot Fe_2O_3$)

$C\overline{C}$ Calcium carbonate ($CaCO_3$) or calcite

CH Calcium hydroxide ($Ca(OH)_2$)

$C\overline{S}$ Anhydrite or Anhydrous calcium sulfate

$C\overline{S}H_2$ Gypsum or Calcium sulfate dihydrate

C-S-H Calcium-silicate-hydrate ($3CaO \cdot 2SiO_2 \cdot 3H_2O$)

CSA Calcium sulfoaluminate

AFm Alumina-ferrite-monosulfate

AFt Alumina-ferrite-trisulfate

AH_3 Aluminum hydroxide $Al(OH)_3$

$C_6A\overline{S}H_{32}$ Ettringite or hexacalcium aluminate trisulfate hydrate ($6CaO \cdot Al_2O_3 \cdot 3SO_3 \cdot 32H_2O$)

AS_2 Metakaolin ($Al_2O_3 \cdot 2SiO_2 \cdot 2H_2O$)

Hc Hemicarboaluminate hydrate (hemicarbonate) ($C_3A \cdot 0.5CaCO_3 \cdot 11.5H_2O$)

Mc Monocarboaluminate hydrate (monocarbonate) ($C_3A \cdot CaCO_3 \cdot 11H_2O$)

Ms Monosulfoaluminate hydrate (monosulfate) ($C_3A.C\overline{S}.12H$)

Acknowledgements

First, I'm extremely grateful to Mrs. Linda Rice for her trust and immense generosity. She made this research possible, maintaining the connection between her late husband Mr. Edward K. Rice and UCLA engineering.

I also would like to express my deepest and sincere gratitude to my professor, Dr. Eric P. Bescher, for trusting me and giving me the opportunity to work on this project. His guidance and expertise enabled me to carry out this research.

I want to thank Omkar Deo for his assistance, scientific and technical support. He made himself as available as possible when needed and provided me with valuable advice.

I also have to acknowledge all the members of CTS Cement Manufacturing Corporation that helped me throughout this project in a good working atmosphere, showing kindness, benevolence and providing helpful feedback.

Many thanks to Prof. Sergey Prikhodko and Prof. Ignacio Martini for their help and support in the SEM and chemistry lab at UCLA. I learned a lot.

Thanks to Dr. Jaime Marian, Dr. Bruce S. Dunn and Dr. Jenn-Ming Yang for serving on my thesis committee.

Thanks to all the classmates, friends and tennis partners who were a breath of fresh air at the most stressful times.

You all made this a rich learning experience, academically, scientifically, socially, and personally.

Finally, I would like to thank my family for its unwavering support.

1. INTRODUCTION

Low embodied CO_2 binders refer to types of binders that produce less carbon dioxide (CO_2) emissions during production. Binders are materials that hold the aggregates (sand, gravel, etc.) together in concrete, and typically the production of binders involves high-temperature heating processes that release significant amounts of CO_2. Portland cement has traditionally been the most commonly used binder in concrete production. However, Portland cement production results in significant CO_2 emissions, accounting for approximately 8% of global CO_2 emissions [1]. To produce portland cement, limestone, clay, and other raw materials, such as iron oxide, bauxite, and silica, are heated in a large rotating furnace called a kiln to a temperature of 1450°C. Fossil fuels are burned to reach this high temperature, accounting for 40% of Portland cement's carbon emissions [2]. The remaining 60% of carbon emissions are due to the decomposition of limestone into lime and carbon dioxide. Efforts are being made to develop alternative binders with a lower carbon footprint. These low embodied CO_2 binders include some relatively new types of cementitious materials such as calcium sulfoaluminate (CSA) cements, including belitic CSA or BCSA cement, Portland limestone cement (PLC), limestone calcined clay cement (LC^3) as well as commonly used supplementary cementitious materials (SCMs) or pozzolans, such as calcined clay, fly ash, slag, and other alkali-activated binders or geopolymers, all of which are associated with lower CO_2 emissions during their production compared to Portland cement [3].

BCSA is a special class of CSA cement that has a history of nearly 45 years of use in North America, thanks to its several benefits, such as low embodied CO_2, fast setting behavior, high early-age strength, low shrinkage, resistance to chemical attacks (e.g., sulfate, chloride, alkali-silica, carbonation, etc.), and increased long-term durability. It is composed of nearly 50% by weight of belite (C_2S) as its primary component, hence the name - BCSA. It does not contain alite (C_3S), meaning the BCSA clinker can be produced at a lower manufacturing temperature of nearly 1250°C compared to almost 1450°C required for producing portland clinker. It also has a lower requirement for limestone [4]. The BCSA clinker, which is more porous and friable, also requires less grinding effort compared to portland clinker [5]. The production of 1 ton of BCSA cement releases only 0.75 tons of CO_2, resulting in a 25% reduction in CO_2 emissions [6]. Currently, there are only two producers of BCSA cement in the United States - CTS Cement Manufacturing

Corporation and Buzzi Unicem USA. BCSA cement manufactured by CTS Cement is commercially known as Rapid Set® cement and can be used as a standalone (non-blended) replacement for ordinary Portland cement (OPC). Whereas the CSA Cement from Buzzi Unicem USA is mainly used as an additive that can enhance the chemical and physical properties of a cement blend [7].

PLC or Type IL is a relatively recent development in the cement industry. It incorporates limestone as a partial replacement for portland clinker, the main component in OPC. In PLC, 5% to 15% of the clinker is typically replaced with limestone during cement manufacturing [8]. Although this integration of limestone as a partial replacement for clinker in cement production has been explored and studied by researchers and industry professionals for several decades, the widespread adoption and commercial availability of PLC in various regions occurred in the early 2000s [9]. Since its introduction, PLC has gained recognition for its sustainability benefits, including its potential to reduce carbon emissions and its comparable performance to OPC [10]. The use of PLC offers several sustainability benefits compared to OPC. First, limestone is a natural resource that is abundantly available, making it a more environmentally friendly option. Using limestone as a partial replacement for clinker reduces the need for extracting and processing large amounts of raw materials, resulting in a lower carbon footprint for PLC or lower embodied carbon content than OPC [11]. Second, the calcination process of limestone during PLC production releases less CO_2 compared to the production of clinker in OPC. It is estimated that the use of PLC can result in a nearly 15% reduction in CO_2 emissions per ton of PLC produced compared to OPC [11].

LC^3 is one of the newest low-carbon cement that has been developed and tested since 2014 as a collaboration between École Polytechnique Fédérale de Lausanne (EPFL) of Switzerland, three IITs or Indian Institutes of Technology campuses in India, and the Central University of Las Villas in Cuba. LC^3 is composed of 50% by weight of portland clinker, 30% calcined clay, 15% limestone, and 5% gypsum [12]. Using LC^3 for making concrete can reduce CO_2 emissions by up to 40 % compared to OPC because of its increased limestone content and the use of low-grade clays, which are known to be abundant in various regions of the world [12]. Other benefits of LC^3 cement include (a) resource conservation - due to its utilization of lower-grade materials such as

clay waste from the ceramic or cosmetic industry, as well as less-pure limestone, (b) high performance - similar or higher performance compared to OPC at 28 days or later, (c) cost savings - due to utilization of low-cost raw materials and minimal modifications in the production and operation of existing cement plants, and (d) fast implementation - no special training or techniques are needed to use the cement for making concrete. LC^3 can be manufactured directly as a blended cement in a cement plant or a mineral addition of limestone, calcined clay, and gypsum and can be prepared in a ready-mix plant. The limestone calcined clay mineral addition is a better alternative to adapt the clinker factor depending on the desired application.

With the continued increase in demand for cement and, subsequently, concrete for new construction and rehabilitation of existing structures, combined with stricter regulations on carbon emissions, there is an urgent need to address these conflicting challenges. The 2021 IEA report [13] estimates that nearly 4 billion metric tons of cement were produced globally in 2020. Although global cement production reached a high of 4.2 billion metric tons in 2014, it remained around the figure reached in 2021. A widely adopted strategy to reduce carbon emissions in the cement industry is to replace a portion of OPC with low-carbon alternatives or pozzolans. However, this strategy can only be successfully implemented if such replacement results in either enhancing or controlling the properties and performance of concrete made using such blended cements.

The broader adoption of low CO_2 embodied cements or the reliance on existing alternatives such as PLC and LC^3 alone cannot fulfill all the requirements for concrete's performance. Therefore, the primary objective of this study is to evaluate the potential for enhancing the performance of PLC and LC^3-based cements using BCSA in terms of physical properties while also lowering CO_2 emissions.

2. LITERATURE REVIEW

This chapter provides context and background regarding the various aspects of this study. The basis of this study is to evaluate the potential of using BCSA to improve the performance of low embodied binders. Hence, the concept of global warming potential (GWP) of cement and concrete materials is introduced first, followed by the description and previous work on different binders used in this study, such as PLC, LC^3, and BCSA. The description includes composition, hydration, performance, environmental impact, and applications of these binders. Past works on lowering the carbon emissions of such binders and their blends are also reviewed. Lastly, the scope of this study is stated in section 2.8.

2.1. Global Warming Potential of Cement and Concrete

As the demand for construction materials, mainly concrete, continues to increase, it is essential to understand the global warming potential (GWP) of cements and concrete to develop strategies to mitigate their environmental impact.

The GWP of cement measures the climate impact of cement production alone. Cement is a main component of concrete and is produced by heating limestone and other materials at elevated temperatures, which releases significant amounts of CO_2 as a byproduct. The GWP of cement accounts for the direct CO_2 emissions associated with the manufacturing process, typically expressed in CO_2-equivalent units. The most commonly used cement is still portland cement, which has a GWP of approximately 1.25 kg of CO_2 emitted per kg of cement produced [14]. However, alternative cements proportioned with SCMs, such as fly ash and slag, have lower GWPs, with some estimates suggesting GWPs of up to 50% lower than portland cement [15]. In addition, using alternative fuels and implementing energy-efficient technologies can further reduce the carbon footprint of cement production, leading to a lower GWP.

The GWP of concrete considers the emissions associated with the entire life cycle of concrete, including cement production, transportation of materials, construction, use, and end-of-life. It considers not only the emissions from cement but also other components of concrete, such as

aggregates, water, and admixtures. The GWP of concrete includes the emissions associated with the various stages of its life cycle and is also expressed as CO_2-equivalent emissions. It is also dependent on factors such as the type and amount of cement or cementitious mix used, the type and amount of aggregates used, and the distance to transport these ingredients from their manufacturing and storage to their actual production. The use of alternative cements and SCMs can significantly lower the GWP of concrete [15].

Several researchers have conducted studies on the GWP of concrete, exploring the factors influencing its carbon footprint and potential mitigation strategies. Celik et al. conducted a study in 2015 on the life cycle assessment (LCA) of self-consolidating concrete mixtures made with blended portland cements containing fly ash and limestone powder [16]. They found that high volume, or up to 55% by weight replacement of OPC with fly ash, or fly ash and limestone, produces highly workable concrete that has high 28-day and 365-day strengths and extremely high to very high resistance to chloride penetration along with low GWP for concrete production.

Sonebi et al. conducted a study in 2016 focused on the environmental sustainability of cement, concrete, and cement replacement materials in the construction sector [17]. They discussed the carbon footprint, energy consumption, and other environmental impacts associated with different materials. Their study highlighted the importance of integrating sustainability considerations into the material selection, mix design, and construction practices to minimize the GWP of concrete and promote a more sustainable built environment.

Work by Miller et al. in 2018 focused on the global impact of concrete production on water resources and discussed the indirect effects of concrete on global warming [18]. It highlighted the water-intensive nature of cement production and the associated energy consumption, which contributes to CO_2 emissions. Their study stressed the need for water-efficient practices and sustainable sourcing of raw materials to mitigate the environmental impact of concrete. Also, a case study by Yang et al. in 2018 discussed the assessment of the carbon footprint of concrete buildings in China [19]. They analyzed the GWP of various construction elements, including foundation, structure, and finishes, and found that the production of cement and concrete accounted for a significant portion of the total carbon footprint. They also recommended using

low-carbon materials, such as SCMs and alternative binders, as effective measures to reduce the GWP of concrete buildings.

Xing et al. conducted a comprehensive review in 2022 on the LCA of recycled aggregate concrete [20]. Their study highlighted the importance of considering the entire life cycle of concrete, including raw material extraction, production, transportation, use, and end-of-life. Their study emphasized the potential for reducing the GWP of concrete through the use of SCMs, such as fly ash and slag, and the optimization of mix design to minimize cement content.

Past studies have also investigated the GWP of concrete made with alternative binders [21,22]. One study compared the GWP of concrete made with an alkali-activated binder (AAB) and portland cement and found that the GWP of the AAB concrete was approximately 30% lower than that of Portland cement concrete [23]. Another study evaluated the GWP of concretes made with different geopolymers or different precursor materials and found reductions in GWPs by up to 50% compared to portland cement concrete [24]. The use of recycled materials such as recycled concrete or aggregates can further reduce the GWP of concrete. For example, using recycled concrete aggregate can reduce the GWP of concrete by up to 30%. In comparison, the use of supplementary cementitious materials such as fly ash can reduce the GWP of concrete by up to 15% [25].

The GWP of concrete is a critical concern in the construction industry due to its significant contribution to CO_2 emissions. Studies on the GWP of concrete have examined several factors, including cement production, aggregate sourcing, and concrete mix design. By considering alternative cement production methods, optimizing mix proportions, and incorporating SCMs, the carbon footprint of concrete can be reduced. Continued research and implementation of sustainable practices are essential to mitigate the environmental impact of concrete and promote a more sustainable construction industry.

Despite all the previous work on the GWP of various cement and concrete materials, no work has explored the possibility of using BCSA combined with any of the newer low embodied cements such as PLC and LC^3 to lower the GWP and carbon intensity of concrete.

2.2. Portland Limestone Cement

Cement manufacturers around the world are increasingly shifting their production from OPC to PLC. This shift is driven and encouraged not only because of the need to reduce the carbon emissions of traditional OPC but also because PLC is proving to be a better alternative to OPC [26]. However, it should be noted that the performance of PLC can be affected to a certain extent depending on where the limestone blended with PLC is mined or quarried. This is due to some impurities such as silica, alumina, and iron oxide that may be present in the limestone. These impurities can influence the pozzolanic reactivity and the formation of additional hydration products during cement hydration. They can also affect several properties of PLC, including setting time, strength development, and durability [27].

Studies have shown that incorporating limestone in PLC can extend the setting time compared to OPC [28]. This is attributed to the dilution effect caused by the presence of limestone filler, which slows down the initial hydration reactions. However, proper mix design and optimization can effectively control the setting time of PLC without compromising its overall performance. The use of chemical admixtures or adjusting the fineness of the cement can help fine-tune the setting characteristics of PLC.

The presence of limestone in PLC promotes a pozzolanic reaction in addition to the hydration of clinker minerals. The pozzolanic reaction occurs between the calcium hydroxide (CH) liberated during clinker hydration and the silica and alumina present in the limestone filler. This reaction leads to the formation of additional hydration products, such as calcium silicate hydrates (C-S-H) and calcium aluminate hydrates (C-A-H), contributing to the strength development of PLC [29]. However, the rate of strength gain in PLC may be slower in the early stages compared to Portland cement, requiring longer curing periods for optimal performance.

The main components of PLC are C_3S, C_2S, tricalcium aluminate (C_3A), and calcium aluminoferrite (C_4AF), which are similar to OPC resulting in nearly similar hydration. The hydration reactions occurring in PLC are shown below.

Alite reacts with water to form C-S-H and CH:

$$2C_3S + 6H \rightarrow C_3S_2H_3 + 3CH \quad (2.1)$$

$$2C_2S + 4H \rightarrow C_3S_2H_3 + CH \quad (2.2)$$

These reactions are referred to as the silicate reaction. Then, C_3A reacts with gypsum, a calcium sulfate source, to produce ettringite, which is referred to as an aluminate reaction.

$$C_3A + 3C\bar{S}H_2 + 26H \rightarrow C_6A\bar{S}_3H_{32} \quad (2.3)$$

The small quantities of C-S-H and ettringite produced at an early age are responsible for compressive strength, while the continued hydration of alite results in additional C-S-H formation at an intermediate or later age. Belite reacts at a very slow rate compared to alite but forms the same hydration products around 28 days. The reaction of belite with water to form C-S-H also leads to some improvement in compressive strength at later ages.

The reaction of C_4AF in PLC is relatively slower compared to that of C_3A. However, C_4AF reacts with gypsum to form a trisulfate or AFt phase, which is converted into monosulfate or AFm phase once the sulfate has been consumed.

When compared to OPC, a secondary hydration reaction occurs after all the sulfate ions have reacted. At this stage, ettringite reacts with the remaining C_3A to form monosulfate ($C_4A\bar{S}\ H_{12}$) [30].

$$2C_3A + C_6A\bar{S}_3H_{32} + 4H \rightarrow 3C_4A\bar{S}\ H_{12} \quad (2.4)$$

Thermodynamics models suggest that this reaction is affected by the calcium carbonate ($C\bar{C}$) in limestone [31]. If $C\bar{C}$ is present in sufficient quantities, the remaining C_3A does not react with ettringite but with $C\bar{C}$ after the depletion of sulfate. Furthermore, monocarboaluminate ($C4A\bar{C}H11$) and hemicarboaluminate ($C4A\bar{C}0.5H12$) phases are formed instead of a monosulfate phase [32,33].

$$C_3A + C\bar{C} + 11H \rightarrow C_4A\bar{C}H_{11} \quad (2.5)$$

$$C_3A + 0.5\ C\bar{C} + 0.5\ CH + 11.5\ H \rightarrow C_4A\bar{C}_{0.5}H_{12} \quad (2.6)$$

The use of PLC has shown positive effects on durability properties, making it suitable for structures exposed to aggressive environments [8]. The incorporation of limestone filler enhances the resistance of concrete to sulfate attack, chloride penetration, and alkali-silica reaction. The refined pore structure and reduced permeability of PLC contribute to increased resistance against deleterious agents. Furthermore, the utilization of PLC in cement production reduces CO_2 emissions compared to traditional Portland cement. By partially replacing clinker, which is responsible for significant CO_2 emissions during production, PLC helps mitigate the environmental impact associated with cement manufacturing.

PLC generally exhibits similar workability to Portland cement [34]. However, adjustments may be required to maintain consistent performance due to variations in limestone characteristics, including particle size distribution and specific surface area. The presence of limestone filler affects the water demand and rheology of fresh concrete. Proper mix design, including adjustments to water-to-cement ratio and fine aggregate content, along with quality control measures, are essential to ensure the desired workability and consistency of PLC-based concrete mixtures.

PLC can be used in a wide range of concrete applications, including buildings, infrastructure, and pavements. Its enhanced durability characteristics make it particularly suitable for structures exposed to aggressive environments, such as marine environments, wastewater treatment facilities, and roadways [35].

PLC-based concrete can provide increased resistance to chemical attacks, reduced permeability, and improved long-term performance, making it a viable option for various construction projects [35,36]. The utilization of PLC aligns with sustainable construction practices by reducing carbon emissions and preserving natural resources. The use of PLC can contribute to achieving green building certifications, meeting sustainability targets, and supporting environmentally responsible construction practices.

PLC can be blended with other supplementary cementitious materials, such as fly ash or slag, to further enhance performance and optimize sustainability benefits. Combining PLC with these materials allows for a synergistic effect, providing increased strength, improved workability, and

enhanced durability properties. Blending PLC with supplementary cementitious materials also offers a potential solution for utilizing industrial by-products, reducing waste, and maximizing resource efficiency in cement production [37].

PLC offers a viable alternative to traditional Portland cement, providing several advantages in terms of properties, performance, and sustainability. The addition of limestone filler influences the setting time, strength development, and durability of PLC-based concrete. The utilization of PLC results in comparable or enhanced mechanical properties and improved resistance to aggressive environments. Furthermore, PLC contributes to the reduction of carbon emissions and the conservation of natural resources. Proper mix design, quality control, and adjustments to accommodate limestone variations are essential to ensure consistent performance. Continued research and field studies are encouraged to explore the long-term performance and specific applications of PLC in different environmental conditions.

2.3. Limestone Calcined Clay Cement (LC^3)

Calcined clay, also known as metakaolin, is an SCM that can be used in the production of low CO_2 cement. It is produced by heating natural clay minerals, typically kaolinite, to temperatures between 600 to 800°C, resulting in the transformation of the clay into a reactive and amorphous material. Pure metakaolin is used in the paper treatment, ceramics, and refractory sectors, where color and purity requirements are very high. As a result, it is usually sold at approximately three times the cost of cement [38]. Therefore, pure kaolinite clay cannot be used to produce most of the cement available on the market. However, for the cement industry, the requirements for clay are not very stringent, so the use of pure metakaolin is not needed. The precise amount of kaolinite present in calcined clay used for making LC^3 cement can vary depending on the specific formulation and manufacturing process. However, typically, the calcined clay used in LC^3 cement contains a considerable proportion of kaolinite. The exact percentage of kaolinite in calcined clay can depend on factors such as the quality and composition of the clay source, the calcination temperature, and the processing methods employed.

Metakaolin (AS_2) is produced during the calcination of clay containing kaolinite. Metakaolin, being a pozzolan, has reactive aluminosilicates that can enhance the physical properties of cement. It also reacts with CH and water to form C-A-S-H and stratlingite [39].

$$AS_2 + CH + 6H \rightarrow C{-}A{-}S{-}H + C_2ASH_8 \quad (2.7)$$

The reaction between the aluminates in metakaolin and the calcium carbonate in limestone forms monocarbonate (Mc) and hemicarbonate (Hc). However, in the case of PLC, the reaction between aluminates, CH, and $C\overline{C}$ does not form monosulfoaluminate but carboaluminate phases.

$$AS_2 + 0.5\ C\overline{C} + 3.5CH + 8.5H \rightarrow C4A\overline{C}_{0.5}H_{12} \quad (2.8)$$

In comparison to OPC or PLC, Mc and Hc are produced in greater quantities in LC^3, which have a positive effect on the porosity and strength gain of concrete [40].

Following are some important benefits of blending calcined clay with cement to create a low CO_2 cement [8]:

1. Pozzolanic Activity: Calcined clay exhibits pozzolanic properties since it reacts with CH produced during cement hydration to form additional cementitious compounds. These compounds, such as C-S-H and C-A-H contribute to the strength and durability of the resulting cementitious matrix.
2. Improved Strength and Durability: The incorporation of calcined clay in cement can lead to improved strength development, especially in the early stages, due to the additional formation of cementitious compounds. The refined microstructure and reduced porosity resulting from the pozzolanic reaction contribute to enhanced durability properties, such as increased resistance to chloride penetration and sulfate attack [12].
3. Carbon Footprint Reduction: The use of calcined clay as a partial replacement for cement clinker significantly reduces the carbon footprint of cement production. The calcination process for clay requires lower temperatures compared to clinker production, resulting in lower energy consumption and reduced CO_2 emissions. By replacing a portion of the clinker, which is responsible for a significant portion of CO_2 emissions in traditional

cement production, the incorporation of calcined clay helps mitigate the environmental impact of cement manufacturing.

4. Improved Workability: Calcined clay can enhance the workability of cementitious mixtures. It has a fine particle size and high surface area that contribute to improved water dispersion and lubrication, resulting in increased flowability and easier handling during construction. This can be beneficial for various applications, including concrete production and mortar preparation.
5. Compatibility and flexibility: Calcined clay can be blended with different types of cement, including Portland cement and blended cements, offering flexibility in formulation and customization. It can be used in conjunction with other supplementary cementitious materials, such as fly ash or slag, to optimize performance and achieve specific requirements.

Overall, the use of calcined clay in blending with cement offers a sustainable approach to reducing the carbon footprint of cement production. It enhances strength, durability, and workability while providing environmental benefits through the efficient utilization of clay resources and reduced CO_2 emissions.

LC^3, as introduced previously, incorporates calcined clay and limestone as major components. LC^3 cement leverages the synergistic effects of calcined clay and limestone to further enhance its sustainability and reduce CO_2 emissions compared to OPC.

Antoni et al., in 2012, studied four ternary mortar blends composed of portland cement, limestone, and metakaolin to determine the best composition for LC^3 [41]. They substituted 15 to 60% of portland cement with metakaolin and kept the limestone-to-metakaolin ratio constant at 0.50 to promote the reaction between the alumina in metakaolin and the calcite in limestone. They found that $C\overline{C}$ reacts with alumina from the metakaolin, forming supplementary AFm phases and stabilizing ettringite. They also suggested that gypsum addition should be carefully balanced when using calcined clays because it considerably influences the early age strength by controlling the very rapid reaction of aluminates.

Dhandapani et al. focused on investigating the mechanical properties of LC^3 concrete to assess its strength and performance [42]. The study revealed that LC^3 concrete exhibits favorable compressive strength and flexural strength characteristics. The incorporation of calcined clay and limestone does not compromise the overall strength of the concrete. In fact, the pozzolanic reaction between calcined clay and calcium hydroxide results in the formation of additional cementitious compounds, such as C-S-H and C-A-H, which contribute to the overall strength development of LC^3 concrete. The research emphasized that the optimal replacement level of clinker with calcined clay and limestone can be determined based on specific project requirements, allowing for customized concrete formulations with desired strength properties.

Diaz et al. in 2018 investigated the durability aspects of LC^3 concrete to evaluate its performance in an aggressive environment [43]. The study revealed that LC^3 concrete exhibits excellent resistance to chloride penetration and sulfate attack, which are common causes of deterioration in concrete structures. The incorporation of calcined clay and limestone in LC^3 enhances the long-term durability performance of the concrete. The refined microstructure, reduced porosity, and improved pore size distribution resulting from the pozzolanic reaction and filler effect contribute to the enhanced durability properties of LC^3 concrete. Overall, LC^3 concrete showcases comparable or improved durability characteristics when compared to conventional concrete, making it a sustainable choice for infrastructure projects.

Sharma et al., in 2021, conducted a comprehensive review of LC^3 cement, considering its environmental impact throughout its life cycle [44]. The study found that LC^3 significantly reduces the carbon footprint of cement production compared to conventional Portland cement. By partially replacing clinker with calcined clay and limestone, LC^3 achieves a substantial reduction in CO_2 emissions. The lower calcination temperature required for clay compared to clinker production contributes to the environmental benefits, as it leads to lower energy consumption and reduced greenhouse gas emissions. Furthermore, LC^3 cement exhibits comparable or improved mechanical properties compared to Portland cement, making it an economically viable and sustainable alternative for the construction industry.

Lin et al., in a 2022 study, investigated the effects of adding 1% and 2% nano silica by weight of LC^3 on early strength and carbonation resistance of mortar mixtures [45]. They found that a 2% addition of nano-silica led to an increase in the 1-day compressive strength of the LC^3 mixture by 55.8% compared to the mixture with nano-silica addition. However, the effect of nano-silica on mechanical strength was found to decrease with increasing curing age. Their results also indicated that nano silica could accelerate the hydration reactions, reduce the porosity, improve resistance to carbonation, and enhance the durability of LC^3.

In short, by incorporating calcined clay into the blending process, LC^3 cement achieves a significant reduction in CO_2 emissions, improved strength, durability, and enhanced workability. The use of calcined clay in combination with limestone highlights the potential of LC^3 cement as a sustainable and low-carbon alternative to traditional cement, supporting efforts to mitigate the environmental impact of the construction industry.

2.4. Calcium Sulfoaluminate Cements

CSA cements are a class of hydraulic cements renowned for their rapid setting, high early strength development, good durability, and lower carbon footprint compared to portland-based cement [46,47]. Their lower CO_2 emissions are possible because they can be produced at lower sintering temperatures and with the use of less limestone [48]. The four major phases found in a CSA-based cement include anhydrite ($C\hat{S}$), gypsum ($C\hat{S}H_2$), ye'elimite or CSA ($C_4A_3\hat{S}$), and belite (C_2S). $C\hat{S}H_2$ and CSA react to form ettringite, which imparts rapid strength and can also give the cement expansive properties, whereas C_2S provides later-age strength. The concept of using CSA as an additive was first introduced as Type A and K additive. This early work was carried out by Alexander Klein in the late 1950s and 60s to address the high shrinkage of Portland cement [49]. His research was aimed at reducing OPC's drying shrinkage. It consists of a blend of upwards of 70% portland cement, with the remaining being a combination of CSA and $C\hat{S}H_2$. The higher $C\hat{S}H_2$ content causes Type-K mortars to expand at an early age, typically around 0.05% during the first few days of hydration. This expansive phase is then followed by the drying shrinkage of Portland cement until the net shrinkage of the blended mortar or concrete is near zero. Then in the 1970s, Ost introduced a cement that was an improvement over Klein's Type K

cement [50]. It contained no Portland cement and a higher CSA content (~20%) than type K, causing this binder to exhibit rapid strength gain. The main phase in this cement was belite, with CSA being the second-largest constituent. This binder is defined as Type B or belitic CSA. In all, there are four types of CSA cements based on their composition, as shown in Table 2.1.

Table 1: Types of CSA binders [4]

CSA Type	CSA [%]	C_2S [%]	$C\underline{S}$ [%]	Other [%]
Type A – Accelerating Additive	35-45	0-20	10-30	5-55
Type B – Belitic CSA	20-30	30-60	5-25	0-35
Type C – Expansive Additive	10-20	10-30	40-60	0-40
Type K – Shrinkage Compensating Cement	1-10	30-50	1-20	20-70

Figure 1 shows a ternary diagram representing the different types of CSA cement. Typical phases besides CSA and $C\hat{S}$ include C_2S, calcite, mayenite, etc. Typical compositions of different CSA cements are shown as references. This classification was introduced at the 1st International Symposium on Calcium Sulfoaluminate in Murten, Switzerland, by Bescher and Kim [51]. This diagram illustrates that CSA cements can be thought of as a family of binders with various diverse characteristics rather than a single cement – similar to the fact that portland cements are a family of binders with different characteristics.

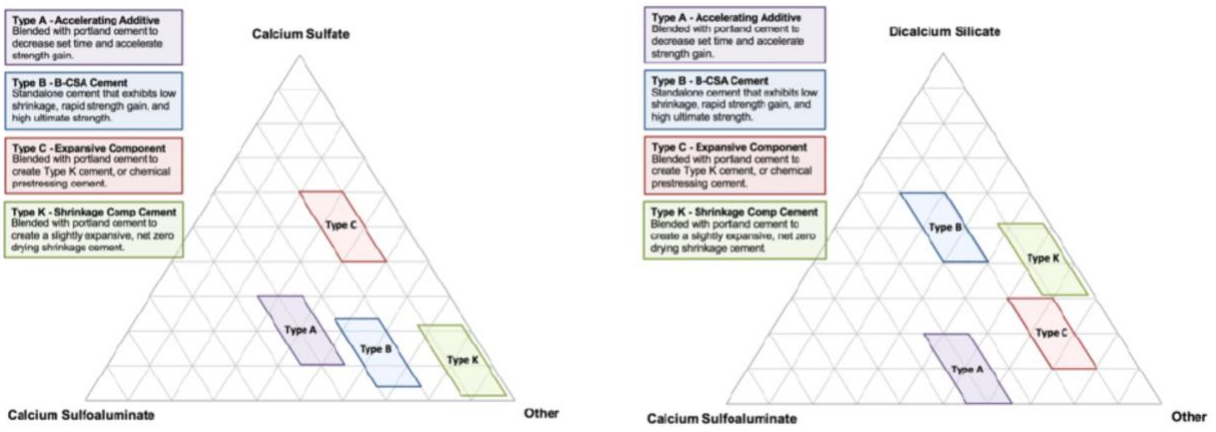

Figure 1: Proposed nomenclature for CSA binders [4]

Depending on the proportion of its components, a CSA cement can exhibit rapid setting, self-stressing, or shrinkage-compensating properties. Type A and type C cements are used as additives and blended with portland cement, while Type K cement is blended with portland cement to reduce shrinkage. Only Type B cement or B-CSA cements can be used as a single component cement. These differences in mineralogy lead to differences in the physical characteristics of the mortars. Commercial BCSA occupies a very small domain in the diagram because for a commercial product to meet regulatory approvals, early strength must be maximized, and expansion minimized.

2.5. Belitic calcium sulfoaluminate cement

BCSA cement is a type of CSA cement in which the major components include belite, CSA, anhydrite ($C\overline{S}$), gypsum ($C\overline{S}H_2$), along with small quantities of calcium aluminoferrite (C_4AF), and mayenite ($C_{12}A_7$) [4]. Sulfates play an important role in the hydration of CSA. When BCSA has a sufficient amount of sulfate, ettringite ($C_3A.3C\overline{S}.32H$) is formed as the main product of hydration. When sulfates are not available in them in sufficient quantities, monosulfate ($C_3A.C\overline{S}.12H$) is formed as a product of hydration [52]. But typically, the hydration of BCSA mostly yields a crystalline form of ettringite along with amorphous aluminum hydroxide (AH_3) regardless of the amount of sulfate present.

$$C_4A_3\overline{S} + 18H \rightarrow C_3A.\ C\overline{S}.\ 12H + 2AH_3 \tag{2.9}$$

$$C_4A_3\overline{S} + 2C\hat{S}H_2 + 34H \rightarrow C_3A.\ 3C\overline{S}.\ 32H + 2AH_3 \tag{2.10}$$

The extremely slow and later stage hydration of belite forms C-S-H or stratlingite (C_2ASH_8), depending on the presence of AH_3.

$$C_2S + 2H \rightarrow C{-}S{-}H + CH \tag{2.11}$$

$$C_2S + AH_3 + 5H \rightarrow C_2ASH_8 \tag{2.12}$$

The hydration of BCSA produces mostly ettringite compared to C-S-H [53]. This formation of ettringite occurs rapidly compared to C-S-H and has a higher degree of crystallinity, and is the main contributor to strength, especially at an early age. Ettringite is also known to have interesting features such as high surface energy and large surface area and is known to be expansive in nature

leading to a significant reduction in shrinkage compared to OPC. The ability of ettringite crystals to grow or swell and adhere to a greater amount of chemically bound water helps it to lower shrinkage compared to C-S-H [54].

BCSA, being an extremely fast setting cement, typically sets in 3 to 5 minutes if no retarder is added [55]. To increase the workability, its setting can be slowed by using various admixtures that can retard its fast-setting behavior. Citric acid is among the most common retarder, though there are other retarders, such as molasses, tartaric acid, or boric acid.

Concretes produced using BCSA cement have dense microstructure, low porosity, and low permeability, thanks to the extensive formation of ettringite during hydration [56]. Concretes produced using BCSA can reach compressive strengths as high as 4,000 psi (35 MPa) in one hour. Since less C-S-H gel is formed during hydration, dimensional changes in BCSA concretes are different from that of Portland and Type-K concretes [57]. BCSA concretes are also not prone to alkali-aggregate reactions or sulfate attacks [56]. The influence of the water-to-cement ratio and the proportions of citric acid on compressive strength were studied as a function of time, and compressive strength tests were conducted on BCSA concrete. The results supported the idea that BCSA concrete can be used efficiently [56].

2.6. CSA and Portland cement blends

Several studies in the past have evaluated the effects of blending OPC and CSA cements to understand their hydration and expansion behavior [58–62]. Chaunsali and Mondal, in 2015, evaluated the expansion and hydration characteristics of various OPC-CSA blends [52]. They found that the hydration of CSA and expansion process were completed within 7 days, irrespective of the CSA cement content of the blends. They also suggested that expansion is governed by the CSA content of the blend, and the expansion itself is due to crystallization stress caused by the supersaturation of ettringite.

Huang et al., in 2021, studied the effects of mixing different proportions of OPC and CSA cements [63]. They noticed that the hydration of CSA in a CSA-OPC blend was found to be faster than that of both belite and alite. Their results also indicated that CSA delays the hydration of belite and alite, while CH enhances the hydration of CSA. The setting time and workability of the OPC-

CSA blends also increased with increasing OPC content. The rapid-strengthening properties of CSA were maintained with a CSA content of at least 40%. In the blends containing less than 40% of CSA, no strength could be measured before 6 hours because of the low amount of ettringite produced and the slow hydration rate of belite and alite. The hydration products formed depended on the amounts of OPC and CSA. Calcium hydroxide was only identified in the blends containing 60 % or more of OPC. Unreacted belite, alite, and CSA were detected at 90 days in the blends with less than 40% of OPC, while small amounts of belite and gypsum were found in the blends containing more OPC.

Another study examined the effect of calcium sulfate on the hydration of OPC-CSA pastes [64]. It was found that without the presence of calcium sulfate, the hydration of alite was found to be delayed in the blends compared to OPC, which had a negative impact on the strength gain. The reaction of sulfate to form AFm was not found in OPC-CSA pastes that did not contain any calcium sulfate. In fact, the ettringite in their system was converted into Mc and Hc. In the presence of calcium sulfate, the OPC-CSA pastes showed the formation of monosulfate after 24 hours, while at later stages, the ettringite was converted into Hc, Mc, and AFm. Also, the calcium sulfate added in the cement pastes contributed to the strength development and the reduction of porosity.

Kothari et al., in 2022, evaluated the fresh and hardened properties of OPC-CSA cement concrete made with different CSA cements, including two types of belite-rich CSA cements [65]. They found that the addition of CSA cement resulted in shorter setting times. For instance, the setting time decreased from 187 min. to 4 min. for a 40% replacement of portland cement with CSA cement. The extent of heat released during the hydration dropped when the OPC was replaced by over 40% of CSA simply due to the lesser extent of ettringite formation and also due to the lack of available sulfates. Their study also showed that additional ettringite was formed due to the delayed reaction of C_3A. A renewed formation of C-S-H and CH occurred due to the delayed reaction of belite. Also, blends containing at least 40% of CSA cements showed lower shrinkage compared to OPC at all ages. In contrast, blends containing less than 40% of BCSA or CSA exhibited a higher shrinkage compared to OPC while still achieving a comparable strength compared to OPC [65].

2.7. Blended cements containing belite, alite, and ye'elimite

A study by Chitvoranund et al. in 2015 investigated the hydration of a blend consisting of calcined clay and alite-CSA cement composed of 50% alite, 10% ye'elimite, and 14% belite [66]. They found that the addition of clay led to a reduction in the amount of portlandite and ettringite and an increase in the amount of monosulfate and C-S-H. They also showed that mixing alite-CSA with 10% of calcined clay increased the volume of hydrated phases and reduced the porosity after 28 days leading to improvements in compressive strengths.

In 2017, Pedersen et al. conducted a study on blended CSA cements prepared by replacing 20% of CSA cement with different SCMs, such as metakaolin and limestone [67]. The researchers evaluated five different ratios of metakaolin to limestone. Despite the absence of portlandite in the blends, both limestone and calcined clay contributed to the hydration process. Notably, limestone was observed to accelerate the belite reaction, whereas calcined clay exhibited a delaying effect on the same reaction. The addition of metakaolin and limestone resulted in increased compressive strength. However, no synergistic effect was observed between metakaolin and limestone.

Researchers at the University of Malaga in 2018 conducted a study on cements containing Belite-Alite-Ye'elimite (BAY) phases and Belite-Ye'elimite-Ferrite (BYF) phases [68]. They found that the main hydration products of these cements were monosulfoaluminate, stratlingite, katoite, and AFt. From their hydration study of pure alite, ye'elimite, and anhydrite, it was inferred that the reaction of alite was retarded up to 7 days after the start of hydration due to the presence of ye'elimite. Their study claimed that alite would only start to react after the hydration of ye'elimite was completed. Other notable observations included: no formation of CH; instead, the hydration of alite produced Aft, and then AFm phases and katoite were formed by the hydration of belite and the reaction between tricalcium aluminate (C_4AF) and alite. In terms of performance, they found that BAY cement achieved a higher compressive strength than BYF cement at all ages.

Mrak et al., in a 2021 study, investigated the influence of gypsum content on belite- and ye'elimite-rich BCSA cements with different clinker phase compositions [69]. They found that for ye'elimite-rich BCSA cement, more ettringite is formed when the amount of gypsum is increased, leading to

higher compressive strengths. This was not the case for belite-rich BCSA cement. They also found that additional C-S-H is formed when the amount of gypsum is increased, and the space-filling properties of C-S-H are not as high compared to ettringite.

2.8. Scope

Binders made with BCSA cement and other low CO_2 embodied cements are currently not available for various field applications. Until now, BCSA cement has been used as a single component cement. However, in this study, BCSA is blended with PLC and calcined clay, both of which are low carbon cements that are readily accessible. The main limitations of these Portland-based cements are their extended setting time and low early strength.

The inclusion of BCSA with PLC or PLC and calcined clay is anticipated to reduce the setting time and provide high early age strengths, often within 24 hours, while also reducing the embodied CO_2 of the blends. Blends with higher BCSA content may also affect the dimensional changes occurring due to ettringite formation and help lower the extent of shrinkage often associated with Portland-based cements.

The uniqueness of this research lies in the prospect of improving the properties of low CO_2 embodied binders such as PLC and calcined clay using another low CO_2 embodied material - BCSA. The combinations of ye'elimite, alite, belite, metakaolin, and limestone employed in various proportions are uncommon in most cement formulations. Previous studies elucidating the performance of such blends are lacking. Therefore, the objective of this study is to further minimize the CO_2 emissions associated with PLC and LC^3-like mixes without compromising their strengths. Various proportions of low embodied CO_2 mixes are evaluated to determine the optimal ratios, maximize the properties, and strike a balance between their competing hydration reactions.

3. MATERIALS, MIX PROPORTIONS, AND TEST METHODS

3.1. Materials

In this study, commercially available BCSA, PLC, and calcined clay were used. Sand that complies with the ASTM C778 standards was used during the mortar mixing.

3.1.1. BCSA

A commercially obtained BCSA known as Rapid Set® cement manufactured by CTS Cement Manufacturing Corporation was used in this study. Figure 2 shows the diffraction pattern of unhydrated BCSA**.** Ye'elimite, belite, and anhydrite peaks can be identified.

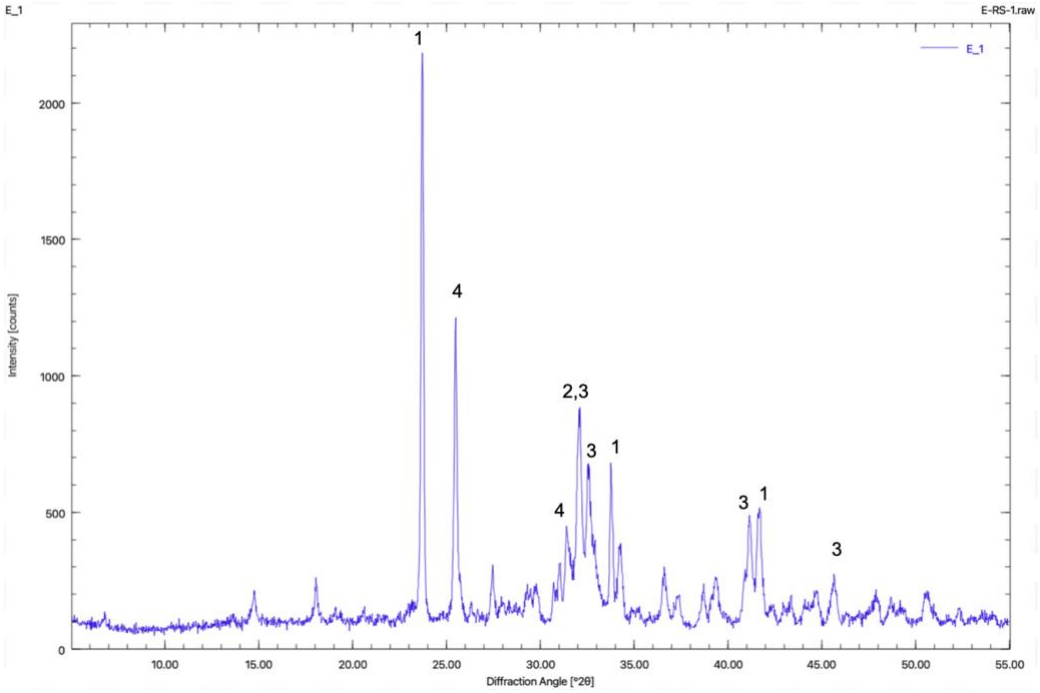

Figure 2: Diffraction pattern of unhydrated **BCSA** 1: ye'elimite (COD: 9009938) 2: belite-α (COD: 1546027) 3: belite-β (COD:1535815) 4:anhydrite (COD: 5000040) 5: ettringite (COD:9011103)

Table 2: Mineralogical (XRD) and chemical (XRF) composition of the BCSA or Rapid Set® cement [4]

Phases	**wt.-%**	**Oxides**	**wt.-%**
β-C_2S	43.6	SiO_2	14.3
α`-C_2S	4.4	TiO_2	0.58
Anhydrite	10.6	Al_2O_3	15.4
Bassanite	3.7	Fe_2O_3	0.9
Quartz	0.4	Mn_2O_3	-
Ye'elimite	27.4	MgO	1.4
Brownmillerite	1.8	CaO	49.5
Periclase	1.6	Na_2O	0.2
Gehlenite	1.7	K_2O	0.6
Perovskite (CT)	1.3	P_2O_5	0.3
Calcite	2.6	LOI	2.2
Dolomite	0.9	SO_3	14.9

3.1.2. PLC

The PLC or Type IL cement used was produced at a plant in Hannibal, MO, by the Continental Cement Company. Figure 3 shows the diffraction pattern of unhydrated PLC. Alite, belite, C_3A, and gypsum peaks can be identified.

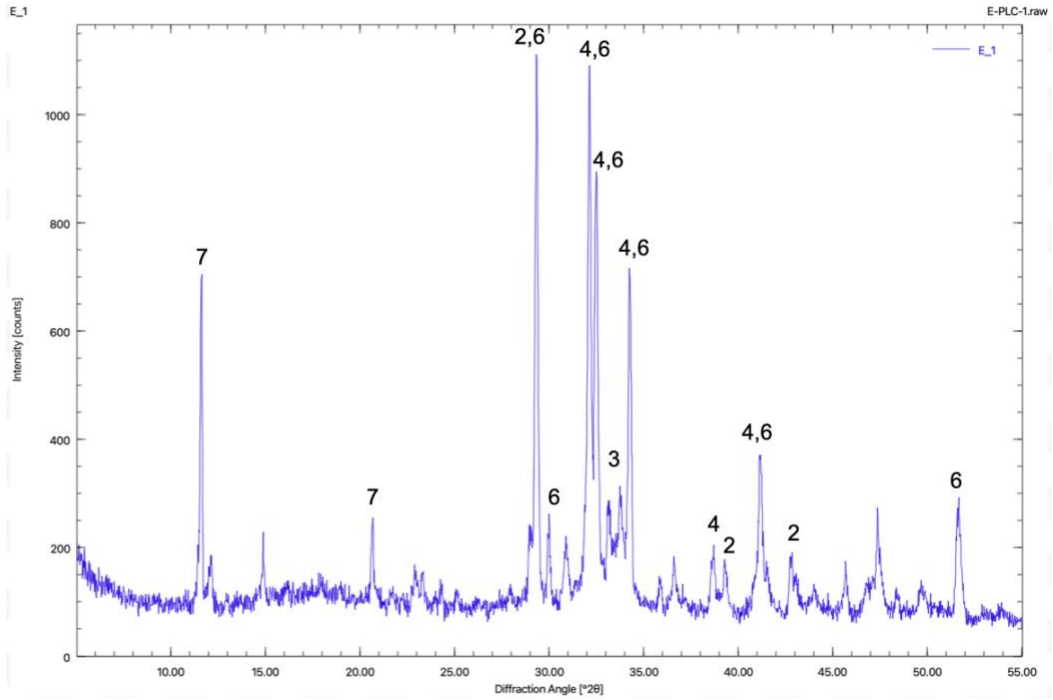

Figure 3: Diffraction pattern of unhydrated **PLC** 1: calcium hydroxide (COD: 1529752) 2: calcite (COD: 2100992) 3: C3A (COD: 1000039) 4: belite (COD: 1535815) 5: ettringite (COD: 9015084) 6: alite (COD: 9016125) 7: gypsum (COD: 9007887)

Table 3: Mill certificate phase composition for PLC

Adjusted Potential Phase Composition *(C 150)*		
C3S (%)	---	53
C2S (%)	---	13
C3A (%)	---	6
C4AF (%)	---	9
C3S+4.75*C3A (%)	---	84

3.1.3. Calcined Clay

A commercially available calcined clay called Metaforce® was obtained from GCC of America Inc. This product was defined as a Class N Pozzolan that complied with several requirements in terms of chemical composition and physical properties per ASTM C168 (Standard Terminology Relating to Thermal Insulation). For example, the maximum water requirement was 115%, and the value reported on the mill certificate was 103%. The Blaine fineness was found to be 787 m^2/kg; however, there was no limit specified per ASTM C168.

The Blaine fineness, which indicates how fine or coarse the cement is, was determined per ASTM C204 (Standard Test Methods for Fineness of Hydraulic Cement by Air-Permeability Apparatus). The Blaine fineness of the Rapid Set® used was approximately 600 m^2/kg, while for PLC, it was 434 m^2/kg per its mill certificate. A high Blaine number indicates higher fineness or smaller particle size of the cement.

Figure 4 shows the diffraction pattern of calcined clay. An XRD analysis was performed to determine the composition of Metaforce®. Quartz, kaolinite, illite, and dickite peaks can be identified.

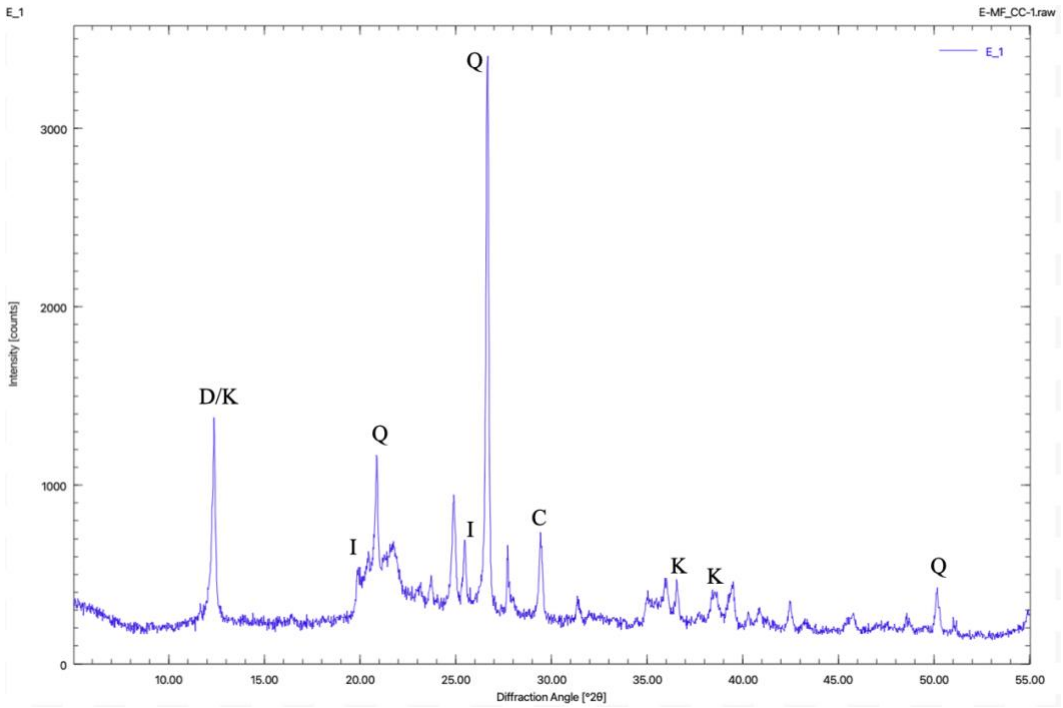

Figure 4: Diffraction pattern of Calcined Clay Q: quartz (COD:1536406) K: kaolinite (COD: 9014999) I: Illite (COD: 9009665) D : Dickite (COD: 9003081) C: calcite (COD: 2100992)

The value obtained per Rietveld refinement for the mineral composition complies with what is stated in the Mill Certificate (see Appendix 7.1).

Table 4: Mill certificate mineral composition of Calcined Clay or Metaforce®

CHEMICAL		
Item	**ASTM C618 Spec. Limit**	**Test Result**
SiO_2 (%)	-	57.1
Al_2O_3 (%)	-	26.7
Fe_2O_3 (%)	-	0.80
SiO_2 (%) + Al2O3 (%) + Fe2O3 (%)	70.0 min	84.6
MgO (%)	6.0 max	0.20
Na_2O (%)	-	0.35
K_2O (%)	-	0.24
SO_3 (%)	4.0 max	0.85
Equivalent Alkalis (%)	-	0.51
Moisture content (%)	3.0 max	0.06
Loss on Ignition (%)	10.0 max	1.92

3.2. Mixture Proportions

Two sets of cementitious mixtures were prepared in this study. The first set was composed of mixes prepared using Portland Limestone Cement (PLC) cement and 10%, 30%, and 50% by weight of BCSA. The second set of mixes is composed of three components: BCSA, PLC, and Calcined Clay (Metaforce®), wherein the proportion of CC is kept constant at 30% by weight while PLC cement is replaced with 20%, 40%, and 60% by weight of BCSA. Mixtures prepared using only PLC and BCSA cements were also prepared for comparison.

The BCSA+PLC+CC (Calcined Clay) mixes include all the components of the LC^3 cement. LC^3 is composed of Portland clinker, limestone, gypsum -that can be found in PLC- and calcined clay. So, an LC^3 mix was approximately replicated to have a point of comparison.

An additional mix called "LC^3" was also prepared, containing 30% CC and 70% PLC. The amount of calcined clay compared to the other constituents is the same as in LC^3. However, the amounts of limestone, gypsum, and calcined clay are slightly different. Table 5 shows the mix designations and their proportions in weight %s of all the mixtures used in this study.

Table 5: Mix proportions for PLC, BCSA, and CC blends used in this study

Mix Type	Mix Designation	PLC (wt.%)	BCSA (wt.%)	CC (wt.%)
Single	**PLC**	100	0	0
	BCSA	0	100	0
Binary (Set-A)	**90-PLC + 10-BCSA**	90	10	0
	70-PLC + 30-BCSA	70	30	0
	50-PLC + 50-BCSA	50	50	0
Ternary (Set-B)	**50-PLC+20-BCSA+30-CC**	50	20	30
	30-PLC+40-BCSA+30-CC	30	40	30
	10-PLC+60-BCSA+30-CC	10	60	30

Mortar samples were prepared per ASTM C305 (Standard Practice for Mechanical Mixing of Hydraulic Cement Pastes and Mortars of Plastic Consistency) for measuring setting time, flow, compressive strength, and shrinkage. The water, cement, and sand were mixed in a bowl using a mixer equipped with a paddle. The cement:sand ratio is 1:2.75, and the water-to-cement (w/c) ratio was kept constant at 0.50. The paddle can be rotated or moved in a planetary motion at fast, medium, or slow speed.

The water is placed in the bowl before mixing. The cement is added and mixed with water at a slow speed for 30 seconds. Then, sand is added gradually for 30 seconds while still mixing at a slow speed. All the components were mixed at medium speed for 30 more seconds. The mixer was stopped for 90 seconds to scrape down the mortar for 15 seconds and let the mortar stand for the remaining 75 seconds.

Paste mixtures were prepared using a lab vortex mixer for measuring the heat of hydration using calorimetry, TGA/DTG, XRD, and SEM. Table 6 shows the weights of the various mixtures prepared in this study for preparing twelve 2 in. cubes and two 1 in. x 1 in. 11.25 in. bars.

Table 6: Batch weights for twelve cubes (2 in. x. 2 in.) and 2 bars (1 in. x 1 in. 11.25 in.)

Mix type	Mix Designation	PLC (g)	BCSA (g)	CC (g)	Sand (g)	w/c ratio	Water (g)
Single	**PLC**	1334	0	0	3668.5	0.50	667
	BCSA	0	1334	0	3668.5	0.50	667
Binary (Set-A)	**90-PLC + 10-BCSA**	1200.6	133.4	0	3668.5	0.50	667
	70-PLC + 30-BCSA	933.8	400.2	0	3668.5	0.50	667
	50-PLC + 50-BCSA	667	667	0	3668.5	0.50	667
Ternary (Set-B)	**50-PLC+20-BCSA+30-CC**	667	266.8	400.2	3668.5	0.50	667
	30-PLC+40-BCSA+30-CC	400.2	533.6	400.2	3668.5	0.50	667
	10-PLC+60-BCSA+30-CC	133.4	800.4	400.2	3668.5	0.50	667

3.3. Test Methods

This section briefly describes all the test methods used in this study.

3.3.1. Flow Test and Setting Time

ASTM C1437 (Standard Test Method for Flow of Hydraulic Cement Mortar) was followed to measure the flow of the mortar mixtures using a specified flow table. A conical mold is placed on the center of the flow table. The truncated cone is filled with fresh mortar and then lifted. The flow table raised and dropped 25 times. The mortar spreads on the plate, and its diameter is measured in four directions using the caliper specified in ASTM C230 (Standard Specification for Flow Table for Use in Tests of Hydraulic Cement). The sum of the four values is the flow in percentage % relative to the original diameter of the mortar in the conical mold before tamping.

The setting time was determined per ASTM C191 (Standard Test Methods for Time of Setting of Hydraulic Cement by Vicat Needle). A thin Vicat needle is deposited and dropped on the surface of cement samples. If there is no mark on the surface, the final setting time is reached. The initial setting time can be determined well before. The Vicat needle can be dropped on the surface of the cement after the sample is made. If the needle cannot sink more than 25 mm, the initial setting time is reached.
There is also an ASTM C266 method that requires two needles. The initial and final setting times are measured by using, respectively, a heavy and light weighted Gilmore needle.

3.3.2. Isothermal Calorimetry

Measurements were carried out using an I-Cal 2000 HPC calorimeter from Calmetrix, Inc. The heat released by the cement pastes was monitored during the first 24 h of hydration. The heat generated is conducted to a heat sink after passing through heat flow sensors. The 2-channel calorimeter is linked to a computer using a USB cable. The data collection software used was CalCommander. The thermal power (mW/g) and cumulative heat release (J/g) can be displayed by the software.

10 grams of cement were mixed with 5g of water in small plastic containers by using a lab vortex mixer. Before running the experiment, the cement and water were conditioned separately in the calorimeter at 23°C for 24 hours.

3.3.3. Length-Change

Changes in lengths of the mortar bars were measured per ASTM C-157 (Standard Test Method for Length Change of Hardened Hydraulic-Cement, Mortar, and Concrete). Mortar or concrete samples undergo dimensional changes over time due to the loss of water and the formation of expansive phases during the curing process. The lengths of the samples may increase or decrease over time depending on the type of binder and the nature of curing, leading to either expansion or shrinkage. In this study, the length-change measurements were made using the recommended dial gauge on two replicates for each mix. All the mixtures were air-cured, and their readings were taken at 1, 4, 7, 14, and 28 days. A reference bar was used to set the dial gauge to zero. The length change percentage at a given age is calculated with this formula:

$$L = \frac{L_x - L_i}{G} \times 100 \quad (3.1)$$

Where L_x is reading at x age, L_i is the initial reading. G is the nominal gauge length. It can be equal to 250 or 10, depending on the size of the molds used. In our case, G is equal to 10.

3.3.4. Compressive strength

Compressive strengths were measured per ASTM C109 (Standard Test Method for Compressive Strength of Hydraulic Cement Mortars). 2"×2" cubes were made in metallic molds. Two cubes were broken with a press at 1, 7, 14, and 28 days. The two values are averaged to obtain the compressive strength at each age.

Additional measurements were made at 1h30 and 3 hours for the fast-setting mixes. All the cubes were cured in lime-saturated water.

3.3.5. X-Ray Diffraction (XRD) and Rietveld analysis

XRD is a technique that involves exposing a sample to a beam of X-rays and measuring the intensity and angle of the diffracted X-rays that are scattered by the atoms in the sample. This technique is used for identifying and quantifying the various crystalline phases present in a sample. In this study, powdered samples from each mix were scanned and analyzed using a Bruker® D2 Phaser bench-top X-Ray Diffractometer equipped with a Cu-kβ source of radiation and a Scintillator detector. This analysis aimed to evaluate the phases formed during the hydration of various mixes prepared in this study using PLC, BCSA, and Calcined Clay. For each mix, the samples were analyzed before their hydration (in their raw or unreacted form) and at two levels of hydration - 7 and 28 days. Each sample used for XRD was prepared by either crushing or forming a powder that passed through a 200 mesh (75 microns) sieve to ensure the sample was as homogeneous and well distributed as possible. A well-distributed sample can ensure that the X-rays can interact with the atoms in the sample more uniformly, leading to a more representative diffraction pattern with improved quality. This improved quality is also necessary for quantifying the phases present in the sample using Rietveld analysis.

For evaluating the samples cured at 7 and 28 days, the samples were first mixed with isopropyl alcohol to stop their hydration for nearly 24 to 48 hours and were then dried and crushed into small pieces. The samples were then passed through the 200 mesh (75 microns) before preparing them for scanning and analysis. An application called DIFFRAC.MEASUREMENT was used for running the scan. Each sample was scanned at an increment or step size of 0.02° 2θ for 3 seconds from 5° to 55° 2θ at 0.384° 2θ/min. The total time to scan each sample was approximately 2 hours and 10 minutes.

The phase identification and quantitative Rietveld analysis were performed with the open-source application called Profex Version 5.0.1. To verify the reliability of the results obtained from Profex, other applications from Bruker, such as DIFFRAC.EVA and TOPAS were also used for phase identification and quantification. The structure files required for the Rietveld analysis were obtained from the Crystallography Open Database (COD).

3.3.6. Thermogravimetric analysis (TGA)

TGA is used to monitor the weight loss of a sample as it is gradually heated. During heating, hydrates and minerals undergo various thermal reactions that often occur over a typical temperature range, resulting in a mass change. The mass loss percentage (TG curve) and its derivative (DTG curve) can be plotted against the temperature. The DTG curve makes it easier to identify consecutive mass losses associated with the phases present in the sample, which are indicated by peaks on the DTG curve.

TGA can identify crystalline phases and can be used to confirm XRD results. Additionally, it can identify amorphous phases, such as the C-S-H phase, which cannot be detected using XRD. C-S-H is the primary constituent responsible for compressive strength, and thermogravimetric analysis was primarily conducted to identify this phase.

The measurements were performed using a Perkin Elmer thermogravimetric analyzer "TGA 800". The samples were heated in nitrogen gas from 30°C to 1000°C at a rate of 30°C/min, with a gas flow rate of 20 mL/min.

3.3.7. Scanning Electron Microscopy (SEM)

SEM is an imaging method that can produce a high-resolution image of a sample. The surface of the sample is scanned with a beam of high-energy electrons. Depending on how these incident electrons react with the sample, the scattered electrons or rays will carry different information. An inelastic interaction produces secondary electrons, while an elastic interaction produces backscattered electrons. Secondary electrons (SEs) come from the surface of the sample. Secondary electron imaging can give more topographical information about that region of the sample. Backscattered electrons (BSEs) come from within the sample. The brightness of a BSE image varies according to the atomic number of the sample enabling the identification of different phases.

SEM can be used to study the microstructure of cement samples. Ettringite crystals, C-S-H and CH, can be observed. The observations based on the SEM images can be used to support the XRD and compressive strength results.

Thin cement pieces were examined at high vacuum using an FEI scanning electron microscope “NOVA 230 NanoSEM" equipped with an ETD (Everhart-Thornley detector) secondary-electron detector. The samples were placed in a bottle of isopropanol at 28 days to stop the hydration. The cement pieces were dried, pasted on an SEM stub, and then gold coated to make the sample conductive and prevent the charging effect.

3.4. Carbon emissions

The amount of greenhouse gasses emitted can be expressed in kg of CO_2 equivalent, which is the quantity of CO_2 that would have the same global warming impact. The Global Warming Potential (GWP) is a metric of sustainability that takes the contribution of all greenhouse gasses. It refers to the CO_2 equivalent of all the greenhouse gasses emitted per m^3 of concrete produced, a lower GWP showing a concrete mix's greater sustainability and lower CO_2 emissions.

The CO_2 emissions of an equivalent concrete mix prepared using the various cements and their blends used in this study can be calculated by proportionally adding the product of the mass percentage of each cement with its equivalent CO_2 emissions value obtained from its Environmental Product Declaration (EPD). PLC and BCSA release 846 [11] and 673 [6] kg of CO_2 per ton of cement produced, respectively, whereas the calcined clay is estimated to have a $CO_{2\text{-eq}}$ emissions value of 300 kg of CO_2 per ton.

An equivalent concrete mix is assumed to have a 6.5 sack content, which corresponds to 611 lbs./yd^3. The CO_2 emission value can be expressed in kg/m^3, knowing that 1 lb./yd^3 = 0.593 kg/m^3.

Table 7: CO_2 emissions of the binders used in this study in kg/m3

Mix	**CO_2 emissions (kg/m^3)**
BCSA	244
PLC	307
90-PLC+10-BCSA	300
70-PLC+30-BCSA	288
50-PLC+50-BCSA	275
10-PLC+60-BCSA+30-CC	177
30-PLC+40-BCSA+30-CC	190
50-PLC+20-BCSA+30-CC	202
LC[3]	200

The CO_2 emissions are reduced by increasing the percentage of cement substitution by SCMs. However, it is still essential to achieve high compressive strength. Carbon emission per unit compressive strength (or CO_2 intensity) is a sustainability index that assesses the performance of cement or concrete. The CO_2 intensity can be expressed in kg/m^3 of CO_2 equivalent per MPa of the cement blend at a given age.

$$CO_2\ intensity = \frac{CO_2\ emitted}{compressive\ strength} \tag{3.2}$$

4. RESULTS AND DISCUSSION

This chapter provides the results of all the tests carried out in this study. Since all the mixtures were prepared at a constant w/c ratio of 0.50, the flow and set times were first measured to gauge the level of workability before preparing samples for further evaluation and testing. The results of the first set of mixtures (Set-A) are described in section 4.2, while the same for Set-B are described in section 4.3.

4.1. Flow test and setting time

Figure 5 shows the flow test results per C1437 for both sets of mixes prepared in this study, i.e., blends of (a) BCSA and PLC, and (b) BCSA, PLC, and CC, as well as the BCSA and PLC mix for comparison.

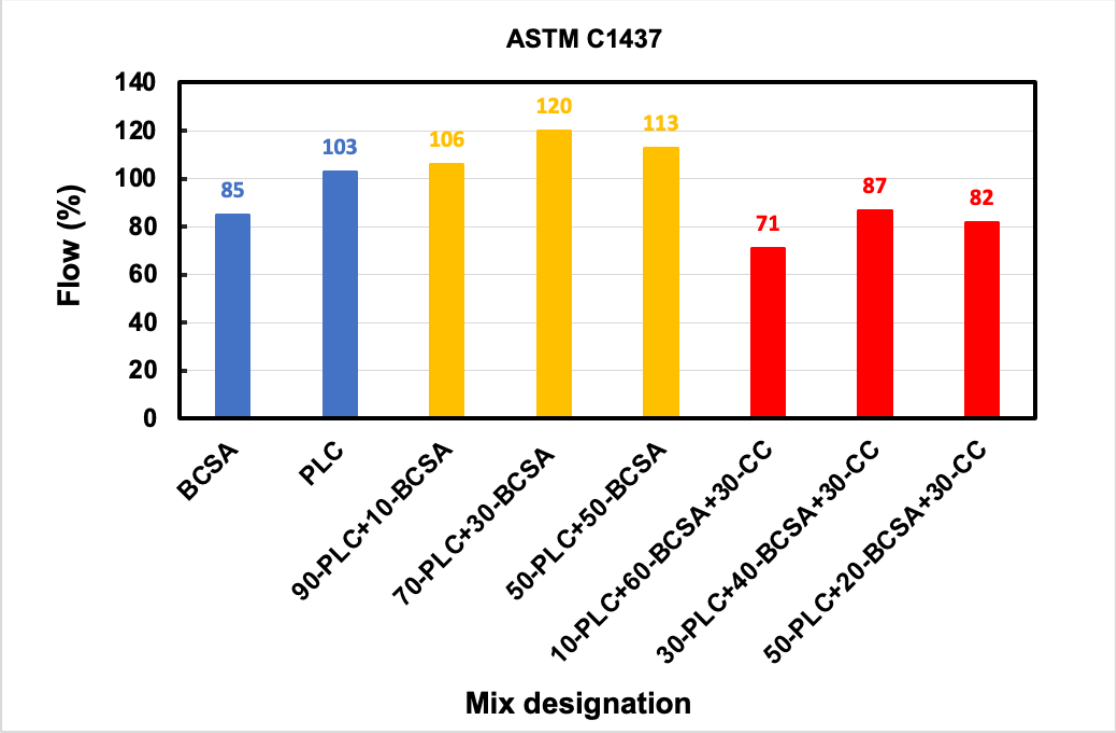

Figure 5: Flow table test results per C1437 for single (blue), binary (yellow), and ternary (red) mixes.

As shown in the figure, the BCSA mix had a flow of only 85 (%), while for the PLC mix, it was 103 (%). Per C109, the optimal flow of a mortar mix should be approximately 110±5 (%) at a specified w/c; however, both the reference mixes (BCSA and PLC) had flows below this optimal value. Despite having lower than optimal flow values, the reference mixes were still workable for casting samples at the set w/c of 0.50. The lower flow for the BCSA mix relative to the PLC mix could be due to the finer particle size of the BCSA cement compared to the PLC cement. The use of a binder with a finer particle size yields lower flow values due to an increase in the surface area of the mix compared to a binder with a coarser particle size, especially when similar w/c ratios are used. The lower flow value of the BCSA mix could also be because BCSA is inherently a fast-setting cement compared to PLC, and the mix may already be in the process of setting on the flow table even before all the measurements were taken since no retarder was added.

Based on the flow values of the reference mixes, it may seem that the flow values of the PLC and BCSA blends would be either lower than the PLC mix or in between those of the reference mixes; however, the blended mixes had higher flow values. This could be due to some agglomeration effect of the two binders, which resulted in decreased surface area of the blends. Whereas the lower flow for the PLC and BCSA blends with CC could be due to an additional increase in the surface area of the mixes due to the addition of fine CC and variations in dissolution rates of different phases present in these blends. Despite the lower flow values of the blends proportioned with CC, all the mixes were found to be workable for preparing samples.

Figure 6 shows the initial and final setting times of all the mixtures used in this study. Significant differences between the set times were observed between the BCSA and the PLC mix. The BCSA mix achieved a final set in only 32 minutes, whereas for the PLC mix, the final set occurred after 6 hours or 360 minutes. This observation is apparent due to the rapid setting behavior of the BCSA cement, whereas the PLC mix had a setting behavior that is more consistent with an OPC mix.

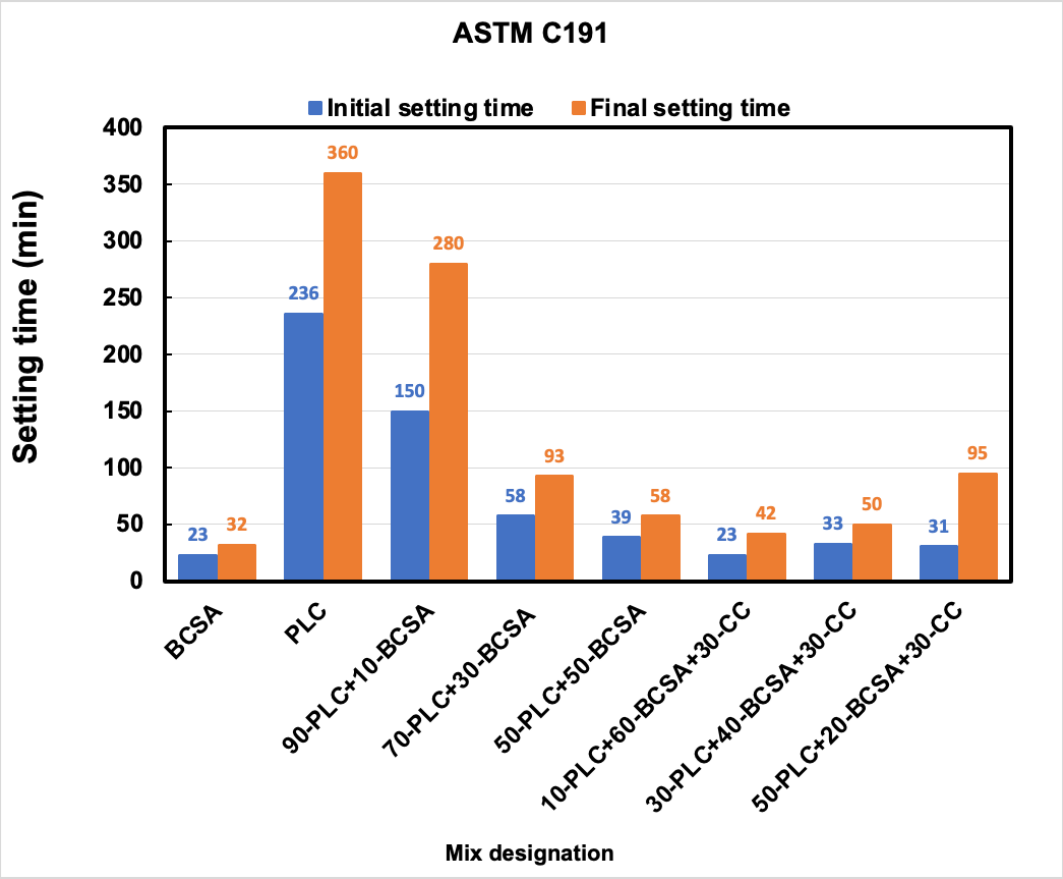

Figure 6: Setting times per ASTM C191 for all mixes included in this study

The setting times of the PLC and BCSA blends were found to be in between those of PLC and BCSA. An inverse correlation between the BCSA content of the mix and its setting time was observed. This fact was also evident in the PLC, and BCSA blends with CC. The inclusion of CC appeared to have accelerated the set times even further compared to blends with no CC, indicating that the possibility of agglomeration may not have occurred in these blends. However, the lower set times of the blends with CC could be due to their increased surface areas resulting in limited availability of free water that may have helped prolong the setting.

4.2. BCSA and PLC blends

4.2.1. Calorimetry

Figure 7(a) shows the profiles of the heat of hydration for BCSA, PLC, and their blends. These profiles were obtained at 70°F (or 21°C) using the I-Cal 2000 HPC calorimeter from nearly 0 to 24 hours of hydration, while the same is shown in Figure 7(b), but only until 5 hours.

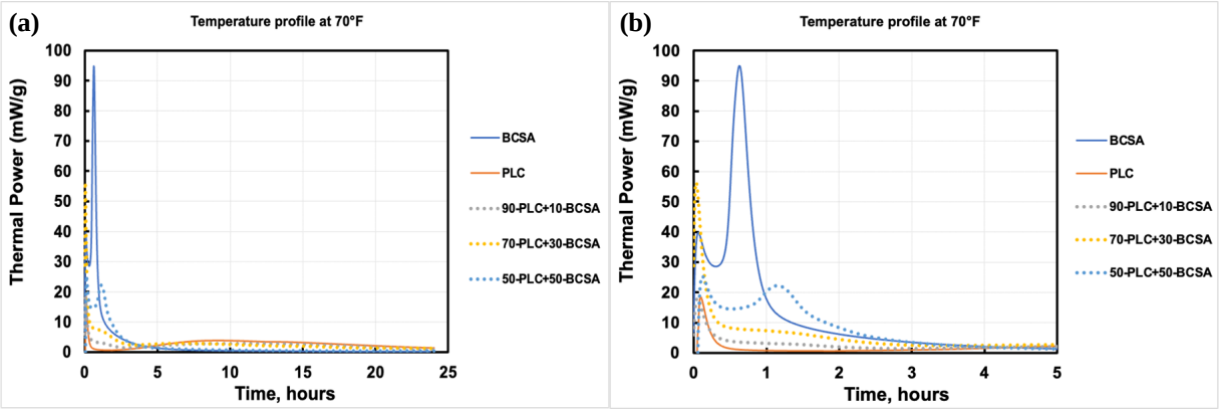

Figure 7: Heat of hydration of BCSA, PLC, and their blends from (a) 0 to 24 hours, (b) 0 to 5 hours

During the first two hours of hydration, the BCSA mix generates the highest amount of heat (blue profile), followed by the blends of BCSA and PLC, and the PLC mix, as shown in Figure 7(a).

It is common to see two exothermic peaks in a typical heat of hydration curve for any cementitious mix - these two peaks are called initial and secondary. The initial peak, seen more clearly in Figure 7(b), typically occurs within the first 30 minutes of hydration in the case of either BCSA or PLC and is also known as the dissolution peak. A dissolution peak occurs during the rapid dissolution of the calcium and sulfate phases present in the cement. For BCSA cement, the initial peak occurs due to the rapid reaction of gypsum and ye'elimite (CSA) to form ettringite with aluminum hydroxide (AH_3) as the by-product. In contrast, for PLC, the initial peak is a result of the reaction of extremely fast-reacting phases such as C_4AF and C_3A that are present in smaller proportions to form C-A-$\hat{S}$-H gel. This gel forms around other unreacted phases of the cement, such as alite, thereby limiting the access of water and controlling the rate of hydration. This results in a period

known as the dormant phase that lasts anywhere between 2 to 6 hours, depending on the amount of gypsum present in the cement.

The secondary peak, in the case of BCSA, occurs only about 30 minutes after the initial peak and is mostly due to the reaction of CSA to form ettringite, along with the remaining reaction of anhydrite and gypsum to form additional ettringite. The increased peak intensity is also due to the reaction of anhydrite to form additional ettringite. In contrast, for PLC, the secondary peak occurs several hours after the initial peak or after the dormant phase, as described earlier, and is due to the reaction of alite (C_3S) to form calcium silicate hydrate (C-S-H) gel and calcium hydroxide (CH). Since BCSA is a fast-setting cement, the secondary peak is observed between 30 minutes and 1 hour, as seen in Figure 7(b). Whereas for the PLC mix, the secondary peak is observed between 8 and 10 hours of hydration.

Figure 7(b) also shows some interesting hydration kinetics at play for the PLC and BCSA blends during the first 2 hours of hydration. The intensity of the initial peak does not correlate with the proportion of BCSA in the mix for all the blends. In other words, the intensities of the initial peaks for the PLC and 90-PLC+10-BCSA are nearly the same, whereas the intensity of the initial peak for the 70-PLC+30-BCSA blend is much higher than that of the BCSA mix. This could be due to the synergistic reaction of the fast-reacting phases in this blend. Also, in the case of the 50-PLC+50-BCSA mix, the intensity of the initial peak is in between those of the 70-PLC+30-BCSA mix and the 90-PLC+10-BCSA mix. This may indicate that for this blend, there could be some competing reactions occurring between the fast-reacting phases of these two cements that cause a reduction in the amount of heat released.

Figure 8 shows the cumulative or total heat release as a function of time for BCSA, PLC, and their blends.

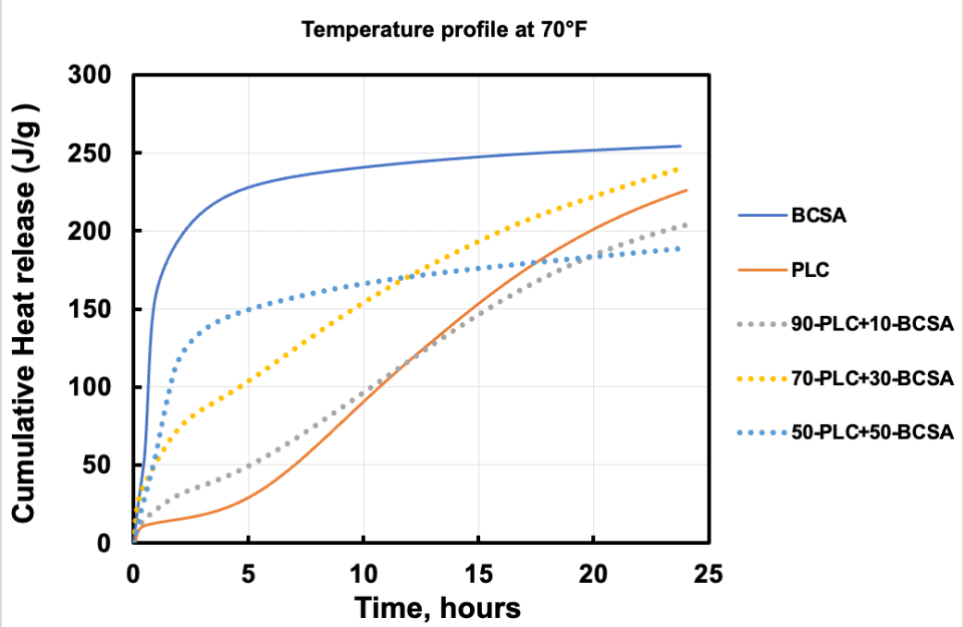

Figure 8: Total or cumulative heat release as a function of time for BCSA, PLC, and their blends

During the first 5 hours after mixing with water, the total heat released due to hydration in every mix is observed to correlate with the amount of BCSA in the mix. In other words, the total heat released is higher for mixes with higher BCSA content. This observation is apparent because the total heat released during this period is dominated by the reaction of CSA to form ettringite. In the case of PLC, the total heat released during the first 5 hours is only due to the reactions of the limited amounts of ferrite and aluminate phases, as stated previously.

After nearly 5 hours of hydration, the amount of heat released is a function of the amount and reaction of alite present in the mix. This is the reason there are two distinct slopes in the total heat release curves for the blends, although this is rather hard to observe in the case of the 50-PLC+50-BCSA mix. This is because the reaction of CSA to form ettringite releases relatively more heat than the amount of heat released by a similar amount of alite during hydration. Also, importantly the reaction of CSA to form ettringite consumes more water than the reaction of alite to form C-S-H, which leads to lower-than-expected heat release for the blends proportioned using a higher

BCSA compared to PLC, e.g., 50-PLC+50-BCSA mix. These differences in the amounts of water available for the reaction of alite also explain the differences in the total heat released at 24 hours of hydration for the blends. A more detailed study may be required to quantify the amounts of water and phase changes occurring during this period to explain this hydration kinetics. This is, however, beyond the scope of this study and may be considered as part of future work.

The main takeaways from this calorimetry study on BCSA and PLC blends are:

- Two distinct peaks - initial and secondary are observed in the heat of hydration profiles of BCSA, PLC, and their blends.
- For the BCSA mix, the initial peak occurs due to the reactions of gypsum and CSA to form ettringite. In contrast, the secondary peak, which follows shortly, occurs mainly due to the reaction of CSA and the remaining gypsum to form ettringite and AH_3.
- For the PLC mix, the initial peak occurs due to the reactions of the limited amounts of the ferrite and aluminate phases. In contrast, the secondary peak, which occurs after the dormant phase, occurs mainly due to the reaction of alite to form C-S-H and CH.
- The total heat release curves for the BCSA, PLC, and their blends show two distinct slopes depending on their blended proportions and reaction stages.

4.2.2. Shrinkage

Figure 9 shows the length-change or shrinkage results of air-cured mortar bars as a function of time for BCSA, PLC, and their blends.

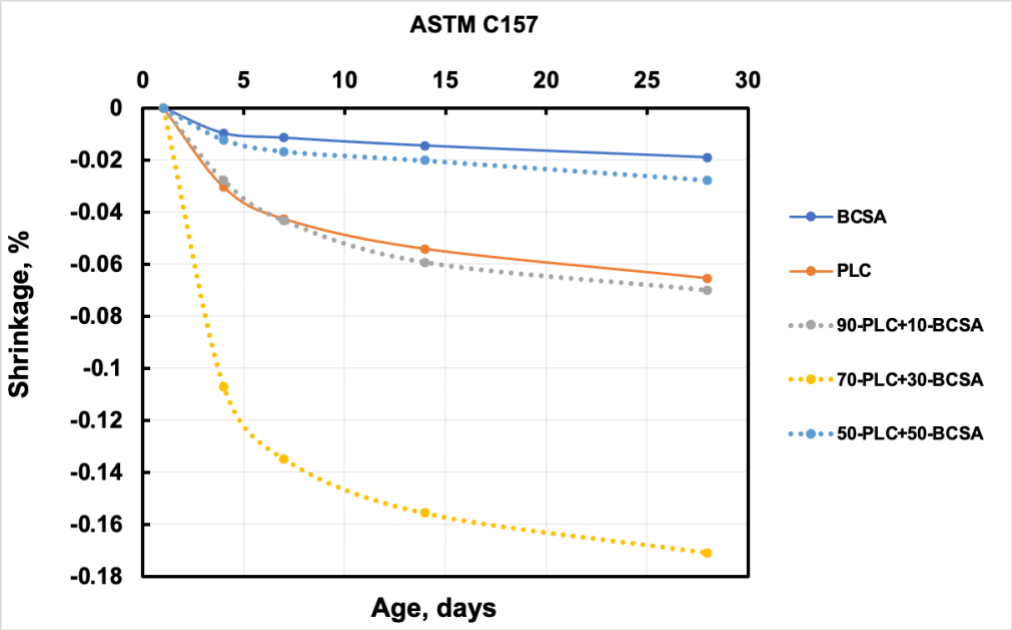

Figure 9: Shrinkage results per C157 for BCSA, PLC, and their blends

Shrinkage can occur in a mix due to loss of water during the hardening process, more so during air-curing. Since all the mixtures in this study were air-cured after they were demolded, all the measurements for length changes are essentially shrinkage results. In terms of the individual mixes, the main product of hydration of BCSA cement is ettringite, which holds a significant amount of chemically bound water. In other words, each molecule of ettringite holds 32 H_2O molecules. In contrast, the main product of hydration of the PLC cement is C-S-H, which holds only 3 H_2O molecules. This major difference in the chemical structures of the hydrated products in these cements results in significant differences in the free water that gets released from the mix as the hydration continues. This explains the main difference in the extent of shrinkage between the BCSA and PLC mixes - the PLC mix shrinks over 3 times more than the BCSA mix at 28 days.

The shrinkage of the **50-PLC+50-BCSA** mix at 28 days is found to be only slightly more than that of the pure BCSA mix. This could be possible since the majority of water in the mix might be chemically bound in ettringite, while the remaining might be bound with C-S-H and CH, and only

a small proportion of water is lost during the curing process resulting in a higher shrinkage than the BCSA mix.

The slightly higher shrinkage at 28 days for the **90-PLC+10-BCSA** mix compared to the PLC mix is negligible.

The **70-PLC+30-BCSA** mix also showed an unusually high shrinkage at all ages compared to all other mixtures. These shrinkage measurements were repeated; however, similar results were obtained. Figure 10 shows the results of the repeated length-change measurements for the **70-PLC+30-BCSA** blend.

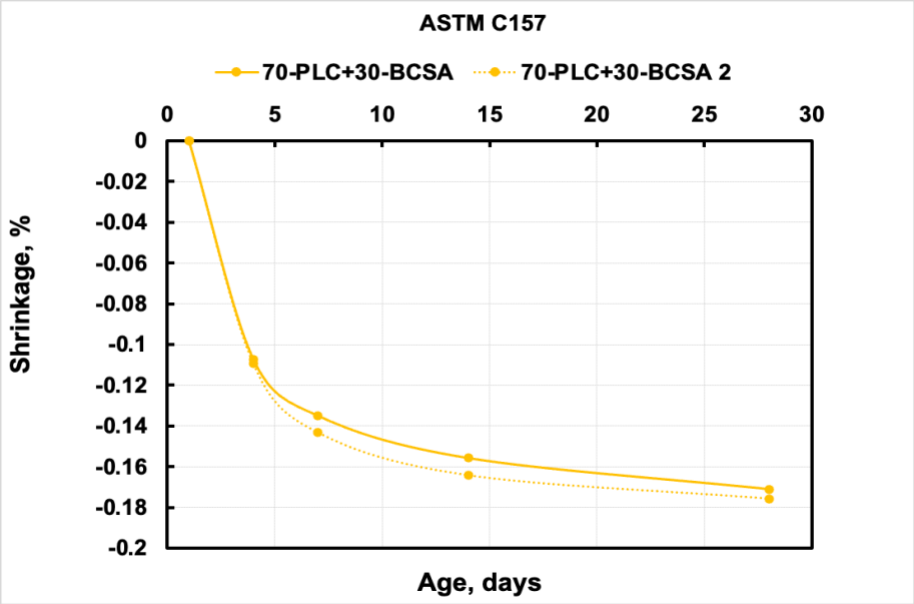

Figure 10: Repeated shrinkage measurements for the 70-PLC+30-BCSA mix

Similar results were obtained in OPC+CSA, and OPC+BCSA blends [65]. Blends containing at least 40% of BCSA or CSA were found to show a lower shrinkage compared to OPC at all ages. Blends containing less than 40% of BCSA or CSA exhibited a higher shrinkage compared to OPC but still achieved a comparable strength compared to OPC [65].

In conclusion, the BCSA mix had a relatively lower shrinkage, i.e., nearly 3 times lower shrinkage than the PLC mix at 28 days. The **50-PLC+50-BCSA** blend has the same shrinkage behavior as BCSA. The 50% of BCSA in this mix has a greater impact on shrinkage compared to the other constituents. The **90-PLC+10-BCSA** blend has the same shrinkage behavior as PLC; the addition

of 10% of BCSA does not affect the shrinkage. The **70-PLC+30-BCSA** blend shows a higher shrinkage compared to PLC. That behavior has already been observed in previously published data [65]. Some additional investigations are needed to understand the reactions leading to that high shrinkage.

4.2.3. Compressive strength

Figure 11 (a) shows the compressive strength development for air-cured BCSA, PLC, and their blends for the first 24 hours or 1 day, while Figure 11 (b) shows the same for up to 28 days.

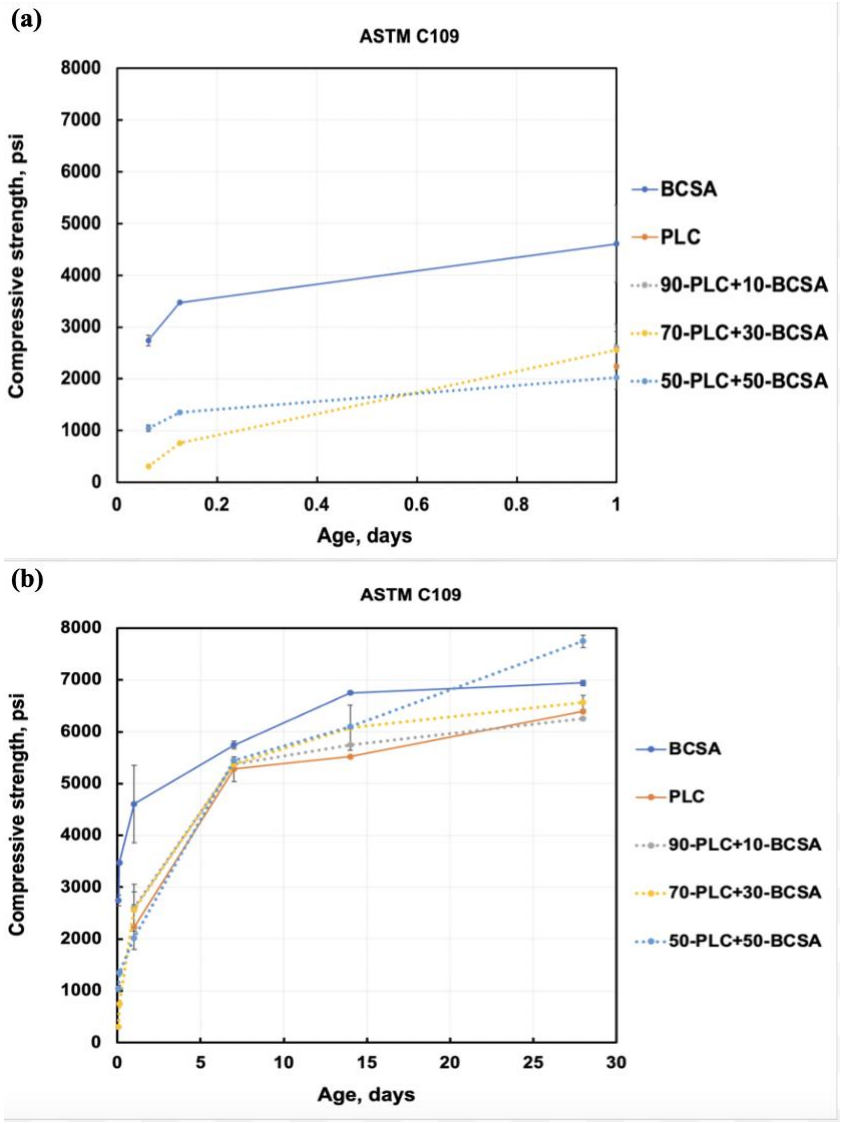

Figure 11: Compressive strength results per C109 for BCSA, PLC, and their blends for (a) for the first 24 hours or 1 day and (b) up to 28 days

From Figure 11(a), it is noted that during the first 24 hours, strengths could be measured only for mixes with at least 30% BCSA, which include only three mixes - 70-PLC+30-BCSA, 50-PLC+50-BCSA, and BCSA. This is due to the fast hydration of CSA to form ettringite, which is responsible for this very early-age strength. This is also the curing duration during which the rate of hydration of CSA is at its maximum, as evidenced by the reasonably high strengths reached by the mixes in proportion to their BCSA contents. Mixes with higher proportions of PLC (70+ %) do not hydrate as fast as those with BCSA since the rate of hydration of C_3S to form C-S-H is not as fast compared to that of CSA to form ettringite, as stated previously. In fact, at this early stage of hydration, most of the PLC-based mixes are in their dormant stage of hydration. The two blended mixes, which achieve at least 2,000 psi in 1 day, may prove to be useful for applications that require concrete mixes where very early-age strengths along with low embodied CO_2 or GWP are required.

From Figure 11(b), it is noted that between 1 and 7 days of curing, the strengths of all the mixes with PLC converge to approximately 5,400 psi. Although it may be a coincidence that these mixes achieve similar strengths at 7 days, the increases in strengths are due to the acceleration of hydration of C_3S to form C-S-H. This is the time interval during which the hydration of C_3S is at its maximum, as evidenced by the steep increases in strengths for all PLC-containing mixes. During this time interval, the rate of hydration of CSA reduces for the BCSA-containing mixes and appears to reduce further beyond 7 days and until nearly 14 days of curing.

Between 7 and 14 days, the increase in strengths observed for the PLC and BCSA blends is primarily due to the additional hydration of C_3S and the small amounts of CSA still available in these blends. Depending on the availability of aluminates present, some portion of the CH (a byproduct of the hydration of C_3S) may also take part in forming additional ettringite leading to further gains in strength [46, 47] as seen in Figure 11(b). This secondary hydration of CH to form additional ettringite continues beyond 14 days as long as reactants are available. Also, at nearly 14 days of curing, the majority of strength gain, made possible by the hydration of CSA, approaches a plateau, indicating minimal amounts of CSA may be available for further hydration in the BCSA mix.

At 28 days of curing, it is interesting to observe that two of the PLC and BCSA blends (90-PLC+10-BCSA and 70-PLC+30-BCSA) achieve similar strength as the PLC mix. However, the 50-PLC+50-BCSA mix outperforms the strengths of all other mixes, including the BCSA mix. This is due to the secondary reaction of the byproducts of the alite's hydration (CH) to form additional ettringite at curing levels beyond 7 and 14 days.

The main takeaways from the compressive strengths of BCSA, PLC, and their blends are:

- The increase in strength gains over time (until 28 days) in the BCSA, PLC, and their blends can be explained by the different rates and relative proportions of the hydration of their main phases, i.e., CSA in the case of BCSA and C_3S in the case of PLC.
- The strengths achieved by 24 hours (1 day) are primarily due to the hydration of CSA, while the strengths achieved around 7 to 14 days are primarily due to the hydration of C_3S.
- The secondary hydration of CH to form additional ettringite beyond 7 days of curing also contributes to further strength gains for PLC and BCSA blends.
- Very early-age strengths (up to 1 day) could only be measured in PLC and BCSA blends with at least 30% BCSA, and
- The mix that achieved the highest compressive strength at 28 days was the 50-PLC+50-BCSA mix.

4.2.4. XRD

This section highlights results from the Rietveld analysis of XRD scans of PLC, BCSA, and their blends. The discussions here are focused only on four to six important crystalline phases that were quantified in these mixes. Other important phases found in PLC, such as C-S-H, C_3A, C_4AF, and in BCSA, such as AH_3, stratlingite, etc., being mostly amorphous, could not be detected and are not included in this analysis. A complete list of phases quantified using Rietveld, as well as the full XRD scans for all of these mixes, is provided in section 6.1.

Figure 12 shows the amounts of the four main phases in (a) PLC and (b) BCSA mixes as a function of curing time. For PLC, these phases include belite or C_2S, ettringite or $C_6A\overline{S}H_{32}$, alite or C_3S, and portlandite or CH, while for BCSA, ye'elimite or CSA, and anhydrite or $C\overline{S}$ are included along with belite and ettringite.

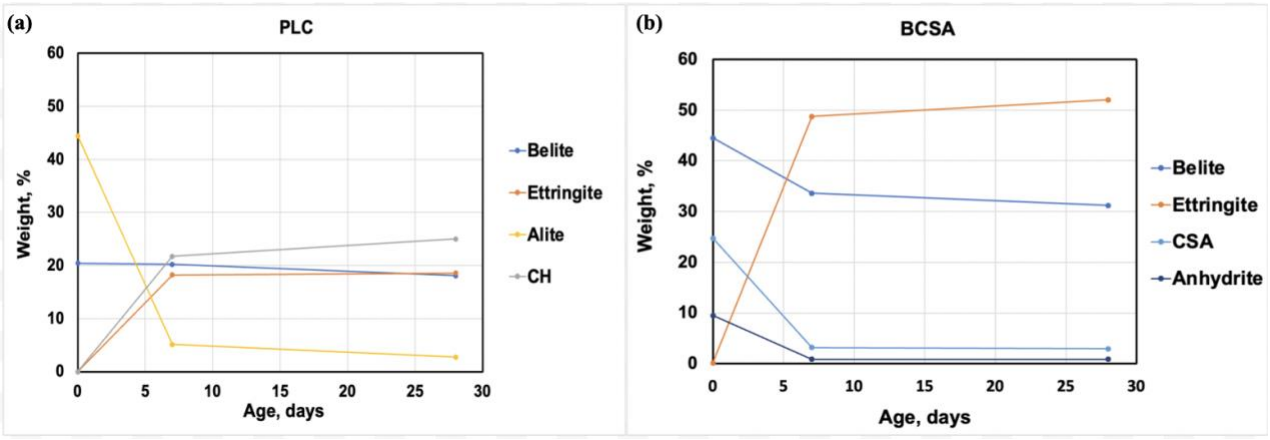

Figure 12: Variation of main phases in (a) PLC and (b) BCSA as a function of curing time

Prior to mixing with water or before hydration, the proportions of these four phases in PLC and BCSA are shown at day 0. Ettringite and CH, being products of hydration, are not present before the start of hydration or day 0. As discussed in prior sections on calorimetry (4.2.1) and compressive strengths (4.2.3), the rate of reactions for alite in PLC and CSA in BCSA are different and play a significant role in the first 7 days of the hydration process. As shown in Figure 12(a) for PLC, a significant proportion, or ~40%, of alite by weight is reacted in the first 7 days to form C-S-H (not shown) as the primary product of hydration and CH as the secondary product. Although the amount of C-S-H formed in 7 days could not be estimated using this technique, it is

interesting to note that ~22% of CH by weight is formed at this age. Since CH is not the main strength-imparting phase in the hydration of PLC, the strength of the PLC mix measured at 7 days is primarily due to the amounts of C-S-H and ettringite formed (~18% by weight). The ettringite measured at 7 days for the PLC mix is most likely due to the hydration of aluminates like C_3A and C_4AF and sulfates (SO_4^{-}) present in the pore solution. It should also be noted that only a minor amount (<1% by weight) of belite hydrates during the first 7 days of curing. This is in contrast with the hydration of belite in the BCSA mix (see Figure 12(b)), where ~10% by weight of belite is hydrated, primarily due to its reaction with the available amounts of gypsum and anhydrite to form ettringite. Also, for BCSA, a significant amount or ~80% of the available CSA is reacted (i.e., from 25% by weight to ~5% by weight) to form ettringite in the first 7 days. This leads to a very high proportion of ettringite being produced in the mix in only 7 days of curing.

Between 7 and 28 days of curing, additional C-S-H (not shown) and CH are formed in the case of PLC, albeit at a relatively slower rate as the hydration proceeds. This fact is observed from the gradual reduction of alite and a minor amount of belite, as well as a small increase in the amount of CH during this period. At the same time, for BCSA, a small increase in the amount of ettringite is observed, possibly due to the reaction of the remaining amount of CSA and a minor proportion of belite.

Overall, these XRD results provide a good representation of the reactions taking place in the hydration of some of the main phases in PLC and BCSA cements.

Figure 13 shows the variations of five major phases as a function of curing time for the PLC, and BCSA blends starting with (a) 90-PLC+10-BCSA, (b) 70-PLC+30-BCSA, and (c) 50-PLC+50-BCSA. The proportions of the five major phases before hydration (or at day 0) correspond with the mix proportions of these blends.

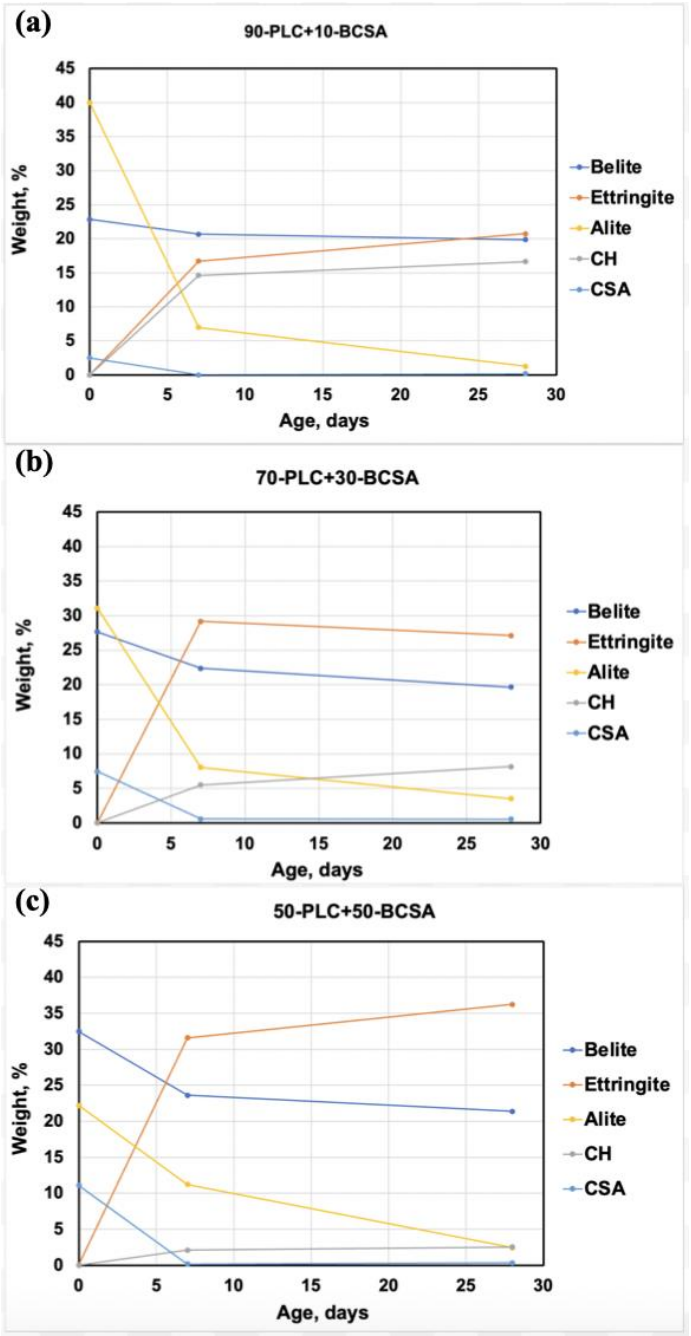

Figure 13: Variation of main phases in PLC and BCSA blends as a function of curing time

Following are some general observations from Figure 13:

- Majority of the hydration reactions involving CSA and alite occur during the first 7 days, as noted previously.

- The amounts of ettringite produced in the blends at 7 and 28 days can be correlated with the amounts of CSA and alite to a certain extent.

- At 7 days of curing, the 50-PLC+50-BCSA mix produces only ~3% additional ettringite compared to the 70-PLC+30-BCSA. There are two possible reasons for this:

  (a) different rates of hydration of CSA and alite. Mixes with higher CSA compared to alite, i.e., mixes with more BCSA than PLC, will hydrate faster relative to mixes with lower amounts of CSA, leading to the consumption of more water that can be made available for the hydration of the remaining alite to produce C-S-H and CH. Hence, in the 50-PLC+50-BCSA mix, most of the water in the mix is consumed during the hydration of CSA to form ettringite leaving less water for the hydration of alite, and

  (b) A certain proportion of CH converts back into the formation of additional ettringite [51], leading to more ettringite in mixes with higher PLC than BCSA.

The main takeaway from the XRD and Rietveld analysis is:

- Quantifying the major phases formed in PLC, BCSA, and their blends as a result of curing for 7 and 28 days sheds light on their different rates of hydration and helps explain the differences in the performance of the mixes to a certain extent.

  For example, the highest compressive strength achieved by the 50-PLC+50-BCSA mix at 28 days compared to all other mixes is most likely due to the greater proportions of both ettringite (measurable) and C-S-H produced from both primary and secondary reactions (partly measurable).

4.2.5. TGA

The main objective of carrying out the DTG analysis was to find the amount of C-S-H present in each mix to support the understanding of the variations in compressive strengths. Figures 14(a) and (b) show the DTG curves for BCSA, PLC, and their blends at 7 and 28 days, respectively.

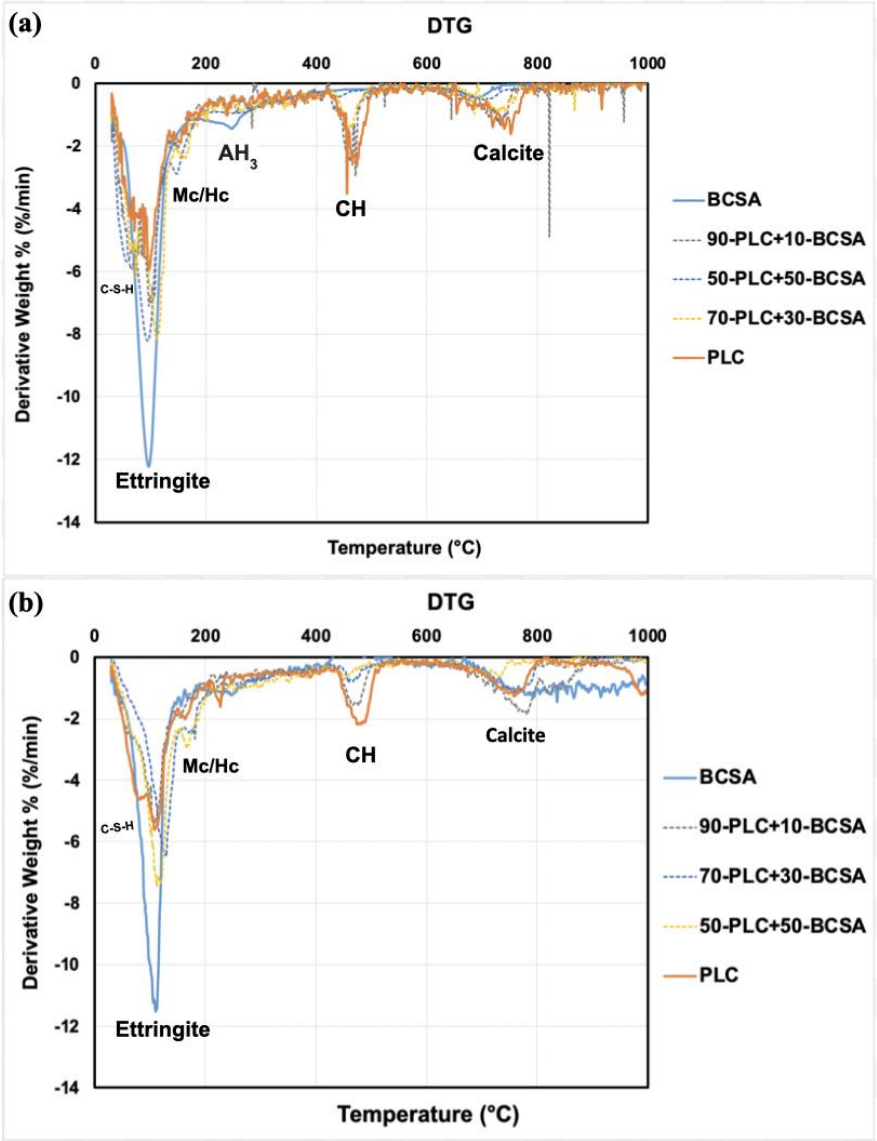

Figure 14: DTG curves for BCSA, PLC, and their blends at (a) 7 days and (b) 28 days

The peaks for C-S-H, ettringite, AH_3, hemicarboaluminate (Hc), monocarboaluminate (Mc), CH, and calcite have been identified [70]. The first set of peaks around 115°C correspond to the dehydration of C-S-H and ettringite, which are found to overlap. The second set of peaks around

170°C represents the decomposition of the monosulfate or AFm phase. The third set of peaks between 400 and 500°C represent the mass-loss of calcium hydroxide, and the fourth set of peaks identified between 750°C and 800°C indicate the mass-loss of calcite. There is also an AH_3 peak around 275°C which is visible on the BCSA curve at 7 days.

At 7 and 28 days, we can identify the ettringite peak at 96°C, which is higher for BCSA. The higher the quantity of BCSA, the greater the peak. This is consistent with the XRD results. We assume that the C-S-H peak is the one around 70°C.

The main takeaway from the TG analysis is that DTG results for ettringite and CH are consistent with XRD results. An increase in the amount of BCSA results in an increase of ettringite. In addition, an amorphous hydration product (AH_3) that could not be detected with XRD was detected in BCSA. C-S-H peak could not be identified with certainty. It is common not to be able to identify some of the hydrated phases because of the overlapping of the thermal decomposition range [70,71].

4.2.6. SEM

Figure 15 shows the SEM images at 28 days for PLC, BCSA, and the **50-PLC+50-BCSA** mix.

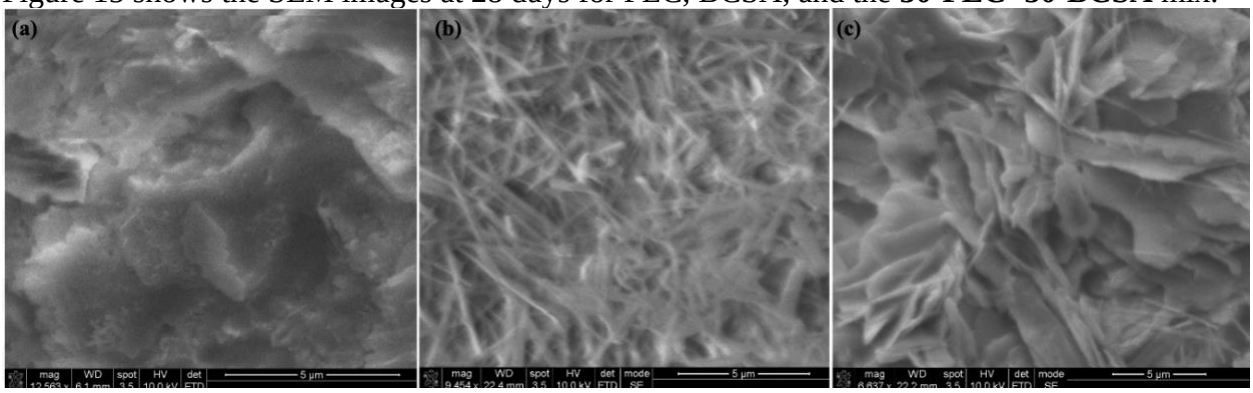

Figure 15: 28 days SEM images for (a) PLC, (b) BCSA, and (c) 50-PLC+50-BCSA

The SEM images confirm the previous findings. Plate-like C-S-H is observed in Figure 15(a), while ettringite crystals are observed in Figure 15(b). The **50-PLC+50-BCSA** SEM image mostly shows plate-like C-S-H and a few ettringite crystals. The **50-PLC+50-BCSA** mix has a denser microstructure compared to PLC. The C-S-H phases are closely packed, which may explain why this mix achieves the highest strength compared to PLC and the other PLC+BSA blends.

This is consistent with the XRD results. It has previously been concluded that C-S-H was responsible for strength at 28 days in the **50-PLC+50-BCSA** mix.

4.3. BCSA, PLC, and Calcined Clay blends

4.3.1. Calorimetry

Figure 16 shows the profiles of the heat of hydration for BCSA, PLC, LC^3, and the **PLC+BCSA+CC** blends. These profiles were obtained at 70°F (or 21°C) using the I-Cal 2000 HPC calorimeter from nearly 0 to 24 hours of hydration, while the same is shown in Figure 16(b), but only until 5 hours.

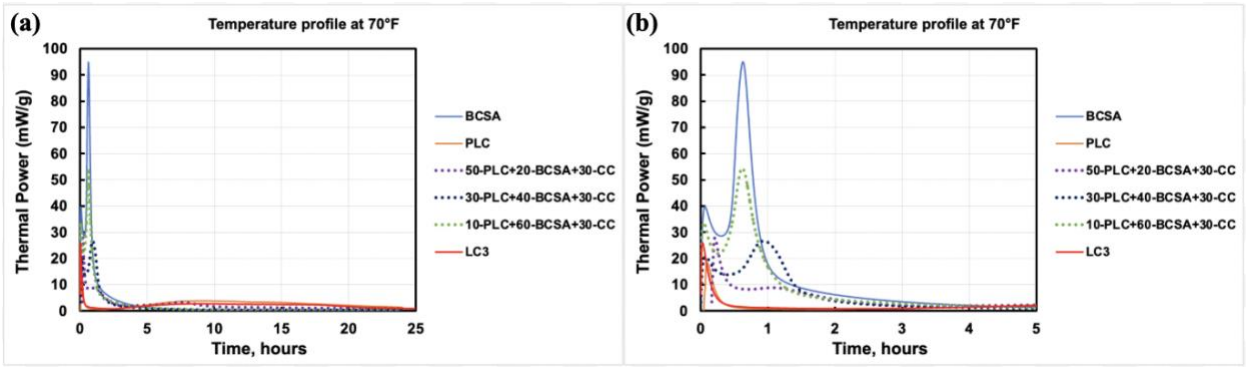

Figure 16: Heat of Hydration of LC3 and the PLC+BCSA+CC blends (a) until 24h (b) until 5h

During the first two hours of hydration, the BCSA mix shows a very high exothermic rate and reaches a maximum rate that is higher compared to all other mixes. The rate of exothermic reaction of the BCSA mix is followed by the **PLC+BCSA+CC** blends, the PLC mix, and finally, the LC^3.

As for the binary blends, two exothermic peaks are observed on the heat of hydration curve of all the cementitious mixes shown in Figure 16(a). The dissolution peak, seen more clearly in Figure 16(b), occurs within the first 30 minutes of hydration due to the rapid dissolution of the calcium and sulfate phases present in the cement.

The secondary peak, in the case of **10-PLC+60-BCSA+30-CC**, occurs only about 30 minutes after the initial peak and is mostly due to the reaction of CSA to form ettringite along with the remaining reaction of anhydrite and gypsum to form additional ettringite. As for **PLC**, the secondary peak on the LC^3 curve occurs several hours after the initial peak or after the dormant phase, as described earlier, and is due to the reaction of alite (C_3S) to form calcium silicate hydrate (C-S-H) gel and calcium hydroxide (CH). Since BCSA is a fast-setting cement, the secondary peak is observed between 30 minutes and 1 hour on the **PLC+BCSA+CC** curves, as seen in Figure 16(b).

Whereas for the LC^3 and PLC mix, the secondary peak is observed between 8 and 10 hours of

hydration.

Figure 16(b) also shows that the intensity of the secondary peak correlates with the proportion of BCSA in the mix for all the **PLC+BCSA+CC** blends. Also, the intensity of the initial peak for the LC^3 mix blend is higher than that of the PLC mix. This could be due to the metakaolin reaction.

Figure 17 shows the cumulative heat release as a function of time for PLC+BCSA+CC blends and LC^3.

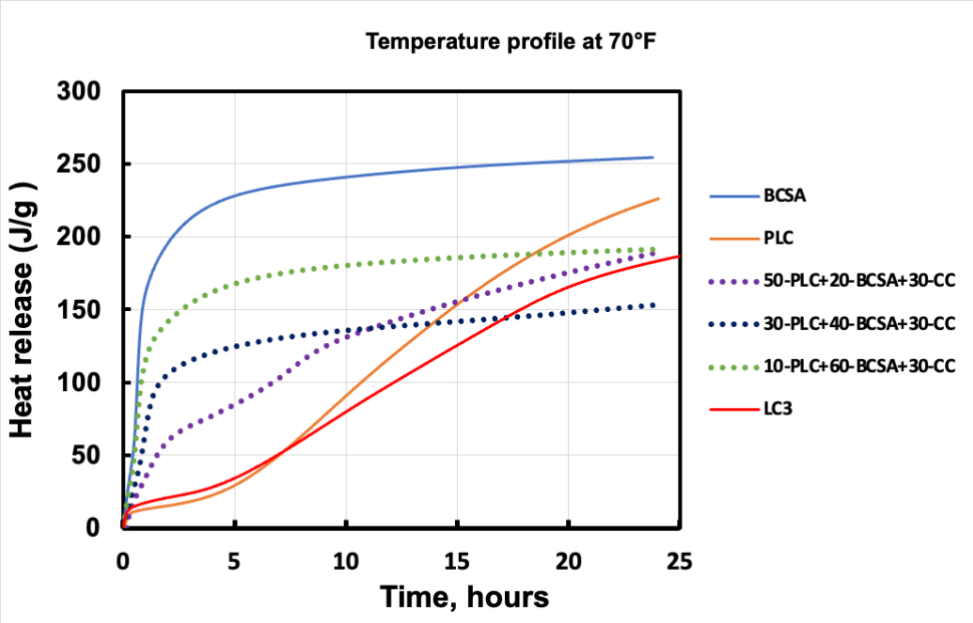

Figure 17: Total or cumulative heat release as a function of time for LC3 and PLC+BCSA+CC blends

During the first 5 hours after mixing with water, total heat released due to hydration is observed to be a function of the amount of BCSA content in the mix. In other words, the total heat released is higher for mixtures with higher BCSA content. This observation is apparent because the extent of the heat release is dominated by the reaction of CSA to form ettringite. A steep increase in heat release is still observed in the **10-PLC+60-BCSA+30-CC** and **30-PLC+40-BCSA+30-CC** during the first 3 hours, even if the amount of BCSA is reduced to half. This fact is also evident in the **50-PLC+20-BCSA+30-CC** mix with the inclusion of only 20 % of BCSA by weight.

The heat release of the **10-PLC+60-BCSA+30-CC** and **30-PLC+40-BCSA+30-CC** blends

increases gradually after 3 hours before reaching a plateau. Most of the water is consumed by the reaction of ye'elimite; the remaining water slowly leads to higher strength.
In the **50-PLC+20-BCSA+30-CC** mix, this initial increase is followed by a dormant period from 3 to ~10 hours, then the hydration of the PLC phases starts.

The main takeaways from this calorimetry study on BCSA, PLC, and CC blends are:

- Figure 16: The first peak is a dissolution peak for BCSA, PLC, and their blends. The height of the second peak is proportional to the amount of BCSA because it is due to the ettringite formation. The peak is slightly delayed for the **30-PLC+40-BCSA+30-CC.**
- Figure 17: During the first 3 hours, a very high amount of heat is generated for the BCSA mix due to the hydration of ye'elimite. After 3 hours, the heat release slowly increases for the blends containing 40 % of BCSA or more. For the blends containing less than 40 % of BCSA, the initial increase is followed by a dormant period; then, the heat release is due to the reaction of the PLC phases.
As for the binary blends, the total heat released due to hydration is higher for mixes with higher BCSA content during the first 5 hours after mixing with water. After nearly 5 hours of hydration, the amount of heat released is a function of the amount and reaction of alite present in the mix.

4.3.2. Shrinkage

Figure 18 shows the shrinkage results for BCSA, PLC, LC^3, and **PLC+BCSA+CC** blends.

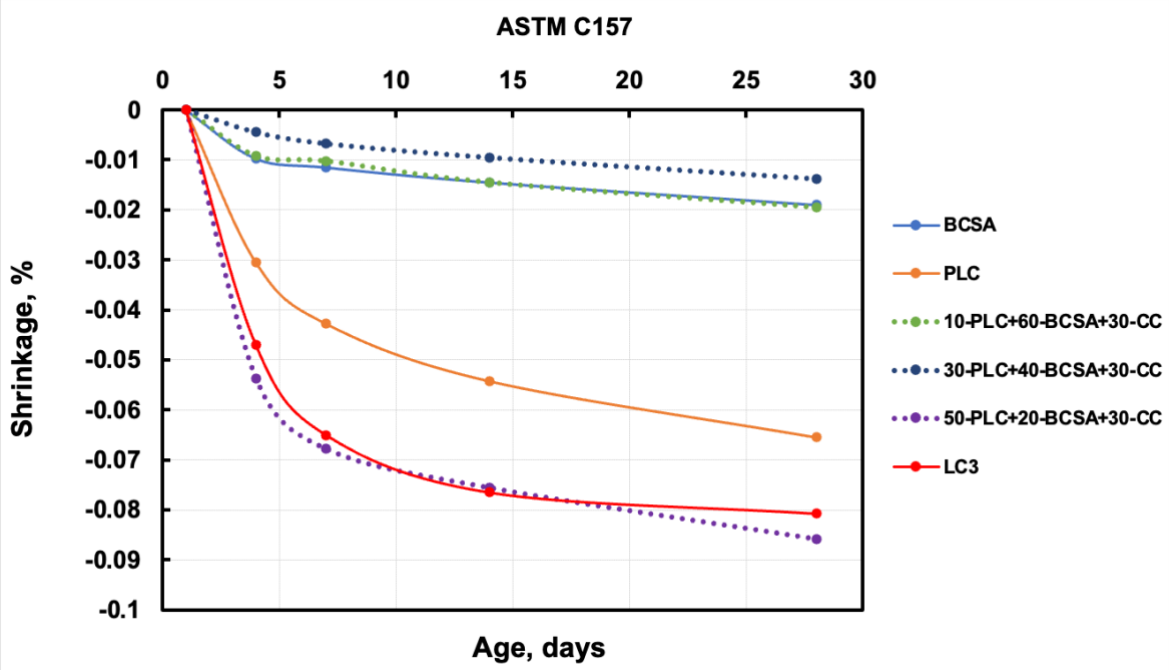

Figure 18: Shrinkage results per C157 for BCSA, PLC, LC3, and PLC+BCSA+CC blends

The extent of shrinkage for an air-cured PLC+BCSA+CC mix can depend on the proportion of BCSA due to BCSA cement's self-desiccating nature [72]. In other words, shrinkage is expected to be inversely proportional to the amount of BCSA in a PLC+BCSA+CC mix. This expectation is found to be valid for all the mixes shown in Fig. 18, with the exception of the **30-PLC+40-BCSA+30-CC** mix. This mix has a lower shrinkage compared to BCSA cement. A lower shrinkage compared to CSA cement was also observed due to the addition of up to 20 % metakaolin [73]. In the **30-PLC+40-BCSA+30-CC** blend, 30% of PLC and 30% of calcined clay enable the pozzolanic reaction of metakaolin. C-S-H gel is produced in the pores, increasing the density of the mortar and reducing shrinkage. The 40% of BCSA also contributes to reducing shrinkage.

It is observed that the **10-PLC+60-BCSA+30-CC** and BCSA shrinkage curves are almost superimposed. This mix has the same shrinkage behavior as BCSA due to 60% of BCSA. The remaining 40% of PLC and calcined clay does not affect the shrinkage properties.

We also observe that the **50-PLC+20-BCSA+30-CC** and LC^3 shrinkage curves are almost

superimposed because these blends have the same shrinkage behavior. This is because 20% of BCSA does not affect the shrinkage.

In conclusion, the PLC+BCSA+CC blends containing at least 60% of BCSA have the same shrinkage behavior as BCSA. The ternary blends containing 20% of BCSA or less have an LC^3 -like shrinkage behavior. The blends containing between 20% and 60% of BCSA can show a lower shrinkage compared to BCSA. In these blends, the pozzolanic reaction of metakaolin and the BCSA present in the blend contributes to reducing shrinkage.

4.3.3. Compressive strength

Figure 19 shows the compressive strengths of BCSA, PLC, and their blends.

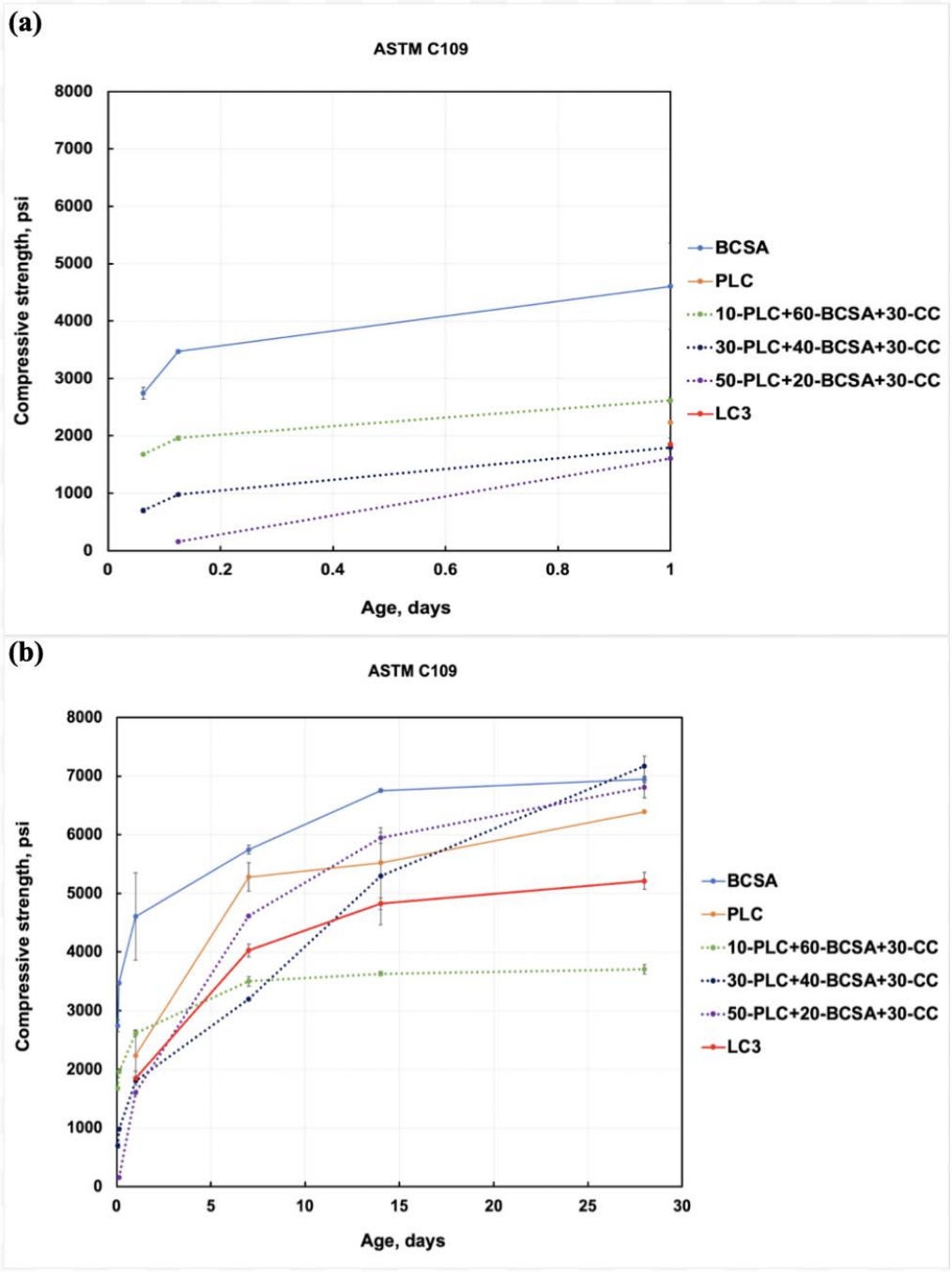

Figure 19: Compressive strength results for PLC+BCSA (a) until 28 days (b) until 24 h

Before 24 hours, strengths for the blended mixtures could be measured only for mixtures with at least 40% BCSA, i.e., for **30-PLC+40-BCSA+30-CC** and **10-PLC+60-BCSA+30-CC**. This is again due to the fast reaction of CSA to form ettringite, and the strengths of these mixtures are a function of their BCSA content. The earliest strength, although very low, could only be measured for the **50-PLC+20-BCSA+30-CC** mix at 3 hours after mixing. The mixtures with at least 40% BCSA (by weight) may prove to be useful in applications where early-age strengths are required.

At 24 hours, the **10-PLC+60-BCSA+30-CC** mix naturally shows the highest strength among other blends owing to its high BCSA content. Mixtures with higher proportions of PLC do not hydrate as fast as those with BCSA since the rate of reaction of alite to form C-S-H is not as fast compared to that of CSA to form ettringite.
Between 1 and 7 days, there is a significant increase in strength for the **50-PLC+20-BCSA+30-CC** blend compared to the other blends. The **30-PLC+40-BCSA+30-CC** mix has the highest increase in strength after 7 days. These two blends achieve similar strength as BCSA at 28 days.

Based on the above strength results, here are the main takeaways:

- The inclusion of BCSA adds some early strength. The compressive strength is proportional to the amount of BCSA before 1 day. The ettringite in BCSA provides strength for up to 7 days, but most of the ettringite is formed before 24 h.
- In the **10-PLC+60-BCSA+30-CC** mix, the 10 % of PLC cannot react with CC because all the water has been consumed to form ettringite and provide early strength. In the **30-PLC+40-BCSA+30-CC** mix, there is less BCSA, so there is more water available. The 30 % of PLC can react with CC to give additional long-term strength. In the **50-PLC+20-BCSA+30-CC** mix, more of the PLC can react with CC. LC^3 does not contain as much alite as PLC, so less C-S-H is formed. Other LC^3 hydration products, such as Mc and Hc, do not provide as much strength as C-S-H or ettringite.
- The ettringite in BCSA is responsible for strengthening the mortar until 7 days, but most of the ettringite is formed during the first 24 hours. Around 7 days, the C-S-H formed by the phases in PLC.

4.3.4. XRD

Figure 20 shows the weight percentage of the main phases as a function of curing time for **PLC+BCSA+CC** blends.

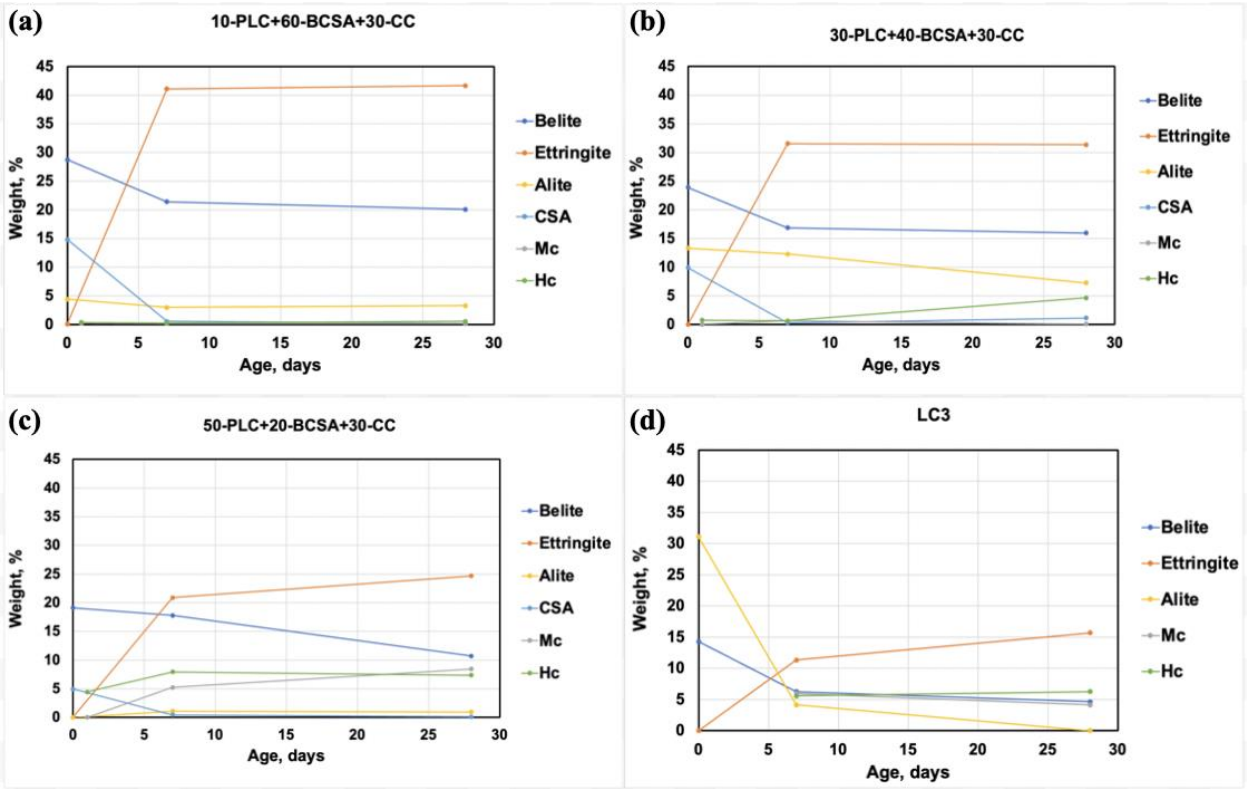

Figure 20: Amount of Belite, CSA, Alite, Ettringite, monocarboaluminate (Mc), and hemicarboaluminate (Hc) as a function of time for PLC+BCSA+CC blends and (d) LC^3

Following observations can be made using the above XRD results:

- The decrease in alite observed for the **30-PLC+40-BCSA+30-CC** blend is found to be higher compared to the **50-PLC+20-BCSA+30-CC** and **10-PLC+60-BCSA+30-CC**. That could explain why this mix achieves a comparable strength as BCSA at 28 days.
- There is little to no Mc and Hc produced in **10-PLC+60-BCSA+30-CC**. That could explain why this mix achieves the lowest strength at 28 days.
- The **50-PLC+20-BCSA+30-CC** mix contains more Hc and Mc. In LC^3, it is known that aluminates (from calcined clay and clinker) react with calcium carbonate (from limestone)

to form Hc and Mc [9]. The **50-PLC+20-BCSA+30-CC** mix also has a clinker/calcined clay ratio close to that of LC^3. The composition of this mix with the actual clinker/calcined clay ratio of LC^3 is "56-PLC+20-BCSA+24-CC*"*. That could explain why this mix achieves a comparable strength as BCSA at 28 days.

The main takeaway from the XRD and Rietveld analysis is:

- The amount of ettringite produced is a function of the BCSA content of the mixtures.
- The **30-PLC+40-BCSA+30-CC** mix had the highest decrease in alite from 7 to 28 days, meaning that more C-S-H is formed and contributes to the late age strength. We also note that Hc is produced in this blend. This shows that there is indeed a reaction between PLC and calcined clay.
- For the **50-PLC+20-BCSA+30-CC** mix, an increase in ettringite from 7 to 28 days was observed because the CH formed in the mix enhances the hydration of ye'elimite. A decrease in belite was also observed from 7 to 28 days. Some components of PLC and calcined clay enhance the reaction of belite.

4.3.5. TGA

Figure 21 shows the DTG curves for BCSA, PLC, and their blends. A sharper ettringite peak (around 100°C) is observed around the mixes that contain more BCSA. The ettringite content increases with increasing BCSA.

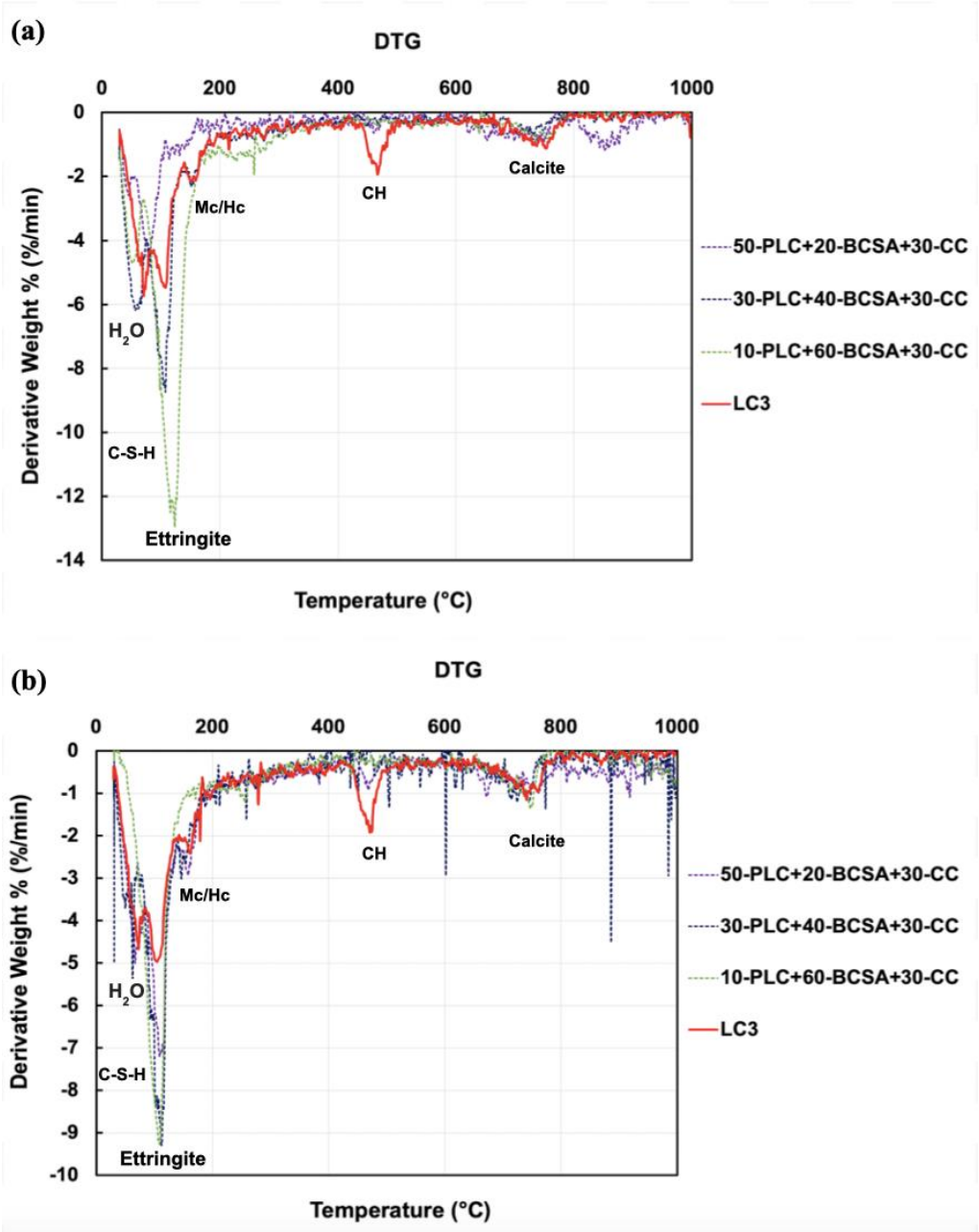

Figure 21: DTG curves for BCSA + PLC blends at (a) 7 days and (b) 28 days

The peaks for ettringite, hemicarboaluminate (Hc), monocarboaluminate (Mc), CH, and calcite have been identified [70]. The peak around 50°C, before the ettringite peak, is due to the evaporation of free water [74]. The is a peak around 850°C on the **50-PLC+20-BCSA+30-CC** curve that could be due to the decomposition of C-S-H. C-S-H transforms into wollastonite when subjected to temperatures around 800°C [48].

The main takeaway from the TG analysis is that the results are consistent with XRD results for ettringite and CH. Here again, the C-S-H peak could not be clearly identified because its temperature range of decomposition overlaps with that of ettringite [70].

4.3.6. SEM

Figure 22 shows the images of (a) **50-PLC+20-BCSA+30-CC** and (b) **10-PLC+60-BCSA+30-CC** blends at 28 days.

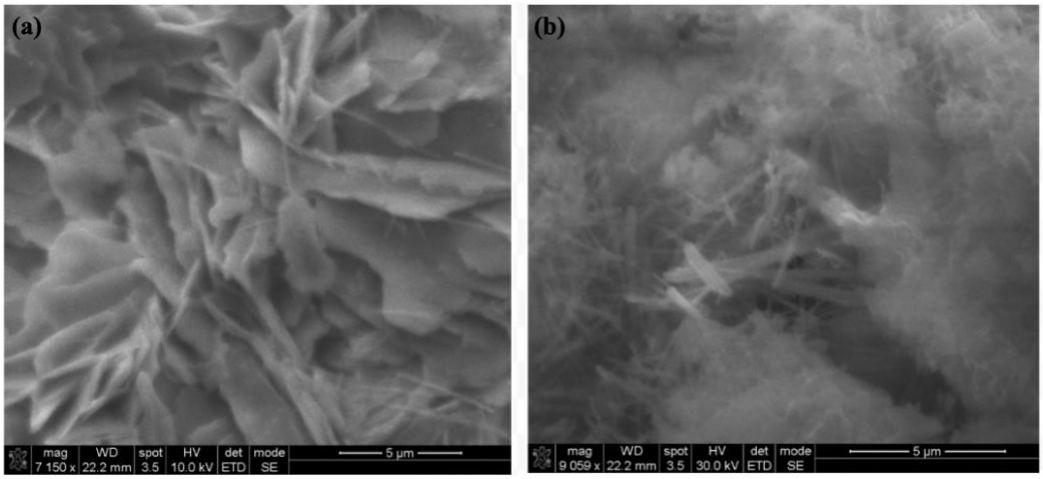

Figure 22: 28 days SEM images for **50-PLC+20-BCSA+30-CC** (a) and (b) **10-PLC+60-BCSA+30-CC**

The SEM images confirm the previous findings. Plate-like C-S-H is observed on the **50-PLC+20-BCSA+30-CC** image, while the **10-PLC+60-BCSA+30-CC** SEM image shows ettringite crystals and C-S-H gel. The **50-PLC+20-BCSA+30-CC** mix has a denser microstructure compared to the **10-PLC+60-BCSA+30-CC** mix. This is consistent with the compressive strength and XRD results. The **50-PLC+20-BCSA+30-CC** blend was found to have comparable strength with the BCSA mix at 28 days, whereas the **10-PLC+60-BCSA+30-CC** blend had the lowest strength. Moreover, it has previously been concluded that C-S-H was responsible for strength at 28 days in the **50-PLC+20-BCSA+30-CC** blend.

4.4. Calculations of Global Warming Potential

Figure 23 shows the GWPs or CO_2 emissions of equivalent concrete mixes proportioned using the same cements and blends used in this study. The CO_2 emissions of these mixes were calculated assuming that each mix has a cement content of 611 lbs./yd^3, or 6.5 sacks per cubic yard. It is observed that the mixes prepared by blending PLC and BCSA showed higher GWPs compared to the BCSA mix but lower than the PLC mix, while the blends prepared with CC or some component of LC^3 show lower GWPs than both BCSA and PLC mixes. The lowest GWP was estimated for the **10-PLC+60-BCSA+30-CC** mix, followed by the **30-PLC+40-BCSA+30-CC** mix.

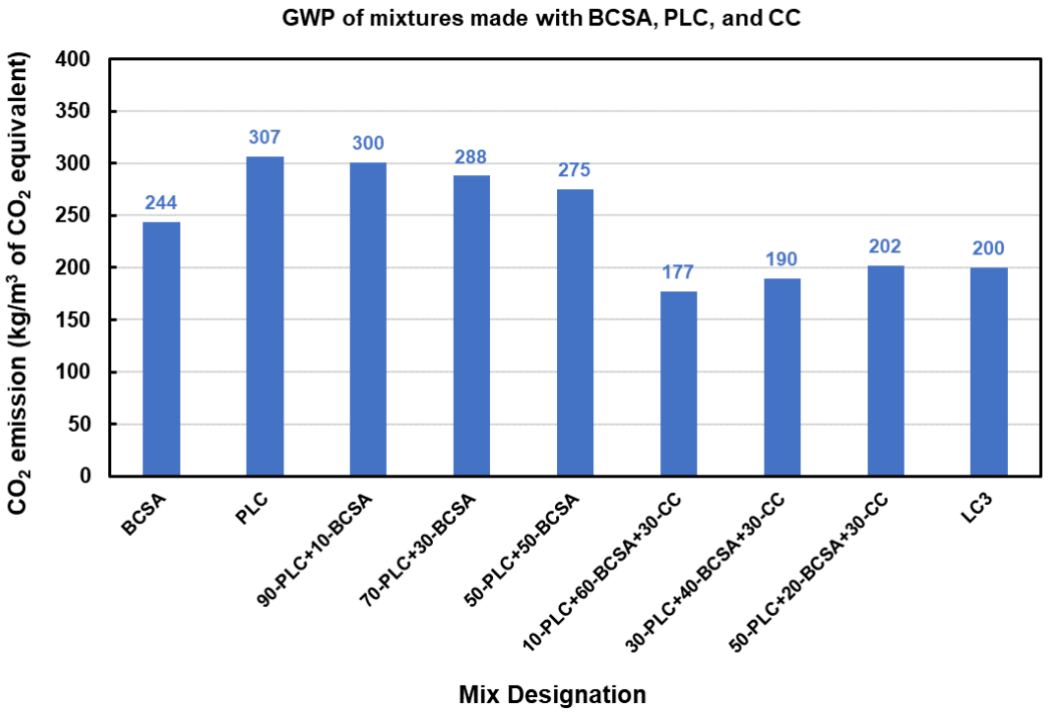

Figure 23: GWP of mixes made with either or in a combination of BCSA, PLC, CC, and their blends

Based on the GWP calculations, the amount of greenhouse gas emitted decreases with increasing BCSA amount for the secondary and ternary blends. It is suggested that if the GWP of a mix is the only criteria for the selection of a mix, then the **50-PLC+50-BCSA** and **10-PLC+60-BCSA+30-CC** are the only secondary and ternary blends, respectively, that have the lowest environmental impact.

Figure 24 shows the CO_2 intensities of all the mixes used in this study based on the compressive strength results at 28 days. The **30-PLC+40-BCSA+30-CC** mix is observed to have a lower CO_2 intensity compared to all other mixes, including the BCSA mix, while the **50-PLC+50-BCSA** mix has nearly the same CO_2 intensity as the BCSA mix. This suggests that the **30-PLC+40-BCSA+30-CC** mix can be considered the preferred mix for applications calling for the mix with the lowest CO_2 intensity at 28 days.

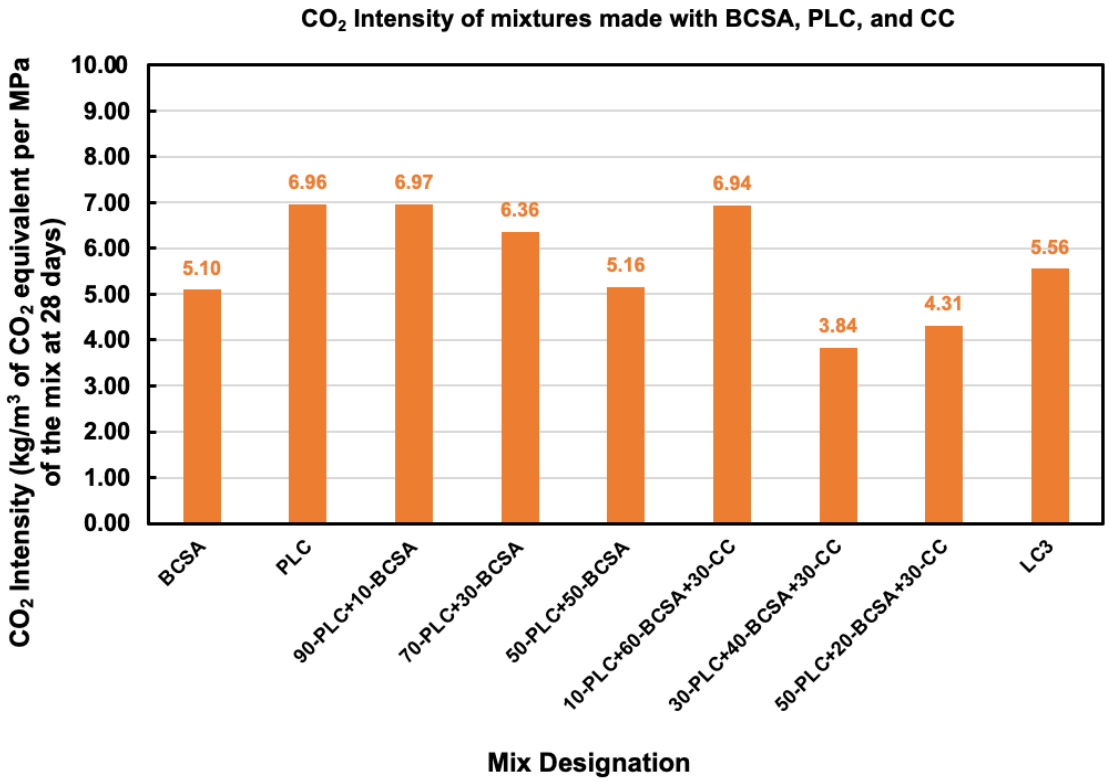

Figure 24: CO_2 intensity of concrete mixes made with BCSA, PLC, and CC based on the 28 days-strength

The **50-PLC+50-BCSA** indeed was found to have the lowest CO_2 intensity based on its performance at 28 days. However, the **30-PLC+40-BCSA+30-CC** blend was measured to have the lowest CO_2 intensity (lower than BCSA) based on its 28-day performance. It was also noted that the **50-PLC+20-BCSA+30-CC** had a lower CO_2 intensity compared to BCSA.

Figure 25 shows the CO_2 intensities of concrete mixes made with BCSA, PLC, and CC based on the compressive strength at 1 and 28 days. There is no trend observed at 1 day. However, we note that the **50-PLC+20-BCSA+30-CC** has a lower CO_2 intensity based on the 1-day strength compared to the **50-PLC+50-BCSA**, although these blends contain the same amount of PLC. This is due to the addition of calcined clay. We can see that the CO_2 intensities of the **50-PLC+50-BCSA** blend and PLC are almost equal, although this mixture contains 50% by weight of BCSA.

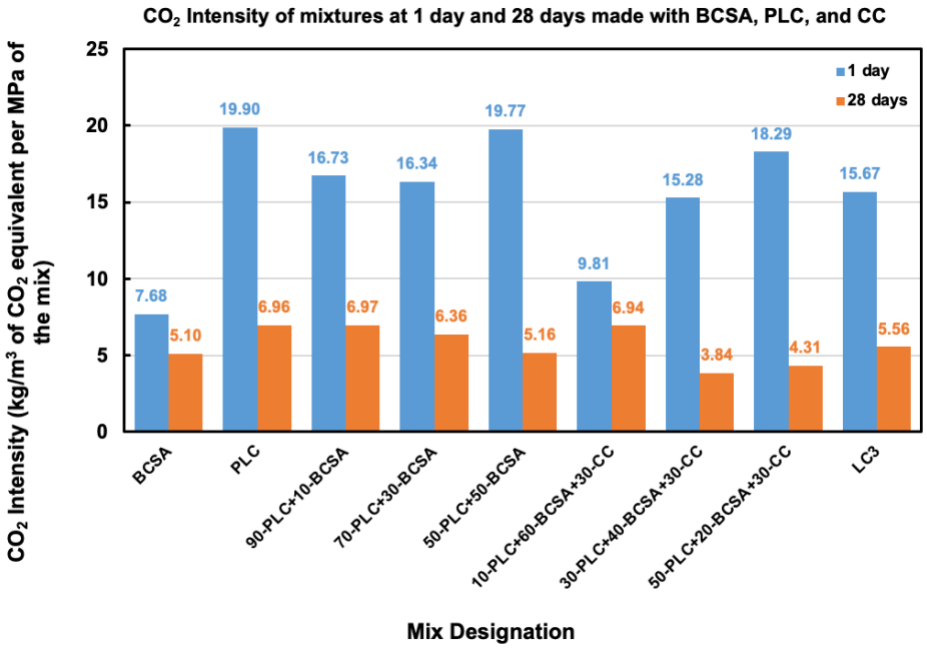

Figure 25: CO_2 intensity of concrete mixes made with BCSA, PLC, and CC based on the compressive strength at 1 and 28 days

Figure 26 shows the CO_2 intensities of concrete mixes made with BCSA, PLC, and CC based on the compressive strength at 1h30, 3h, and 1 day. Early-age CO_2 intensities were calculated because one of these blends was designed in part for the low early-strength of PLC and LC^3. The results for PLC, **50-PLC+50-BCSA**, and LC^3 are not presented because no strength could be measured before 24h. At 1h30 and 3h, the CO_2 intensities decrease with increasing BCSA content. Cement blends that have a low CO_2 intensity at 1h30 and 3h are suitable for applications that require early-strength. The best cement mix for such applications is the **10-PLC+60-BCSA+30-CC** mix, as it contains more BCSA.

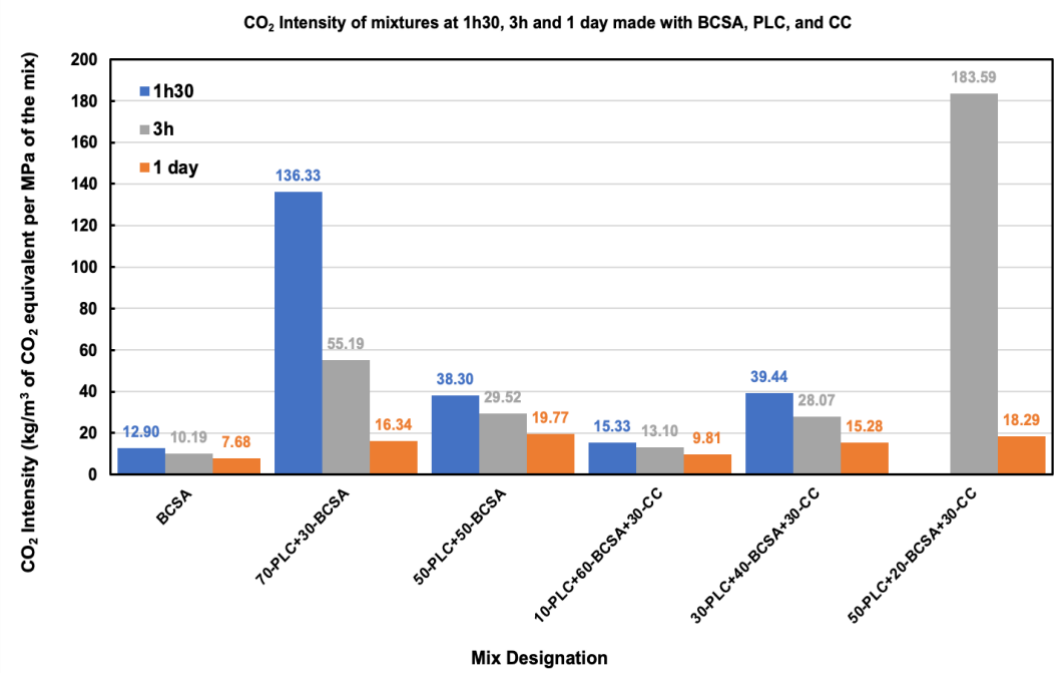

Figure 26: CO_2 intensity of concrete mixes made with BCSA, PLC, and CC based on the compressive strength at 1h30, 3h, and 28 days

The main takeaways from this sustainability study on blends composed of BCSA, PLC, and CC are:

- The CO_2 emissions of the ternary (BCSA+PLC+CC) blends are lower than that of secondary (BCSA+PLC) due to the presence of calcined clay. The same trend is observed for the two sets of blends: the CO_2 emissions decrease with increasing BCSA content.
- The CO_2 emission of the **50-PLC+50-BCSA** is reduced by 10.42% compared to PLC. The CO_2 emission of the **30-PLC+40-BCSA+30-CC** blend is reduced by 5% compared to LC^3 and 38.11% compared to PLC.
- Contrary to evaluation based solely on the CO_2 emissions, the CO_2 intensities based on the 28 days-strength indicate that **50-PLC+50-BCSA** and **30-PLC+40-BCSA+30-CC** contain the optimum proportions of BCSA, PLC, and CC**.**
- The blends containing more BCSA show better performance according to the CO_2 intensities based on the 1h30-strength and 3h-strength.

5. CONCLUSIONS AND FUTURE WORK

Low-carbon cements proposed in the literature are often impractical or at such an early stage of development that they cannot yet be considered as realistic for an industry that is deeply tied to the logistics and the chemistry of Portland cement. In fact, the world still relies on Portland cement for most construction applications despite its shortcomings and high GWP. Efforts are being made to shift the global production of Portland cement to alternative binders such as PLC and LC^3 that promise equivalent performance while lowering both GWP and carbon intensity. The two most practical approaches to low-carbon cements are heavily tied to the Portland cement industry (PLC and LC^3). These alternative binders do not meet the specifications required for certain applications that require high early-age strength in concrete. Such requirements have been partially addressed by using chemical additives or other substitutes that often increase carbon intensity and the cost of producing concrete. In this respect, BCSA has the advantage of being manufactured in Portland cement plants, and of being compatible in concrete placement logistics with OPC. It does not deviate so significantly from 200 years of cement technology that its adoption would be an abrupt revolution in practice. In this work, we explored if it was possible to further reduce the GWP of those materials by adding BCSA to them, while enhancing some of their shortcomings such as low early strength and high shrinkage. A commercially available low-carbon BCSA cement, which can be produced in existing cement plants, and which offers fast-setting, low-shrinkage, and high durability, was used as an additive for improving the performance of other low-embodied binders such as PLC and LC^3. Two sets of mixes were evaluated: one containing BCSA and PLC, the other containing BCSA, PLC, and calcined clay. Compressive strength, shrinkage, flow, and setting time tests were conducted on mortar mixes. Further analysis was conducted to understand the hydration behavior and phases formed using isothermal calorimetry, XRD, TGA/DTG, and SEM. The cement blends were evaluated considering physical/mechanical performance and environmental impact through GWP and CO_2 intensities calculations. The blends developed in this study may be used to meet increasingly low GWP concrete specification especially in the context of the need for faster construction times.

The following conclusions can be drawn from this study:

1. Low embodied CO_2 binders using BCSA, PLC, and calcined clay can meet certain specifications required for high early-age strengths while achieving low GWPs or carbon intensities. Two notable cements that exemplify these features are (a) 50 % PLC and 50% BCSA by weight and (b) 30 % PLC, 40% BCSA, and 30 % calcined clay.

   For example, an early strength of 7.19 MPa (1,043 psi) can be obtained at 1h30 with PLC if 50 % of BCSA is added. Also, an early strength of 6.76 MPa (980 psi) at 3 hours can be obtained by adding 40 % BCSA to LC^3.

   The GWP (or CO_2 emissions) of the **50-PLC+50-BCSA** is reduced by 10.42% compared to PLC, while the GWP of the **30-PLC+40-BCSA+30-CC** blend is reduced by 5% compared to LC^3 and 38.11% compared to PLC. This corresponds to a value of 275 kg/m^3 of CO_2 equivalent for the **50-PLC+50-BCSA** blend compared to 307 kg/m^3 of CO_2 equivalent for PLC and 190 kg/m^3 of CO_2 equivalent for the **30-PLC+40-BCSA+30-CC** blend compared to 200 kg/m^3 of CO_2 equivalent for LC^3.

2. Heat generated from early hydration reactions of these mixes show two distinct peaks - initial and secondary in their exothermic profiles. For the BCSA mix, the initial peak occurs due to the reaction of gypsum and CSA to form ettringite, while the secondary peak, which follows shortly, occurs mainly due to the reaction of CSA and the remaining gypsum to form ettringite and AH_3. For the PLC mix, the initial peak occurs due to the reactions of the limited amounts of the ferrite and aluminate phases, while the secondary peak occurs after the dormant phase, mainly due to the reaction of alite to form C-S-H and CH. The total heat release curves for the BCSA, PLC, and their blends show two distinct slopes depending on their blended proportions and reaction stages. The time interval between the occurrence of the two peaks is also found to be related to the PLC content of the mixes.

3. Shrinkage of the BCSA mix is found to be half that of the PLC mix at 28 days. Also, unlike PLC and BCSA, the binary and ternary blends (of PLC, BCSA, and CC) do not show a discernible trend for shrinkage. The **50-PLC+50-BCSA** and **30-PLC+40-BCSA+30-CC** blends have shrinkage as low as the BCSA mix at all ages.

4. Very early-age strengths (as soon as 1h30 after mixing) of 2.11 MPa (306 psi) and 1.10 MPa (160 psi) could be measured in the binary blends with a minimum of 30% BCSA and in the ternary blends with at least 20% BCSA, respectively. The strengths achieved by 24 hours are primarily due to the hydration of CSA, while the strengths achieved around 7 to 14 days are primarily due to the hydration of C_3S or alite. The secondary hydration of CH to form additional ettringite beyond 7 days of curing also contributes to further strength gains for PLC and BCSA blends. In the ternary blends, the reaction between metakaolin and limestone contributes to strength gain if PLC and CC are available in sufficient proportions. 53.4 MPa (7,745 psi) and 49.4 MPa (7,165 psi) strengths are achieved at 28 days for the **50-PLC+50-BCSA** and **30-PLC+40-BCSA+30-CC** blend compared to 44.1 MPa (6,393 psi) for PLC and 35.9 MPa (5,214 psi) for LC^3.

5. XRD and Rietveld analysis support the observations based on the compressive strength results. Quantifying the major phases produced in PLC, BCSA, and their blends after a 7- and 28-days curing period highlights their different rates of hydration and helps explain the differences in the performance of the mixes to a certain extent. The highest compressive strength achieved by the **50-PLC+50-BCSA** mix at 28 days compared to all other mixes is most likely due to the greater proportions of both ettringite and C-S-H produced from both primary and secondary reactions (partly measurable). The **30-PLC+40-BCSA+30-CC** mix had the highest decrease in alite from 7 to 28 days, meaning that more C-S-H is formed and contributes to the late age strength. A production of Hc was observed in this blend, showing that there is indeed a reaction between PLC and CC. For the **50-PLC+20-BCSA+30-CC** mix, an increase in ettringite from 7 to 28 days was observed because the CH formed in the mix enhances the hydration of ye'elimite. Some components of PLC and CC enhance the reaction of belite, as a decrease in belite was also observed from 7 to 28 days.

6. DTG results are consistent with the XRD results regarding the amount of ettringite and calcium hydroxide, although the goal was to estimate the amount of C-S-H in the blend. The peaks corresponding to other phases, such as calcite, Mc, Hc, and AH_3 (amorphous), can be identified.

The compounds responsible for strength can be identified on the SEM images. Needle-shaped ettringite crystals can be observed on the SEM images of BCSA. Plate-like C-S-H can be observed on the SEM images of PLC. A denser microstructure and closely packed phase are observed on the SEM images of mixes showing a higher or comparable strength to BCSA: **50-PLC+50-BCSA** and **50-PLC+20-BCSA+30-CC**.

7. According to the GWP calculations, the amount of greenhouse gas emitted decreases with increasing BCSA amount for the secondary and ternary blends. If considered alone, the GWP values indicate that the **10-PLC+60-BCSA+30-CC** and **50-PLC+50-BCSA** blends are the ternary and secondary blends, respectively, that have the lowest environmental impact. The **50-PLC+50-BCSA** indeed has the lowest CO_2 intensity. That blend has a comparable CO_2 intensity at 28 days, a higher strength, and a slightly lower shrinkage compared to that of BCSA. However, the same trend is not observed for the ternary blends. The **30-PLC+40-BCSA+30-CC** mix has the lowest CO_2 intensity at 28 days (lower than BCSA) based on its 28-day performance, besides having higher compressive strength and a lower shrinkage compared to BCSA. The **50-PLC+20-BCSA+30-CC** also has a lower CO_2 intensity and a higher strength than that of BCSA at 28 days. However, this blend shows a higher shrinkage compared to BCSA as well as PLC. This highlights the importance of sustainability indices, such as CO_2 intensity, which combine carbon emission and early or long-term strength.

8. As mentioned above, these low embodied CO_2 blends have good mechanical performances at 28 days, and low CO_2 intensities. The CO_2 intensities of the **50-PLC+50-BCSA** and **30-PLC+40-BCSA+30-CC** blends have values of 5.16 and 3.84 kg/m^3 of CO_2 equivalent per MPa of the mix at 28 days compared to 6.96 kg/m^3 and 5.56 kg/m^3 CO_2 equivalent per MPa of the mix at 28 days for PLC and LC^3.

   The CO_2 intensity calculation based on the early-age (1h30 and 3h) strength indicates that the mixes containing more BCSA are better suited for applications that require high early-strength.

This work has made it possible to determine the proportions that lower the CO_2 emission in a **BCSA+PLC** or **BCSA+PLC+CC** blend while still enabling a high strength gain and low shrinkage. The blends containing more BCSA were identified as being suitable for applications that require high early strength.

When BCSA is added in the proper proportions (**50-PLC+50-BCSA** blend or **30-PLC+40-BCSA+30-CC** blend**)**, high compressive strengths are achieved at later ages in addition to higher early strength (1h30 and 3h), lower shrinkage and embodied CO_2 compared to PLC, LC^3 and sometimes even to BCSA cement.

Future work should include:

1. Estimation of water demand for the BCSA and PLC blends (including the ones with CC) to achieve a consistent flow (110 ± 5) or workability.
2. Estimating flow for cement paste mixes using a flow cone test (ASTM C939) or a V-funnel test (ASTM C230).
3. Evaluation of compressive strengths of concrete mixes of BCSA, PLC, and their blends and their correlation with the existing mortar mixes. Similar correlations should be evaluated for length-change or shrinkage measurements of these mixes.
4. Evaluation of GWP of concrete mixes and their correlations with the estimated GWPs based on mortar mixes.
5. Evaluation of long-term performance and durability characteristics, such as alkali-silica reaction, carbonation, corrosion, chloride-ion penetration, freeze-thaw behavior, fatigue behavior, etc., in concrete made using such low CO_2 binders.
6. Evaluate the possibility of achieving improved compressive strengths in such low CO_2 mixtures in proportion with other sustainable materials, including nanomaterials such as graphene oxide, etc.
7. Explore the potential of enhancing the early-age properties of commercially available LC^3 cement using BCSA cement in various proportions.

6. APPENDIX

6.1. XRD-Rietveld refinements

Table 8: Rietveld refinement results for BCSA at 0, 7, and 28 days

Phases	BCSA-0d	BCSA-7d	BCSA-28d
Belite β	43.07	33.13	31.19
Belite α'	1.42	0.45	0
Calcite	1.62	1.87	2.45
Anatase	0	0	0
Anhydrite	9.5	0.89	0.89
Bassanite	6.02	0.23	0.24
Bredigite	-	0.27	1.59
Gypsum	0.85	0.93	1.19
Ellestadite	1.78	2.06	0.47
Ettringite	0.14	48.76	52.01
Brownmillerite	0.48	0.05	0
Jasmundite	1.09	0	0.18
Lime	-	0.04	0.1
Oldhamite	0.6	0	0.04
Periclase	0.43	0.57	0.43
Perovskite	1.68	0.94	0.75
Portlandite	0.57	0.53	0.32
Quartz	0.1	0.44	0.14
Rutile	-	0	0
Stratlingite	1.01	0.83	0.72
Ternesite	4.9	4.83	4.33
Ye'elimite	24.75	3.02	2.73
Ye'elimite orth	0	0.15	0.22
TOTAL	100.01	99.99	99.99

Table 9: Rietveld refinement results for PLC at 0, 7, and 28 days

Phases	PLC-0d	PLC-7d	PLC-28d
Alite*	44.4	5.11	2.71
Calcite	8.94	11.85	14.86
Ferrite	11.90	6.05	4.68
Gypsum	9.13	3.20	5.74
Belite	20.43	20.19	18.06
$CaOH_2$	-	21.73	25.00
C_3A	2.97	0.25	0.10
Ettringite	-	18.21	18.58
Periclase	2.22	2.12	2.93
Hc	-	11.12	2.16
Mc	-	0.18	5.18
TOTAL	99.99	100.01	100

*monoclic+triclinic

Table 10: Results obtained per Rietveld refinement and Mill certificate test results for calcined clay or Metaforce®

Phases	Rietveld refinement results (%)	Mill certificate test results (%)
SiO_2	57.89	57.1
Al_2O_3	24.68	26.7
Fe_2O_3	2.68	0.80
$SiO_2 + Al_2O_3 + Fe_2O_3$	85.25	84.6
MgO	0.08	0.20
Na_2O	0.80	0.35
K_2O	0.62	0.24
SO_3	-	0.85
Equivalent Alkalis	-	0.51
Moisture content	-	0.06
Loss on Ignition	-	1.92

Table 11: Rietveld refinement results for **10-PLC+60-BCSA+30-CC** at 1, 7, and 28 days

Phases	1d	7d	28d
Alite	2.63	2.98	3.30
Belite α'	0.49	0.79	0.79
Bassanite	0.10	0.27	0.26
Brownmillerite	1.29	0.83	0.96
C_3A	0.98	1.65	1.03
Gypsum	1.78	2.24	2.30
Belite	21.88	20.62	19.28
$CaOH_2$	0.04	0.45	0.11
Calcite	5.82	4.84	4.78
Hc	0.36	0.26	0.54
Dickite	3.23	3.18	3.16
Dolomite	0.12	0.48	0.00
Ellestadite	3.31	3.82	3.42
Ettringite	39.03	41.10	41.67
Hematite	0.24	0.00	0.26
Illite	2.60	2.67	2.14
Kaolinite	9.32	7.37	9.84
Lime	0.00	0.00	0.00
Periclase	0.40	0.49	0.48
Mc	0.24	0.21	0.17
Quartz	5.68	5.20	5.31
Ye'elimite orth	0.44	0.48	0.11
Ye'elimite	0.03	0.07	0.09
TOTAL	100.01	100.00	99.99

Table 12: Rietveld refinement results for **30-PLC+40-BCSA+30-CC** at 1, 7, and 28 days

Phases	1d	7d	28d
Alite	9.83	12.29	7.27
Belite α'	1.36	1.10	0.00
Bassanite	0.38	0.00	0.32
Brownmillerite	2.85	1.92	1.70
C_3A	1.74	1.56	1.30
Gypsum	2.17	2.44	2.26
Belite	18.24	16.87	15.96
CaOH2	0.00	0.00	0.15
Calcite	6.01	7.03	6.81
Hc	0.76	0.66	4.65
Dickite	2.98	4.00	4.42
Dolomite	1.27	0.94	1.44
Ellestadite	3.06	2.22	2.33
Ettringite	32.21	31.56	31.37
Hematite	0.25	0.63	0.49
Illite	1.08	1.02	2.96
Kaolinite	9.23	7.34	8.39
Lime	0.00	0.21	0.00
Periclase	0.89	0.88	1.09
Mc	0.03	0.63	0.09
Quartz	4.59	6.41	5.88
Ye'elimite orth	0.69	0.24	0.97
Ye'elimite	0.37	0.07	0.16
TOTAL	99.99	100.02	100.01

Table 13: Rietveld refinement results for **50-PLC+20-BCSA+30-CC** at 1, 7, and 28 days

Phases	1d	7d	28d
Alite	7.09	1.08	0.94
Belite α'	0.55	0.53	0.00
Bassanite	0.00	0.63	0.84
Brownmillerite	3.78	2.47	2.30
C_3A	0.44	0.00	0.21
Gypsum	2.57	6.83	4.58
Belite	17.28	17.27	10.71
$CaOH_2$	3.31	4.04	2.52
Calcite	10.02	7.14	11.67
Hc	4.43	7.93	7.36
Dickite	2.95	3.90	3.83
Dolomite	0.88	2.32	4.27
Ellestadite	2.79	1.55	2.62
Ettringite	24.19	20.87	24.68
Hematite	1.01	0.41	0.00
Illite	2.76	2.11	2.03.62
Kaolinite	6.74	7.02	6.55
Lime	0.00	0.00	0.29
Periclase	0.68	1.31	0.50
Mc	0.00	5.25	8.43
Quartz	5.49	6.89	5.57
Ye'elimite orth	0.57	0.44	0.12
Ye'elimite	2.46	0.00	0.00
TOTAL	99.99	99.99	100.01

Table 14: Rietveld refinement results for **50-PLC+50-BCSA** at 1, 7, and 28 days

Phases	1d	7d	28d
Alite	15.88	11.21	2.43
Belite α'	0	0.72	2.85
Anhydrite	0.18	0	0
Bassanite	1.26	0.38	0.57
Belite	24.27	22.88	18.52
Bredigite	1.18	1.49	1.77
Brownmillerite	2.59	0.27	0.5
C_3A	1.74	1.09	0.94
Gypsum	0.27	0.97	1.84
Calcite	6.22	5.15	6.62
Hc	0.42	10.04	12.30
Dolomite	2.54	2.67	3.07
Ettringite	33.03	31.58	36.23
Lime	0.32	0.35	0.11
Mc	0.07	0.33	2.19
Periclase	1.49	0.72	1.13
Perovskite	1.26	0.51	0
Portlandite	0.65	2.11	2.54
Quartz	0.07	0.16	0.17
Rutile	0.00	0.07	0
Ye'elimite orth	0.00	0	0.34
Ye'elimite	1.54	0.15	0
Stratlingite	1.73	2.11	1.22
Ternesite	3.29	5.02	4.66
TOTAL	100	99.98	100

Table 15: Rietveld refinement results for **70-PLC+30-BCSA** at 1, 7, and 28 days

Phases	1d	7d	28d
Alite	15.45	8.04	3.49
Belite α'	1.69	0.00	2.16
Anhydrite	0.05	0.00	0.00
Bassanite	0.62	1.24	1.78
Belite	20.04	22.36	17.47
Bredigite	0.25	2.89	2.13
Brownmillerite	4.36	1.53	1.16
C_3A	2.46	0.51	0.25
Gypsum	1.14	2.27	3.33
Calcite	9.99	6.94	9.14
Hc	2.71	7.85	8.22
Dolomite	1.08	2.95	3.21
Ettringite	27.23	29.17	27.10
Lime	0.00	0.00	0.36
Mc	0.23	1.99	4.45
Periclase	3.52	1.54	1.70
Perovskite	0.00	0.68	0.00
Portlandite	3.87	5.49	8.14
Quartz	0.09	0.10	0.09
Rutile	0.08	0.06	0.00
Ye'elimite orth	0.24	0.12	0.10
Ye'elimite	2.23	0.45	0.42
Stratlingite	0.00	0.00	0.46
Ternesite	2.69	2.70	4.82
TOTAL	100.02	100.00	99.98

Table 16: Rietveld refinement results for **90-PLC+10-BCSA** at 1, 7, and 28 days

Phases	1d	7d	28d
Alite	16.18	6.98	1.26
Belite α'	1.58	1.79	2.40
Anhydrite	0	0	0.13
Bassanite	0.39	2.11	1.45
Belite	16.89	18.88	17.45
Bredigite	2.09	0.52	0
Brownmillerite	7.74	5.86	3.90
C_3A	0.69	1.38	0.38
Gypsum	1.51	3.94	4.09
Calcite	16.13	11.02	11.84
Hc	0.41	5.06	7.07
Dolomite	1.37	2.01	1.94
Ettringite	19.49	16.72	20.73
Lime	0.00	0	0
Mc	0	1.84	3.11
Periclase	1.80	1.30	1.80
Perovskite	0.58	0	0
Portlandite	9.94	14.62	16.63
Quartz	0.03	0.6	0.4
Rutile	0	0	0.03
Ye'elimite orth	0.14	0	0.17
Ye'elimite	1.12	0	0
Stratlingite	0.13	0.28	0
Ternesite	1.77	5.09	5.23
TOTAL	99.98	100	100.01

6.2. XRD-Main phases

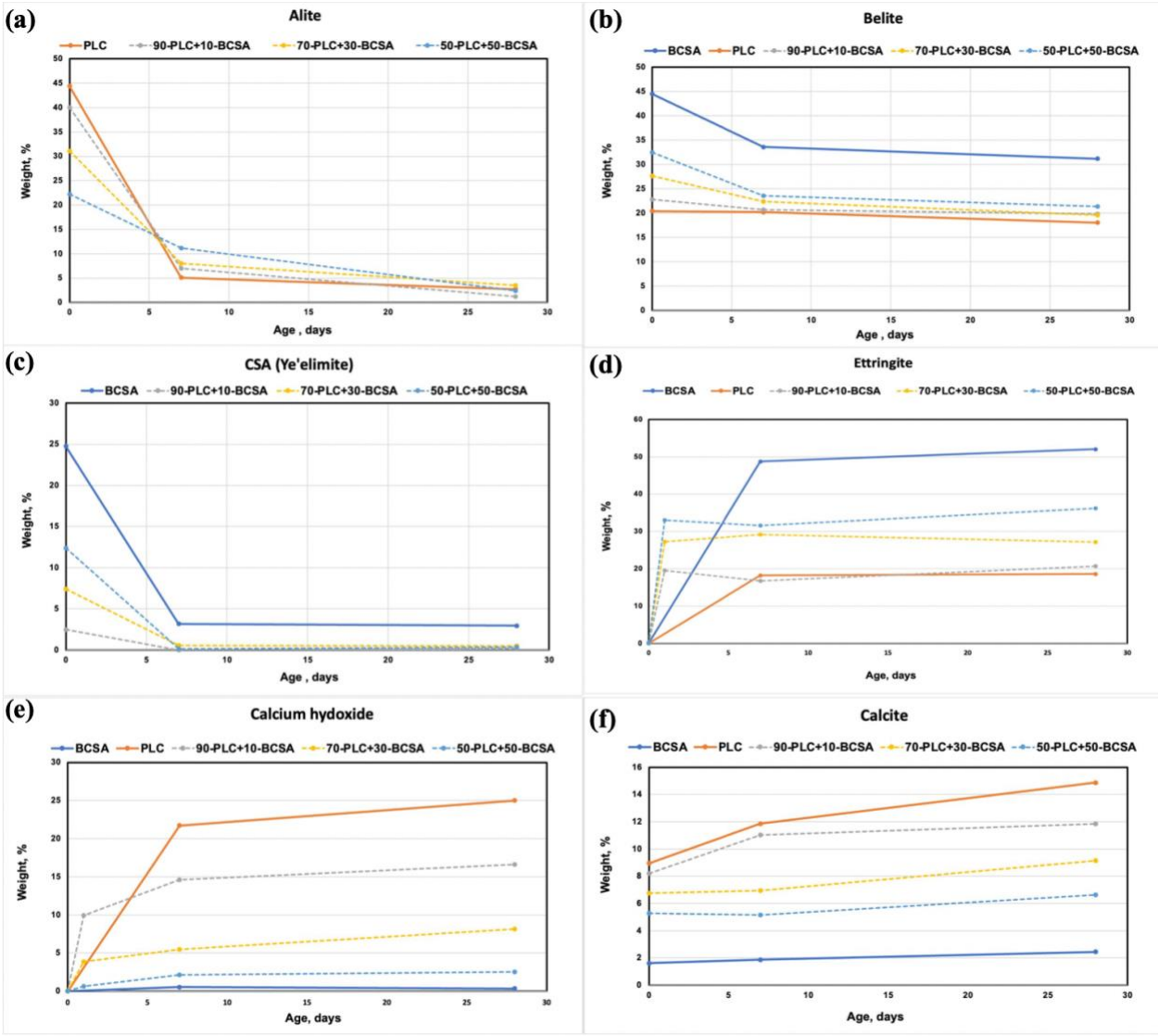

Figure 27: Comparison of the main phases in PLC and BCSA blends as a function of curing time

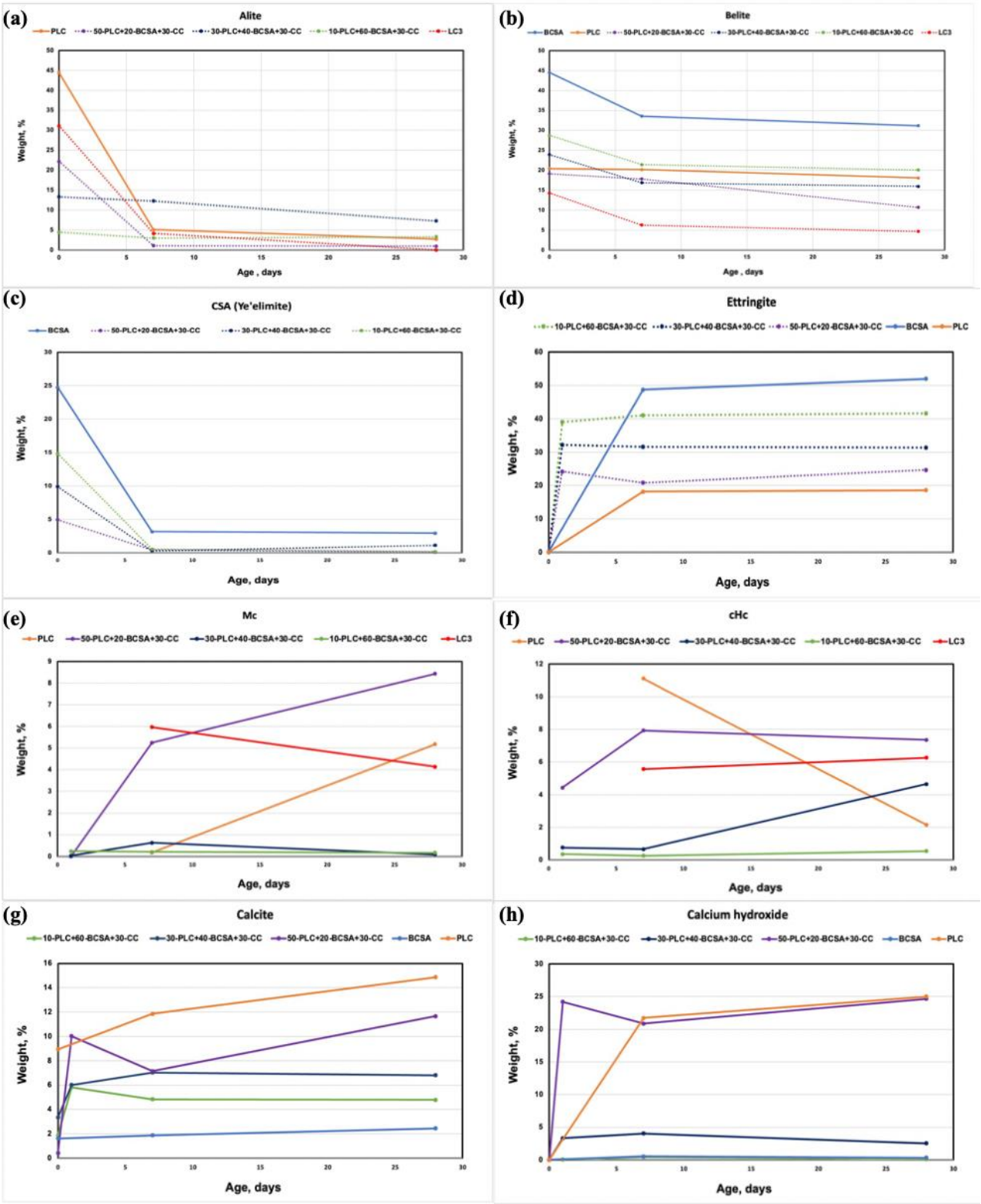

Figure 28: Comparison of the amount of Alite, Belite, CSA, Ettringite, Mc, Hc, and Calcite as a function of time for each blend

6.3. XRD patterns

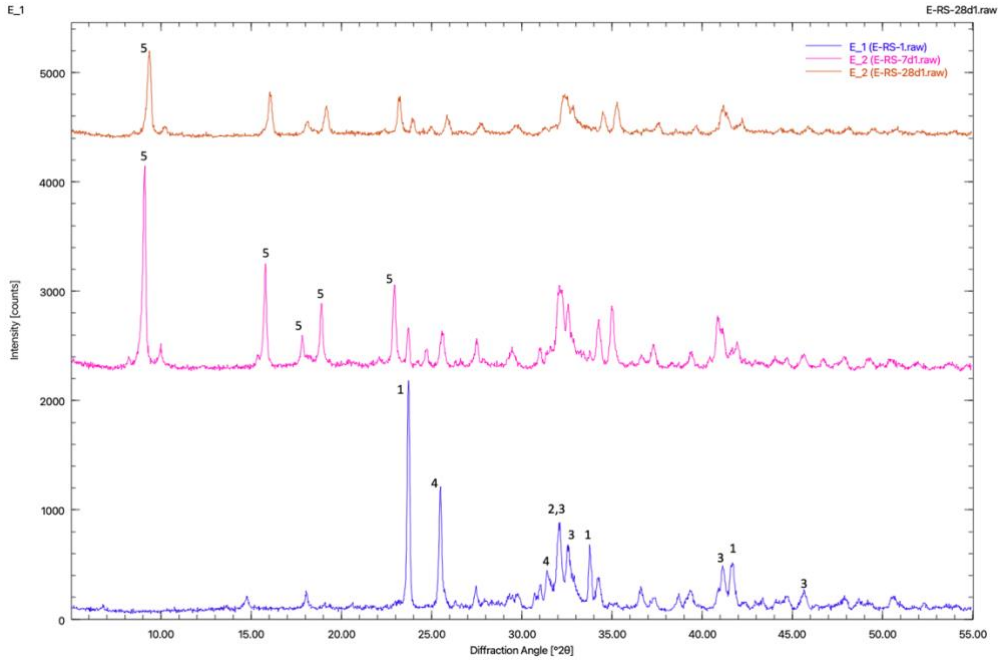

Figure 29: Diffraction pattern of **BCSA** 1: ye'elimite (COD: 9009938) 2: belite-α (COD:1546027) 3: belite-β (COD:1535815) 4:anhydrite (COD: 5000040) 5: ettringite (COD:9011103)

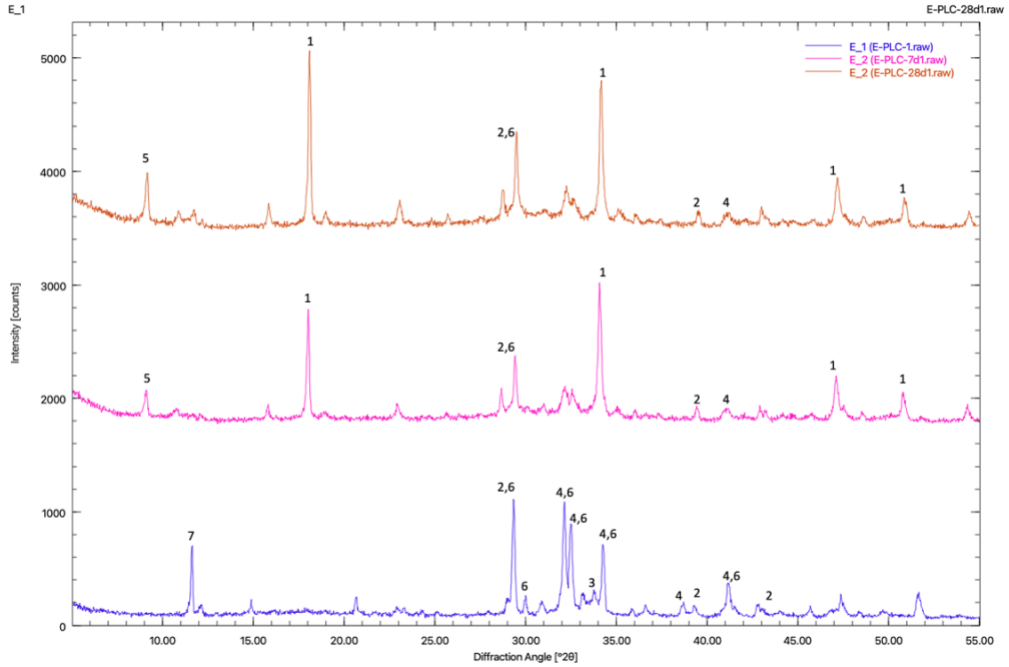

Figure 30: Diffraction pattern of **PLC** 1: calcium hydroxide (COD: 1529752) 2: calcite (COD: 2100992) 3: C3A (COD: 1000039) 4: belite (COD: 1535815) 5: ettringite (COD: 9015084) 6: alite (COD: 9016125) 7: gypsum (COD: 9007887)

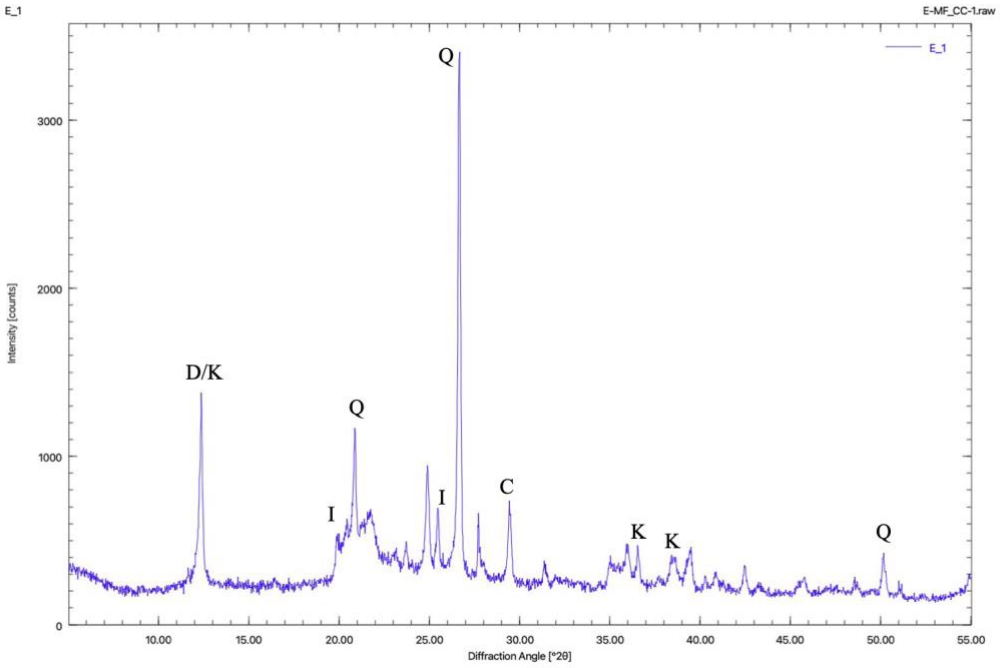

Figure 31: Diffraction pattern of **Calcined Clay** Q: quartz (COD:1536406) K: kaolinite (COD: 9014999) I: Illite (COD: 9009665) D : Dickite (COD: 9003081) C: calcite (COD: 2100992)

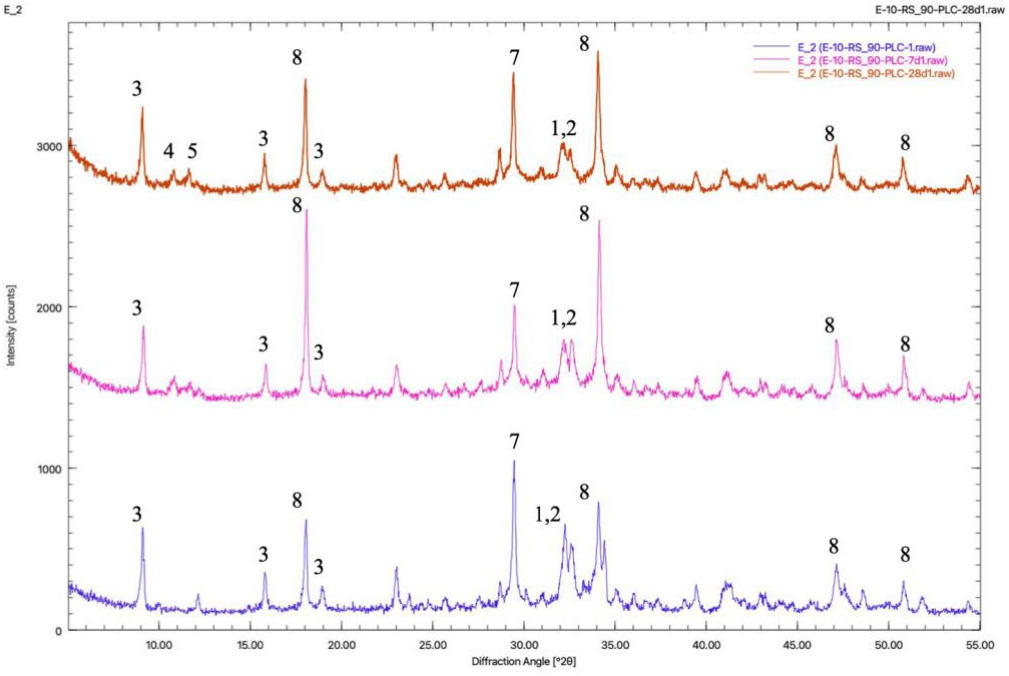

Figure 32: Diffraction pattern of **90-PLC + 10-BCSA** 1: alite (COD: 9016125) 2: belite (COD: 1535815) 3: ettringite (COD: 9015084) 4: Hc (COD: 2105252) 5: Mc (COD: 2007668) 6: kaolinite (COD: 9014999) 7: calcite (COD: 2100992) 8: CH (COD: 1529752) 9: quartz (COD:1536406)

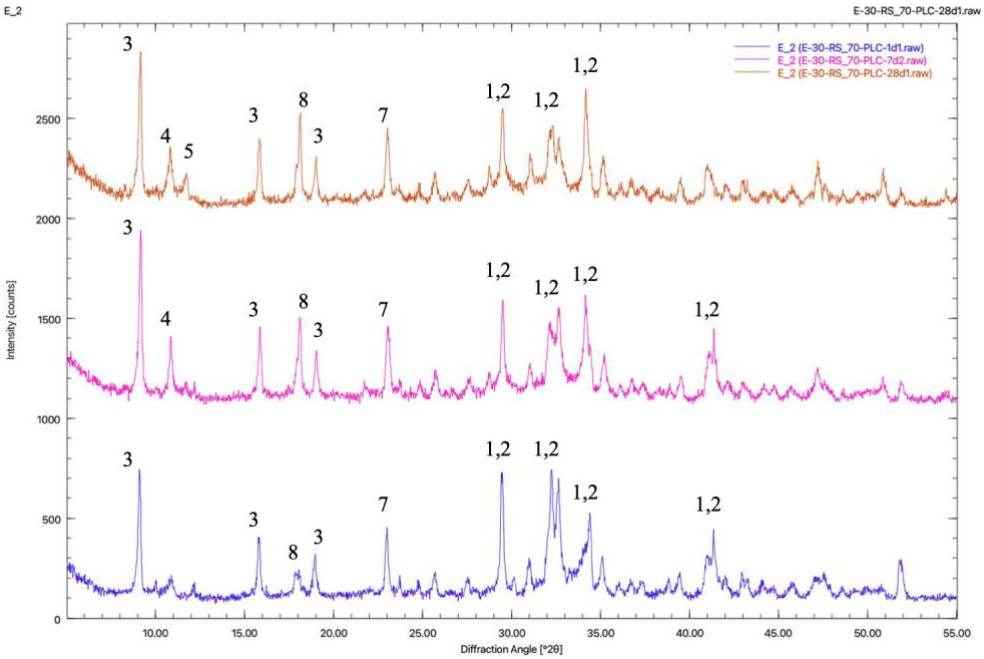

Figure 33: Diffraction pattern of **70-PLC + 30-BCSA** 1: alite (COD: 9016125) 2: belite (COD: 1535815) 3: ettringite (COD: 9015084) 4: Hc (COD: 2105252) 5: Mc (COD: 2007668) 6: kaolinite (COD: 9014999) 7: calcite (COD: 2100992) 8: CH (COD: 1529752) 9: quartz (COD:1536406)

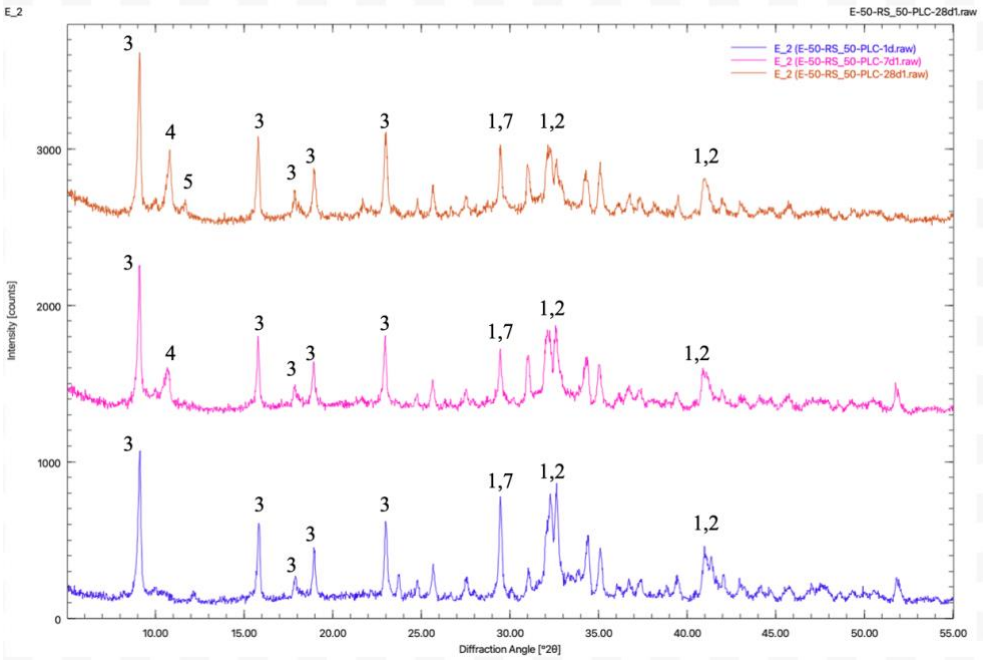

Figure 34: Diffraction pattern of **50-PLC + 50-BCSA** 1: alite (COD: 9016125) 2: belite (COD: 1535815) 3: ettringite (COD: 9015084) 4: Hc (COD: 2105252) 5: Mc (COD: 2007668) 6: kaolinite (COD: 9014999) 7: calcite (COD: 2100992) 8: CH (COD: 1529752) 9: quartz (COD:1536406)

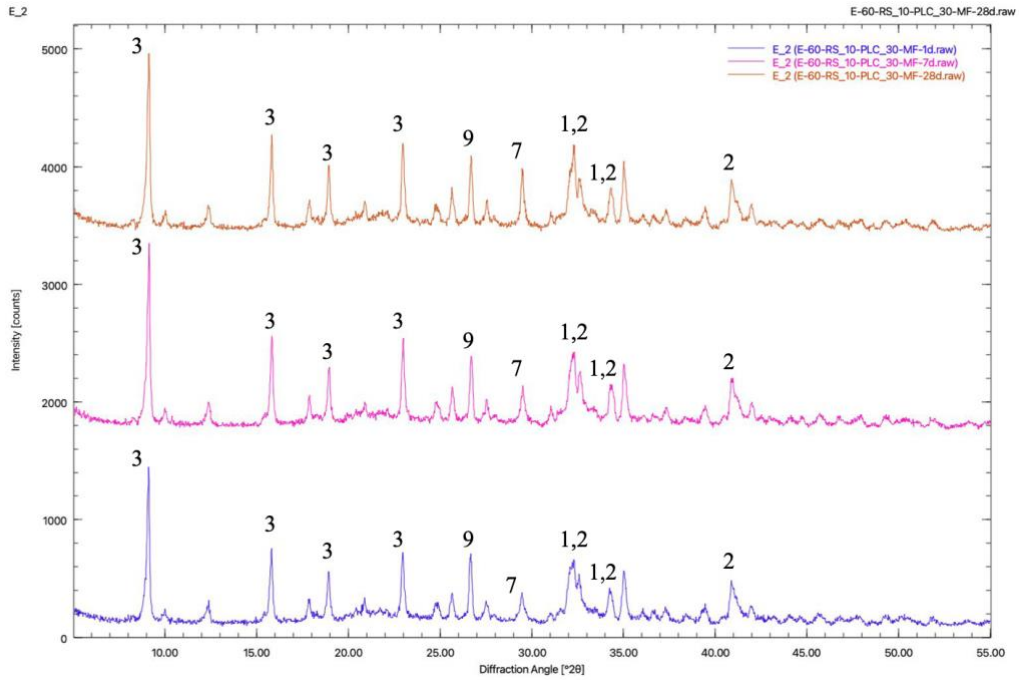

Figure 35: Diffraction pattern of **10-PLC+60-BCSA+30-CC** 1: alite (COD: 9016125) 2: belite (COD: 1535815) 3: ettringite (COD: 9015084) 4: Hc (COD: 2105252) 5: Mc (COD: 2007668) 6: kaolinite (COD: 9014999) 7: calcite (COD: 2100992) 8: CH (COD: 1529752) 9: quartz (COD:1536406)

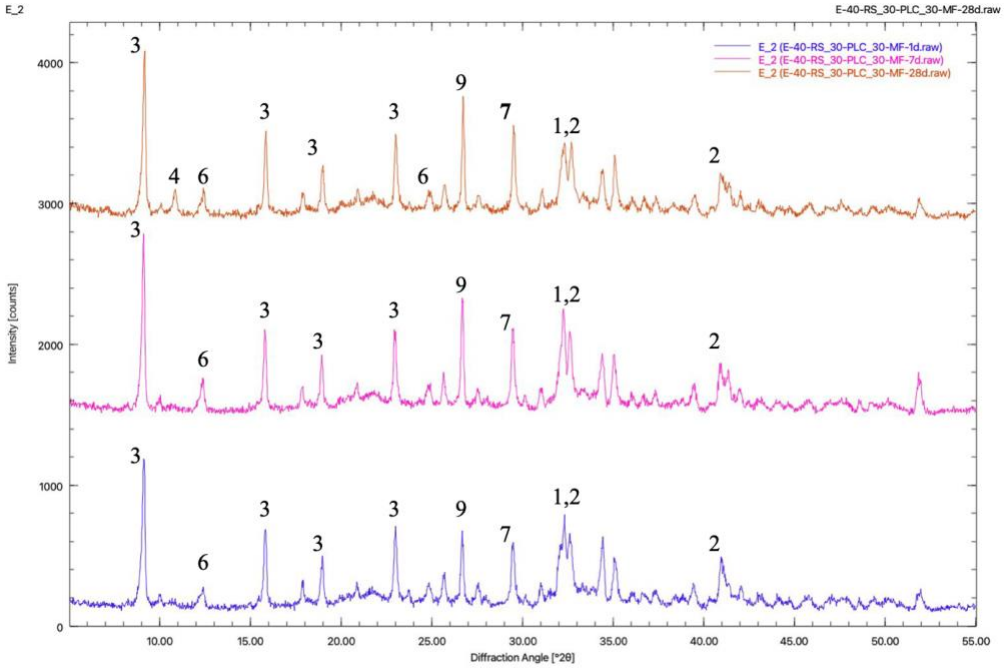

Figure 36: Diffraction pattern of **30-PLC+40-BCSA+30-CC** 1: alite (COD: 9016125) 2: belite (COD: 1535815) 3: ettringite (COD: 9015084) 4: Hc (COD: 2105252) 5: Mc (COD: 2007668) 6: kaolinite (COD: 9014999) 7: calcite (COD: 2100992) 8: CH (COD: 1529752) 9: quartz (COD:1536406)

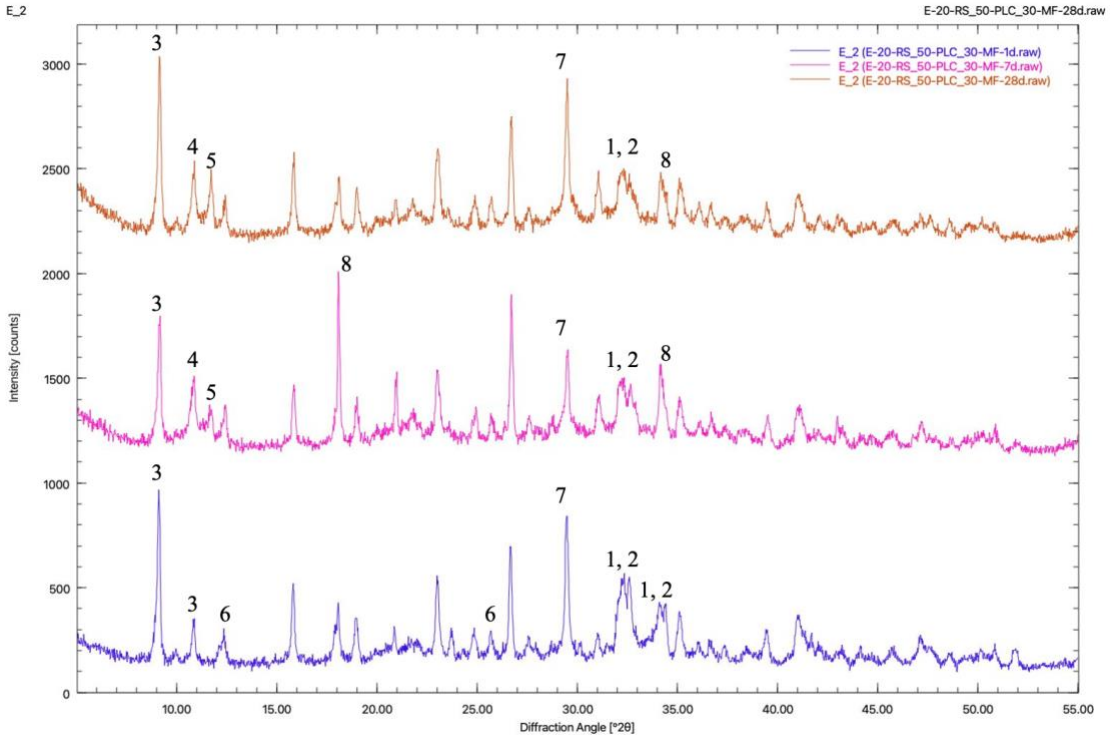

Figure 37: Diffraction pattern of **50-PLC+20-BCSA+30-CC** 1: alite (COD: 9016125) 2: belite (COD: 1535815) 3: ettringite (COD: 9015084) 4: Hc (COD: 2105252) 5: Mc (COD: 2007668) 6: kaolinite (COD: 9014999) 7: calcite (COD: 2100992) 8: CH (COD: 1529752) 9: quartz (COD:1536406)

7. REFERENCES

[1] World Business Council for Sustainable Development (WBCSD). (2021). Low-Carbon Transition in the Cement Industry

[2] https://www.cement.org/docs/default-source/th-paving-pdfs/sustainability/carbon-foot-print.pdf

[3] https://www.cement.org/sustainability/portland-limestone-cement

[4] John Kim, Ken Vallens, and Eric Bescher 2019 Hydration chemistry, performance and use in the United States 15th International Congress on the Chemistry of Cement

[5] Chen I A, Hargis C W and Juenger M C G 2012 Understanding expansion in calcium sulfoaluminate–belite cements *Cem. Concr. Res.* **42** 51–60

[6] https://www.ctscement.com/assets/doc/info/EPDlabel_RapidSet_Labeling_Sustainability_CTS_Cement

[7] https://concretecountertopinstitute.com/free-training/various-csa-cement-brands-and-manufacturers/

[8] Scrivener K L, John V M, and Gartner E M 2018 Eco-efficient cements: Potential economically viable solutions for a low-CO2 cement-based materials industry *Cem. Concr. Res.* **114** 2–26

[9] Voglis N, Kakali G, Chaniotakis E, and Tsivilis S 2005 Portland-limestone cements. Their properties and hydration compared to those of other composite cements *Cem. Concr. Compos.* **27** 191–6

[10] Moir G K and Kelham S 1999 Developments in the Manufacture and Use of Portland Limestone Cement *Spec. Publ.* **172** 797–820

[11] https://www.greenercement.com/_files/ugd/f3d485_04eeabb11d2d4e7ebc2c6a0332c18ebf

[12] Scrivener K, Martirena F, Bishnoi S and Maity S 2018 Calcined clay limestone cements (LC3) *Cem. Concr. Res.* **114** 49–56

[13] IEA (International Energy Agency). (2021). Energy Technology Perspectives 2021: Special Report on Clean Energy Innovation. Paris: IEA

[14] Habert G, Miller S A, John V M, Provis J L, Favier A, Horvath A and Scrivener K L 2020 Environmental impacts and decarbonization strategies in the cement and concrete industries *Nat. Rev. Earth Environ.* **1** 559–73

[15] Miller S A, Horvath A, Monteiro P J M and Ostertag C P 2015 Greenhouse gas emissions from concrete can be reduced by using mix proportions, geometric aspects, and age as design factors *Environ. Res. Lett.* **10** 114017

[16] Celik K, Meral C, Petek Gursel A, Mehta P K, Horvath A and Monteiro P J M 2015 Mechanical properties, durability, and life-cycle assessment of self-consolidating concrete mixtures made with blended portland cements containing fly ash and limestone powder *Cem. Concr. Compos.* **56** 59–72

[17] Sonebi M, Ammar Y and Diederich P 2016 15 - Sustainability of cement, concrete, and cement replacement materials in construction *Sustainability of Construction Materials (Second Edition)* Woodhead Publishing Series in Civil and Structural Engineering ed J M Khatib (Woodhead Publishing) pp 371–96

[18] Miller S, Horvath A, and Monteiro P 2018 Impacts of booming concrete production on water resources worldwide *Nat. Sustain.* **1**

[19] Yang X, Hu M, Wu J and Zhao B 2018 Building-information-modeling enabled life cycle assessment, a case study on carbon footprint accounting for a residential building in China *J. Clean. Prod.* **183** 729–43

[20] Xing W, Tam V W Y, Le K N, Hao J L, and Wang J 2022 Life cycle assessment of recycled aggregate concrete on its environmental impacts: A critical review

[21] Miller S A, Monteiro P J M, Ostertag C P and Horvath A 2016 Concrete mixture proportioning for desired strength and reduced global warming potential *Constr. Build. Mater.* **128** 410–21

[22] Ram K, Serdar M, Londono-Zuluaga D and Scrivener K 2023 Does carbon footprint reduction impair mechanical properties and service life of concrete? *Mater. Struct.* **56** 6

[23] Yang G, Zhao J and Wang Y 2022 Durability properties of sustainable alkali-activated cementitious materials as marine engineering material: A review *Mater. Today Sustain.* **17** 100099

[24] Turner L K and Collins F G 2013 Carbon dioxide equivalent (CO2-e) emissions: A comparison between geopolymer and OPC cement concrete *Constr. Build. Mater.* **43** 125–30

[25] Onyelowe K, Ebid A, Riofrio A, Soleymani A, Baykara H, Kontoni D-P, Madhi H and Jahangir H 2022 Global warming potential-based life cycle assessment and optimization of the compressive strength of fly ash-silica fume concrete; environmental impact consideration *Front. Built Environ.* **8** 1–15

[26] Detwiler R and Tennis P D 1996 THE USE OF LIMESTONE IN PORTLAND CEMENT: A STATE-OF-THE-ART REVIEW

[27] Pacheco-Torgal F, Jalali S, Labrincha J and John V M 2013 Front matter *Eco-Efficient Concrete* Woodhead Publishing Series in Civil and Structural Engineering (Woodhead Publishing) pp i–iii

[28] Tsivilis S, Chaniotakis E, Badogiannis E, Pahoulas G, and Ilias A 1999 A study on the parameters affecting the properties of Portland limestone cements *Cem. Concr. Compos.* **21** 107–16

[29] Tsivilis S, Chaniotakis E, Kakali G, and Batis G 2002 An analysis of the properties of Portland limestone cements and concrete *Cem. Concr. Compos.* **24** 371–8

[30] Taylor H F W 1997 *Cement chemistry* (Thomas Telford Publishing)

[31] Matschei T, Lothenbach B and Glasser F P 2007 The role of calcium carbonate in cement hydration *Cem. Concr. Res.* **37** 551–8

[32] Lothenbach B, Le Saout G, Gallucci E, and Scrivener K 2008 Influence of limestone on the hydration of Portland cements *Cem. Concr. Res.* **38** 848–60

[33] Kakali G, Tsivilis S, Aggeli E and Bati M 2000 Hydration products of C3A, C3S, and Portland cement in the presence of CaCO3 *Cem. Concr. Res.* **30** 1073–7

[34] Neville, A.M. and Brooks, J.J. *Concrete Technology*

[35] Thomas M, Barcelo L, Blair B, Cail K, Delagrave A and Kazanis K 2012 Lowering the Carbon Footprint of Concrete by Reducing Clinker Content of Cement *Transp. Res. Rec.* **2290** 99–104

[36] Thomas M D A, Hooton D, Cail K, Smith B A, Wal J de and Kazanis K G 2010 Field Trials of Concrete Produced with Portland Limestone Cement *Concr. Int.* **32** 35–41

[37] Manglorkar D, Kandhal P and Parker F 1993 EVALUATION OF LIMESTONE COARSE AGGREGATE IN ASPHALT CONCRETE WEARING COURSES

[38] Scrivener K, Martirena F, Bishnoi S and Maity S 2018 Calcined clay limestone cements (LC3) *Cem. Concr. Res.* **114** 49–56

[39] Zunino F and Scrivener K 2021 The reaction between metakaolin and limestone and its effect in porosity refinement and mechanical properties *Cem. Concr. Res.* **140** 106307

[40] Zhou Y, Gong G, Xi B, Guo M, Xing F, and Chen C 2022 Sustainable lightweight engineered cementitious composites using limestone calcined clay cement (LC3) *Compos. Part B Eng.* **243** 110183

[41] Antoni M, Rossen J, Martirena F and Scrivener K 2012 Cement substitution by a combination of metakaolin and limestone *Cem. Concr. Res.* **42** 1579–89

[42] Dhandapani Y, Sakthivel T, Santhanam M, Gettu R and Pillai R G 2018 Mechanical properties and durability performance of concretes with Limestone Calcined Clay Cement (LC3) *Cem. Concr. Res.* **107** 136–51

[43] Díaz E, González R, Rocha D, Alujas A and Martirena F 2018 Carbonation of Concrete with Low Carbon Cement LC3 Exposed to Different Environmental Conditions *Calcined Clays for Sustainable Concrete* RILEM Bookseries ed F Martirena, A Favier and K Scrivener (Dordrecht: Springer Netherlands) pp 141–6

[44] Sharma M, Bishnoi S, Martirena F and Scrivener K 2021 Limestone calcined clay cement and concrete: A state-of-the-art review *Cem. Concr. Res.* **149** 106564

[45] Lin R-S, Oh S, Du W and Wang X-Y 2022 Strengthening the performance of limestone-calcined clay cement (LC3) using nano-silica *Constr. Build. Mater.* **340** 127723

[46] Glasser F P and Zhang L 2001 High-performance cement matrices based on calcium sulfoaluminate–belite compositions *Cem. Concr. Res.* **31** 1881–6

[47] Juenger M C G, Winnefeld F, Provis J L and Ideker J H 2011 Advances in alternative cementitious binders *Cem. Concr. Res.* **41** 1232–43

[48] Liu Y J, Xu Y M and Geng C L 2012 Sulfoaluminate Cement: An Alternative to Portland Cement *Adv. Mater. Res.* **368–373** 478–84

[49] Klein A, Karby T and Polivka M 1961 Properties of an Expansive Cement for Chemical Prestressing *J. Proc.* **58** 59–62

[50] Ost B W A, Schiefelbein B and Summerfield J M 1975 Very high early strength cement

[51] Bolaños-Vásquez, I, Trauchessec, R, and Lecomte, A 2018 Study of calcium sulfoaluminate cements and Portland cement blends International Workshop on Calcium Sulfoaluminate cements (Murten, Switzerland)

[52] Chaunsali P and Mondal P 2015 Influence of Calcium Sulfoaluminate (CSA) Cement Content on Expansion and Hydration Behavior of Various Ordinary Portland Cement-CSA Blends *J. Am. Ceram. Soc.* **98** 2617–24

[53] Kasselouri V, Tsakiridis P, Malami Ch, Georgali B, and Alexandridou C 1995 A study on the hydration products of a non-expansive sulfoaluminate cement *Cem. Concr. Res.* **25** 1726–36

[54] Cohen M D 1983 Theories of expansion in sulfoaluminate - type expansive cements: Schools of thought *Cem. Concr. Res.* **13** 809–18

[55] Burris L E and Kurtis K E 2018 Influence of set retarding admixtures on calcium sulfoaluminate cement hydration and property development *Cem. Concr. Res.* **104** 105–13

[56] H. T A, Kienzle A, and Thomas R J 2022 Engineering properties and setting time of belitic calcium sulfoaluminate (BCSA) cement concrete *Constr. Build. Mater.* **352** 128979

[57] Mehta P K and Klein A 1966 INVESTIGATIONS ON THE HYDRATION PRODUCTS IN THE SYSTEM 4 CAO-3AL203-SO3-CASO4-CAO-H20 *Highw. Res. Board Spec. Rep.*

[58] Pelletier-Chaignat L, Winnefeld F, Lothenbach B, Saout G L, Müller C J, and Famy C 2011 Influence of the calcium sulfate source on the hydration mechanism of Portland cement–calcium sulphoaluminate clinker–calcium sulfate binders *Cem. Concr. Compos.* **33** 551–61

[59] Chaunsali P and Mondal P 2015 Influence of Mineral Admixtures on Early-Age Behavior of Calcium Sulfoaluminate Cement *ACI Mater. J.* **112** 59–69

[60] Le Saoût G, Lothenbach B, Hori A, Higuchi T and Winnefeld F 2013 Hydration of Portland cement with additions of calcium sulfoaluminates *Cem. Concr. Res.* **43** 81–94

[61] Bianchi M, Canonico F, Capelli L, Pace ML, Telesca A and Valenti G L 2009 Hydration Properties of Calcium Sulfoaluminate-Portland Cement Blends *Spec. Publ.* **261** 187–200

[62] Telesca A, Marroccoli M, Pace M, Tomasulo M, Valenti G and Naik T 2013 Expansive and non-expansive calcium sulfoaluminate-based cements

[63] Huang G, Pudasainee D, Gupta R and Liu W V 2021 Extending blending proportions of ordinary Portland cement and calcium sulfoaluminate cement blends: Its effects on setting, workability, and strength development *Front. Struct. Civ. Eng.* **15** 1249–60

[64] Park S, Jeong Y, Moon J and Lee N 2021 Hydration characteristics of calcium sulfoaluminate (CSA) cement/portland cement blended pastes *J. Build. Eng.* **34** 101880

[65] Kothari A, Tole I, Hedlund H, Ellison T and Cwirzen A 2023 Partial replacement of OPC with CSA cements – effects on hydration, fresh and hardened properties *Adv. Cem. Res.* **35** 207–24

[66] Chitvoranund N, Lothenbach B, Sinthupinyo S and Winnefeld F 2015 Reactivity of Calcined Clay in Alite-Calcium Sulfoaluminate Cement Hydration RILEM Bookseries vol 10 pp 373–9

[67] Pedersen M, Lothenbac B, Winnefeld F and Skibsted J 2018 Hydrate Phase Assemblages in Calcium Sulfoaluminate – Metakaolin – Limestone Blends RILEM Bookseries vol 16, ed F Martirena, A Favier and K Scrivener (Dordrecht: Springer Netherlands) pp 352–7

[68] Londoño Zuluaga D 2018 *Eco-cements containing belite, alite, and ye'elimite. Hydration and mechanical properties* http://purl.org/dc/dcmitype/Text (Universidad de Málaga)

[69] Mrak M, Winnefeld F, Lothenbach B and Dolenec S 2021 The influence of calcium sulfate content on the hydration of belite-calcium sulfoaluminate cements with different clinker phase compositions *Mater. Struct.* **54** 212

[70] Scrivener K, Snellings R and Lothenbach B 2015 Thermogravimetric analysis *A Practical Guide to Microstructural Analysis of Cementitious Materials*

[71] Phung Q T, Maes N, and Seetharam S 2019 Pitfalls in the use and interpretation of TGA and MIP techniques for Ca-leached cementitious materials *Mater. Des.* **182** 108041

[72] Hargis C, Kirchheim A, Monteiro P, and Gartner E 2013 Early age hydration of calcium sulfoaluminate (synthetic ye'elimite, C4A3$) in the presence of gypsum and varying amounts of calcium hydroxide *Cem. Concr. Res.* **48** 105–15

[73] Zhou Y, Wang Z, Zhu Z, Chen Y, Wu K, Huang H, Anvarovna K G and Xu L 2022 Influence of metakaolin and calcined montmorillonite on the hydration of calcium sulphoaluminate cement *Case Stud. Constr. Mater.* **16** e01104

[74] Cao Y, Wang Y, Zhang Z, Ma Y, and Wang H 2023 Thermal stability of limestone calcined clay cement (LC3) at moderate temperatures 100–400 °C *Cem. Concr. Compos.* **135** 104832